Form: PGR_Submission_200701

NOTICE OF SUBMISSION OF THESIS FORM: POSTGRADUATE RESEARCH

APPENDIX 1:
Specimen layout for Thesis Summary and Declaration/Statements page to be included in a Thesis

DECLARATION

This work has not previously been accepted in substance for any degree and is not concurrently submitted in candidature for any degree.

Signed ..... (candidate) Date 20/7/2011

STATEMENT 1

This thesis is being submitted in partial fulfillment of the requirements for the degree of ...PhD.....(insert MCh, MD, MPhil, PhD etc, as appropriate)

Signed ..... (candidate) Date 20/7/2011

STATEMENT 2

This thesis is the result of my own independent work/investigation, except where otherwise stated. Other sources are acknowledged by explicit references.

Signed ..... (candidate) Date 20/7/2011

STATEMENT 3

I hereby give consent for my thesis, if accepted, to be available for photocopying and for inter-library loan, and for the title and summary to be made available to outside organisations.

Signed ..... (candidate) Date 20/7/2011

STATEMENT 4: PREVIOUSLY APPROVED BAR ON ACCESS

I hereby give consent for my thesis, if accepted, to be available for photocopying and for inter-library loans **after expiry of a bar on access previously approved by the Graduate Development Committee.**

Signed ..... (candidate) Date .....

Development and plasticity of the mouse primary visual cortex

Adam Ranson

A dissertation submitted for the degree of

PhD in Neuroscience

Cardiff School of Biosciences

Cardiff University

UMI Number: U567132

All rights reserved

INFORMATION TO ALL USERS
The quality of this reproduction is dependent upon the quality of the copy submitted.

In the unlikely event that the author did not send a complete manuscript
and there are missing pages, these will be noted. Also, if material had to be removed,
a note will indicate the deletion.

UMI U567132
Published by ProQuest LLC 2013. Copyright in the Dissertation held by the Author.
Microform Edition © ProQuest LLC.
All rights reserved. This work is protected against
unauthorized copying under Title 17, United States Code.

ProQuest LLC
789 East Eisenhower Parkway
P.O. Box 1346
Ann Arbor, MI 48106-1346

Abstract

The development of the connectivity of the primary visual cortex depends upon an interplay of genetic factors, and environmental factors such as visual experience. In the studies which follow I have investigated the molecular mechanisms by which visual experience alters the connectivity at synapses between the neurons which constitute the visual system. In vitro studies of synaptic plasticity have yielded a deep understanding of ways in which neurons *could* alter their connectivity, but less is known about whether these mechanisms are utilised in vivo and by which brain regions. Broadly speaking, the following studies examine plasticity processes *in vivo,* in both the developing and adult visual cortex of mice which are known to have deficits in plasticity measured in vitro and ex vivo. Plasticity was assessed by monocular eye closure which is known to induce both a loss of cortical responsiveness to the closed eye (after 3 days) and a more gradual gain in cortical responsiveness to the open eye (after 6 days). This process is known as ocular dominance plasticity.

Ocular dominance plasticity was assessed in juvenile mice lacking the GluR1 AMPAR (alpha-amino-3-hyroxy-5-methylisoxazole-4 propionic acid receptor) subunit which results in long term potentiation and long term depression deficits in the hippocampus and somatosensory cortex. In mice lacking GluR1, intrinsic signal responses were observed to be basally depressed and retinotopic map organisation appeared to be defective, although ocular dominance was observed

to basally normal. After 3d of monocular experience plasticity deficits were observed in GluR1 knockout mice in the monocular cortex and in binocular cortical layer 4, while plasticity appeared normal in more superficial binocular cortex. After 6d monocular experience, open eye potentiation was absent in mice lacking GluR1.

Ocular dominance plasticity was also assessed in adult mice lacking GluR1. Ocular dominance plasticity after 6d monocular experience was observed to be normal in GluR1$^{-/-}$ mice as was adult recovery from monocular experience. Facilitation of OD plasticity after short monocular experience (3d) due to prior experience was however impaired in mice lacking GluR1.

A penetrant strain difference was observed in juvenile ocular dominance plasticity between two C57BL/6J sub strains of mice (C57BL/6J and C57BL/6JOlaHsd) whereby open eye 'homeostatic' potentiation was completely absent in the C57BL/6JOlaHsd strain. This was accompanied by a complete lack of dark exposure induced synaptic scaling as measured ex vivo. In contrast in adulthood both strains showed robust and comparable open eye potentiation, suggesting a mechanistic difference between juvenile and adult plasticity. Preliminary data suggests that while juvenile open eye potentiation is homeostatic, in adulthood it may be more of an LTP like process as it appears to be dependent upon CaMKII autophosphorylation.

Acknowledgements

The work presented in this thesis is my own with the exception of two experiments. First, in chapter 3 immunohistochemical straining was performed by Mr Timothy Gould. Second, the in vitro electrophysiology experiments presented in chapter 6 were performed by Dr Claire Cheetham.

I would like to thank here my supervisors, Frank Sengpiel and Kevin Fox, for their enthusiasm in supporting my work, for patiently teaching me, for interesting discussions and feedback, and for permitting me the freedom to explore avenues which I considered interesting. I would like to thank all past and present members of the labs in which I've worked for support and encouragement during the rough and the smooth periods of my PhD. I would particularly like to acknowledge Claire Cheetham for her enthusiasm and for agreeing to our fruitful collaboration which has helped to tie together and strengthen several of the findings presented in this thesis. I would also like to acknowledge Miriam Mann of Mark Hübener's group who in the early days of the PhD kindly introduced me to many of the techniques which I have used, and Mike Stryker's lab members for assistance in developing the periodic intrinsic signal imaging protocol.

Finally I would like to thank my family for their love and always showing interest and pride in my work, and the close friends I've made in Cardiff for making things fun, particularly Denis Bureau, Linda Erlandsson, Anne Kirtley, Paola Moffa-Sanchez, Ana Moragues-Faus, Poppy Nicol and Tom Vowels.

Abbreviation and units of measurement

ΔR/R	Difference in reflectance/reflectance
μM	Micrometres
μV	Microvolts
6J	The C57BL/6J mouse strain
6JOlaHsd	The C57BL/6JOlaHsd mouse strain
ACSF	Artificial cerebrospinal fluid
AMPA	alpha-amino-3-hyroxy-5-methylisoxazole-4 propionic acid
AP5	2-amino-5-phosphonopentanoate
Arc	activity-regulated cytoskeleton-associated protein
BDNF	Brain-derived neurotropic factor
BPM	Beats per minute
BZ	Binocular zone
C/deg	Cycles per degree
CCD	Charge-coupled device
CPP	3-(2-Carboxypiperazin-4-yl)propyl-1-phosphonic acid
C-terminal	Carboxyl-terminus
d.f.	Degrees of freedom
DE	Acute dark exposure
dLGN	Dorsal lateral geniculate nucleus
DR	Dark rearing from eye opening

EPSP	Excitatory postsynaptic potential
fEPSP	Field excitatory postsynaptic potential
FS	Fast spiking parvalbumin-positive large basket cells
GABA	Gamma-aminobutyric acid
GAD	Glutamic acid decarboxylase
GluR1	AMPAR subunit 1
HFS	High frequency stimulation
Hz	Hertz
i.m.	Intramuscular
I.Q.R.	Interquartile range
IPSP	Inhibitory postsynaptic potential
L2/3	Cortical layer 2/3
L4	Cortical layer 4
LFS	Low frequency stimulation
LTD	Long term depression
LTP	Long term potentiation
MD	Monocular deprivation
mEPSP	Miniature postsynaptic potential
mGluR1	Metabotropic glutamate receptor
MI	Monocular enucleation
Mm	Millimetres
mM	Milimolar

Ms	Milliseconds
mV	Millevolts
MZ	Monocular zone
MΩ	Megaohms
nA	Nanoamps
nm	Nanometres
NMDA	N-methyl-D-aspartate
NSF	N-ethylmaleimide-sensitive fusion protei
OD	Ocular dominance
ODI	Ocular dominance index
OI	Optical imaging of intrinsic signals
P	Postnatal day
pA	Picoamps
PSD	Postsynaptic density
RGC	Retinal ganglion cell
ROI	Region of interest
s.c.	Subcutaneous
S.E.M.	Standard error of the mean
Ser	Serine residue
TNF-α	Tumour necrosis factor
TTX	Tetrodotoxin
V1	Primary visual cortex

V2	Secondary visual cortex
VEP	Visually evoked potential
αCaMKII	Alpha-calcium/calmodulin-dependent protein kinase II

Table of contents

Table of figures

Chapter 1. Introduction

1.1 Introduction

The consistency of the morphology of biological organisms is in large part genetically determined. The enormity of this feat of organisation is particularly apparent during brain development when, in the case of humans, tens of billions of neurons are organised into prototypical circuits made up of trillions of synaptic connections. These circuits once developed form the substrate for all cognitive functions. However the fine scale connectivity of many brain circuits can not be accounted for by genetic factors alone and depends upon an interplay of genetic and environmental factors. A much studied example is the primary visual cortex where structured input from the environment relayed via sensory organs is critical to the development of normal connectivity (Katz & Shatz, 1996).

1.2 Cortical map development

There are many problems with trying to understand the role that experience plays in formation of a highly complex brain circuit such as that which produces language. One hurdle is that the brain activity associated with complex cognitive processes is widely distributed in the brain and consequently difficult to measure directly. Early stages of sensory systems in contrast are in many respects more amenable to measurement and are guided in their development by environmental factors which are more readily manipulable. The development of the sensory systems which constitute the early stages of sensory processing has been

explored as model systems in order to understand how genetic products and the environment interact to shape brain circuits.

Early sensory circuits possess some key features which make studying their development a relatively tractable problem. The spatial layout of sensory processing areas often reflects features of the structure of the stimuli being sensed and of the sensory organs. For example the rodent somatosensory cortex contains histologically identifiable 'barrels', each of which contain neurons which respond preferentially to a single whisker. These barrels are laid out with the same topology as the vibrissae on the animals snout (Woolsey & Van der Loos, 1970). Similarly in the auditory cortex there exists a 'tonotopic' map whereby neighbouring sound frequencies activate neighbouring cortical regions (Nelken *et al.*, 2004; Kalatsky *et al.*, 2005) (Figure 1.1B). In visual processing areas 'retinotopy' is present in many structures, whereby activity in neighbouring retinal cells leads to activation of neighbouring cortical neurons (Allman & Kaas, 1971; Kalatsky & Stryker, 2003) (Figure 1.1A). Another advantage of studying circuit development in sensory systems is that the environmental factors which play a part in development are relatively easily experimentally manipulated.

A pivotal epoch in the development of understanding of the importance of environment in brain circuit and particularly sensory brain circuit development began in 1963 with a series of Nobel prize winning studies by Torsten Wiesel and David Hubel exploring the effects of sensory experience manipulation on the development of the cat visual system. This work compared the previously

A

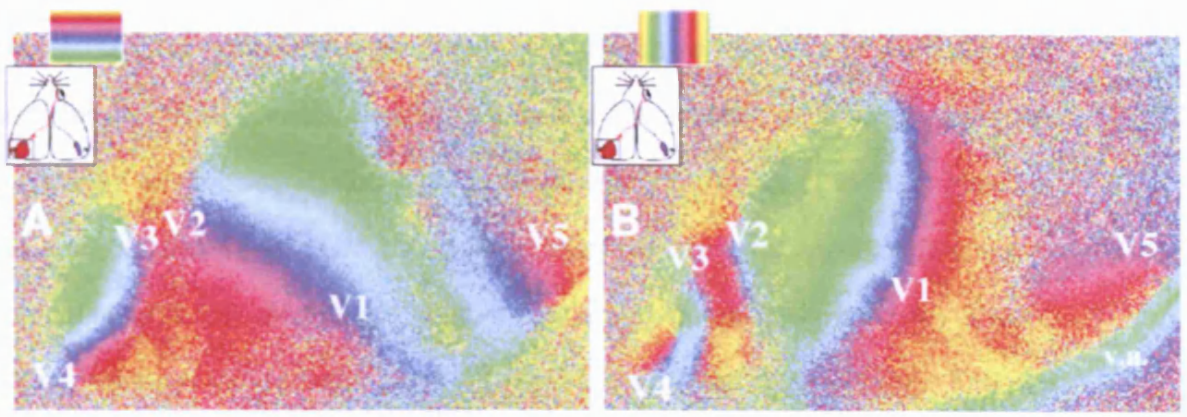

B

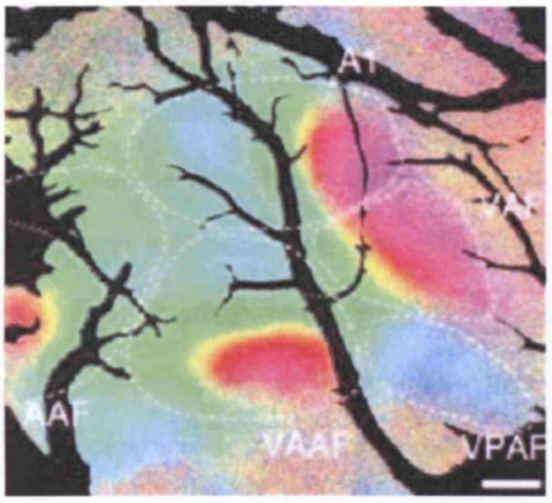

Figure 1.1 Rodent cortical sensory maps.
A: Retinotopic maps of primary visual cortex obtained by intrinsic signal imaging (from Kalatsky & Stryker, 2003). V1, primary visual cortex; V2-V5 are other visually responsive areas; v.a., vascular artefact. *B: Tonotopic maps of primary auditory cortex obtained by intrinsic signal imaging (from Kalatsky et al., 2005).* A1, primary auditory cortex; VAF, ventral auditory field; VPAF, ventral posterior auditory field; VAAF, ventral anterior auditory field; AAF, anterior auditory field.

established characteristics of normal cat visual cortex cell receptive fields (Hubel & Wiesel, 1959) with those of cats reared with abnormal visual experience. In the visual cortex of primates and many mammalian carnivores (for example cats and ferrets) the retinally innervated lateral geniculate nucleus is normally comprised of well segregated eye specific layers which project to the cortex. In the cortex, projecting LGN axons form approximate eye specific patches in cortical layer 4 that are thought not to be experience dependent (Crowley & Katz, 2000), although this remains a controversial finding (Wickelgren, 2000). The eye specificity of these patches is refined in an experience dependent manner and they form the template for further projections upwards into the cortex which make up eye specific cortical columns.

In 1963 Wiesel and Hubel published work exploring the characteristics of cat binocular visual cortical neurons (i.e. neurons that normally receive correlated input from both eyes), which had been deprived of input from the contralateral eye (known as monocular deprivation) during the critical period (Wiesel & Hubel, 1963). This resulted in a behaviourally assayable blindness in this eye (Dews & Wiesel, 1970), the cause of which was electrophysiologically determined to be a loss of responsiveness of cortical neurons to the deprived eye (Wiesel & Hubel, 1963). A further study of binocular deprivation (Wiesel & Hubel, 1965) demonstrated that this effect of reduced response of the deprived eye was largely dependent upon normal input from the open eye as depriving both eyes did not result in the same dramatic loss of eye driven activity. A further study provided evidence that the development of normal binocular cells that were

driven by both eyes was dependent upon correct alignment of the eyes (Hubel & Wiesel, 1965).

1.3 The mouse visual system

As the most thoroughly genetically characterised and manipulable mammalian species, the mouse has emerged as the subject of intense study of cortical map development and the molecular means by which the environment influences circuit formation. I will now provide an overview of the mouse visual system.

1.3.1 The eye and the retina

The mouse eye has an axial length of approximately 3mm and is characterised by a relatively large cornea and lens (Chalupa & Williams, 2008). As is typical of animals adapted to live in low light conditions the retina of the mouse is dominated by rod photoreceptors which make up 97% of the photoreceptive cells (Chalupa & Williams, 2008) and are present at a peak density of 100,000 cells/mm^2. In contrast retinal cones are present at a peak density of 16,000 cells/mm^2. Similar to other non-primate mammals the mouse does not possesses a pitted cone filled foveal region of the retina but instead possesses an area centralis within which both rod and cone photoreceptor density is maximum (Chalupa & Williams, 2008). In the mouse the peak wavelength sensitivity of rod cells is 497 – 500 nm while the peak sensitivity of cone cells depends upon the relative quantity of expression of two photoreceptors: one with a UV peak sensitivity of 360 nm and another with a peak sensitivity of 508 nm

(Chalupa & Williams, 2008). Rod photoreceptor cells relay light signals via rod bipolar cells on to horizontal amacrine interneurons which in turn 'piggyback' onto the cone ON and OFF bipolar cell pathway. Signals are then relayed on to retinal ganglion cells (RGCs). Cone photoreceptors in contrast relay light signals via cone bipolar cells directly to RGCs. Bipolar cell's dendritic neurotransmitter receptor response to photoreceptor released glutamate determines whether they are photoreceptor ON or OFF sensitive.

The photoreceptors in the mouse retina converge onto approximately 48,000 – 65,000 RGCs (Drager & Olsen, 1980) with a peak density of 8,000 cells/mm^2 (Drager & Olsen, 1981). In the mouse RGCs have receptive field sizes of around 2-10° in diameter which are functionally similar to those observed in other mammals in the sense of possessing an antagonistic centre surround configuration and exhibiting a varying degree of direction selectivity (Chalupa & Williams, 2008). In the mouse 2-3% of RGCs project ipsilaterally (Drager & Olsen, 1980) and provide input to the binocular region of the cortical retinotopic map and correspond to the central 30-40° of visual space.

1.3.2 The dorsal lateral geniculate nucleus (dLGN)

In the mouse the dLGN receives direct retinal input from RGCs and relays visual information to the primary visual cortex. The mouse dLGN is organised retinotopically and while it does not contain eye specific laminae as have been observed in primates and carnivores, there is a binocular segment which contains both contralateral and ipsilateral eye responsive relay cells. Of the

binocular visual space inputs there is a difference in degree of convergence between contralateral and ipsilateral RGC afferents onto dLGN recipient relay cells. Specifically while a point in binocular visual space will stimulate around 9 times as many contralateral as ipsilateral RGCs, the volume of the binocular dLGN occupied by contralateral RGC afferents is just 2.4 times the volume occupied by ipsilateral afferents (Coleman *et al.*, 2009), which is approximately the degree of contralateral dominance observed in the binocular cortex (Gordon & Stryker, 1996; Frenkel & Bear, 2004a; Cang *et al.*, 2005). The typical spatial acuity of dLGN cells has been observed to be around 0.03 c/deg with a maximum value of around 0.5c/deg (Grubb & Thompson, 2003) which is consistent with cortical electrophysiological and functional imaging assessments which have been made of mouse visual acuity cut-off (Porciatti *et al.*, 1999; Heimel *et al.*, 2007). The dLGN relay cells transmit visual information to the cortex via their axons which make up the optic radiation.

1.3.3 The visual cortical areas

In the posterior region of the occipital neocortex there are a number of retinotopically organised areas which receive either direct thalamic visual input or receive projections from within the primary visual cortex. The primary visual cortex (V1) is one of the most studied of the visual cortical areas in the mouse and is constituted of cytoarchitectonic area 17. V1 is approximately $3mm^2$ in area and contains a retinotopically organised map of the contralateral visual field. In this map more medial areas correspond to the more horizontally peripheral visual field while more posterior areas correspond to the more vertically elevated

areas of the visual field (Drager, 1975; Gordon & Stryker, 1996; Kalatsky & Stryker, 2003). V1 primarily receives input from the dLGN via the axons of dLGN relay cells which form a projection known as the optic radiation, which for the most part makes excitatory synapses onto the dendrites of layer 4 stellate cells. There is also a substantial degree of direct thalamocortical input to layer 3 (Liu *et al.*, 2008). In addition the mouse cortex receives callosal projections from the contralateral cortex via the commisural fibres which terminate mostly in layers 1-3 and 5 and in retinotopic terms into the lateral, most binocular regions of the V1 cortical map (Mizuno *et al.*, 2007; Restani *et al.*, 2009). These transcallosal projections are thought to be partially explanative of the high degree of binocularity in mouse cortex in the absence of a large number of ipsilateral RGCs innervating the dLGN (although see Coleman *et al.*, 2009).

1.3.4 Receptive field properties of mouse visual cortical cells

The visual cortical neurons of mouse V1 possess many of the receptive field properties observed in other mammals such as spatial frequency and orientation selectivity and simple vs. complex receptive fields (Drager, 1975; Niell & Stryker, 2008; Kerlin *et al.*, 2010).

Single unit studies have assessed the maximum spatial frequency preference of excitatory V1 neurons in the mouse to be approximately 0.3c/deg with the vast majority of neurons exhibiting tuning in the range of 0.01 to 0.08c/deg (Niell & Stryker, 2008), see Figure 1.6A. This is broadly consistent with observations of spatial frequency tuning in the dLGN (Grubb & Thompson, 2003). The spatial

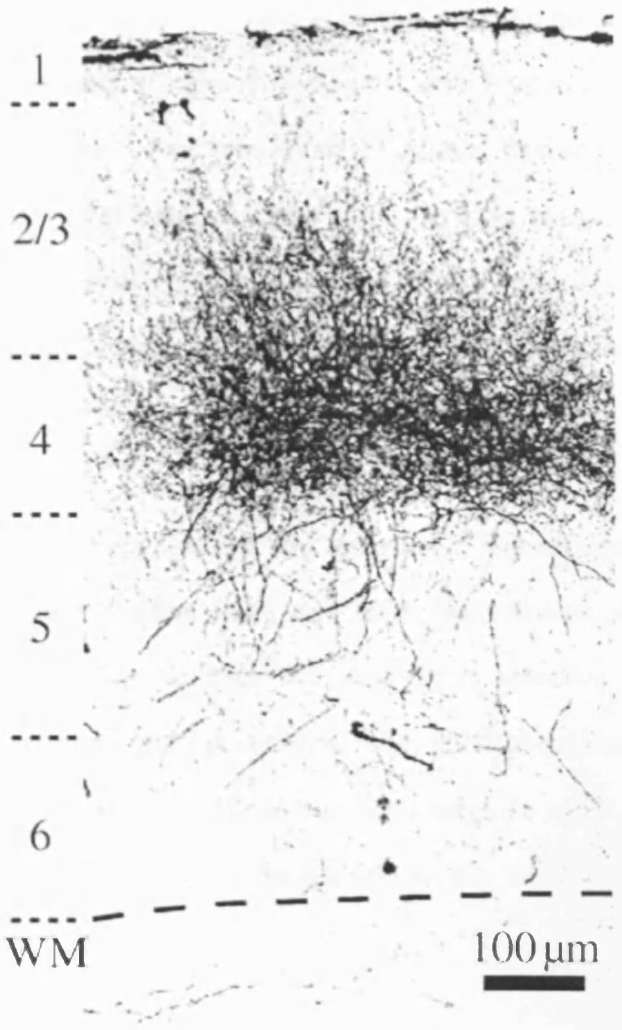

Figure 1.2 Thalamocortical axons labeled by injection of biotin-conjugated dextran into the dLGN. Axons can be seen to project most densely into layer 4 but also into layer 2/3 (from Smith *et al.*, 2009).

frequency cut off has been determined to be approximately 0.5-0.6c/deg (Grubb & Thompson, 2003; Prusky & Douglas, 2003; Heimel *et al.*, 2007). Amongst excitatory cells spatial frequency tuning is similar between cortical layers with the exception of layer 6 where population mean spatial frequency tuning is around 0.02c/deg (Figure 1.6). The bandwidth of spatial frequency tuning is also comparable across most cortical layers with a typical mean spatial frequency tuning width of approximately 2.5 octaves; the exception is cortical layer 5 in which a mean tuning width of closer to 3.5 has been observed (Niell & Stryker, 2008).

Poor orientation selectivity was initially reported in the mouse (Drager, 1975), however more recent studies have described experiments in which 74% of excitatory visually responsive cells are orientation selective (Niell & Stryker, 2008). Cells are most orientation selective in layer 2/3 of the mouse visual cortex with a median tuning half-width at half maximal response of 20 degrees reported by Niell & Stryker (2008) which is comparable to the 19-25 degrees reported in the cat (Van Hooser, 2007).

Electrophysiological analysis of putative inhibitory neurons (putative because they have been identified by spike waveform) and calcium imaging of genetically and immunologically identified classes of inhibitory cells suggests that throughout the visual cortex GABAergic neurons are tuned to lower spatial frequencies (on average 0.02c/deg). Additionally there is evidence that the receptive field properties of GABAergic neurons is in large part determined by the receptive field

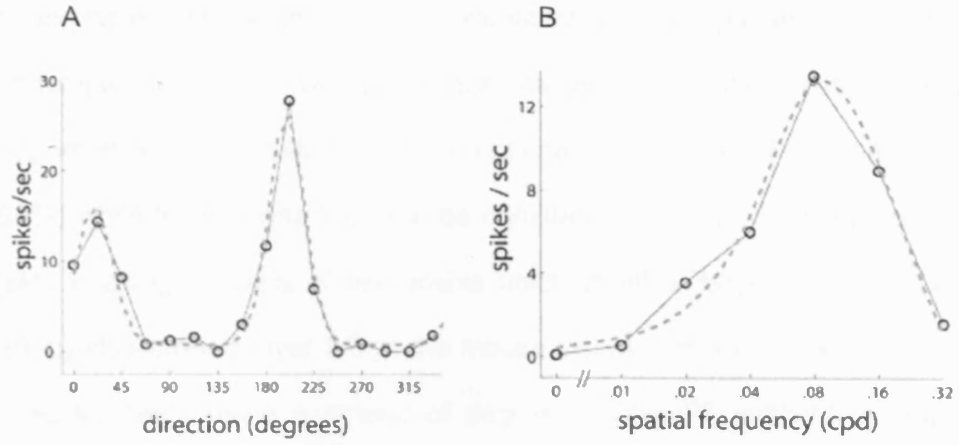

Figure 1.3 Example tuning curves of neurons recorded in mouse V1 (from Niell & Stryker, 2008)
A: An orientation selective cell. B: Spatial frequency tuning of the same cell orientation.

properties of the excitatory neurons in their local vicinity (Kerlin *et al.*, 2010). This might go some way in explaining why GABAergic neurons are relatively non-tuned in mice (which lack clustering of orientation tuning) compared to cats (which posses clustering of orientation tuning) (Hasenstaub & Callaway, 2010).

Mice have also been observed to possess the simple (or linear) and complex (or non-linear) receptive fields observed in other mammals considered to be more visually developed (Hubel & Wiesel, 1962). Niell & Stryker (2008) quantified the degree of linearity (simpleness) of single unit receptive fields by measuring spiking in response to a drifting grating. A periodically modulated response (relative to average spiking rate) was indicative of a simple receptive field whereby a cell responds preferentially to a certain orientation in a certain position in the visual field. In contrast, a visually evoked spiking response that is not periodically modulated is indicative of a more complex receptive field that might

for example respond to a certain orientation of edge presented in a range of retinotopic locations. Using this quantitative classification method, a greater proportion of simple cells have been observed in layer 4 (67%) than in layer 2/3 (53%) while layer 5 was found to be dominated by cells with complex receptive fields (making up 52% of responsive units) (Niell & Stryker, 2008). Liu et al. (2010) also probed layer 2/3 of the mouse visual cortex for simple and complex receptive fields using a criteria of degree of ON/OFF subfield overlap. This quantification yielded a bimodal distribution of overlap indices further suggesting a dichotomy exists between simple and complex cells in mouse V1 (Figure 1.4).

In contrast to the cortical maps of many carnivorous mammals and primates, no columnar clustering of receptive field properties has so far been observed in mouse V1, that is mice lack ocular dominance columns and orientation pinwheels. Recent advances in in vivo cellular resolution imaging have confirmed the evidence from earlier electrophysiological studies of a 'salt and pepper' organisation of mouse V1 maps (Ohki *et al.*, 2005; Mrsic-Flogel *et al.*, 2007)(Figure 1.7). The only super-cellular level of organisation of receptive field properties observed so far in the mouse is the retinotopic map. The retinotopic map has been measured in vivo by electrophysiological (Drager, 1975; Gordon & Stryker, 1996; Kalatsky *et al.*, 2005) and functional imaging techniques (Schuett *et al.*, 2002; Kalatsky *et al.*, 2005; Smith & Hausser, 2010), and ex vivo in tracer experiments (Wang & Burkhalter, 2007).

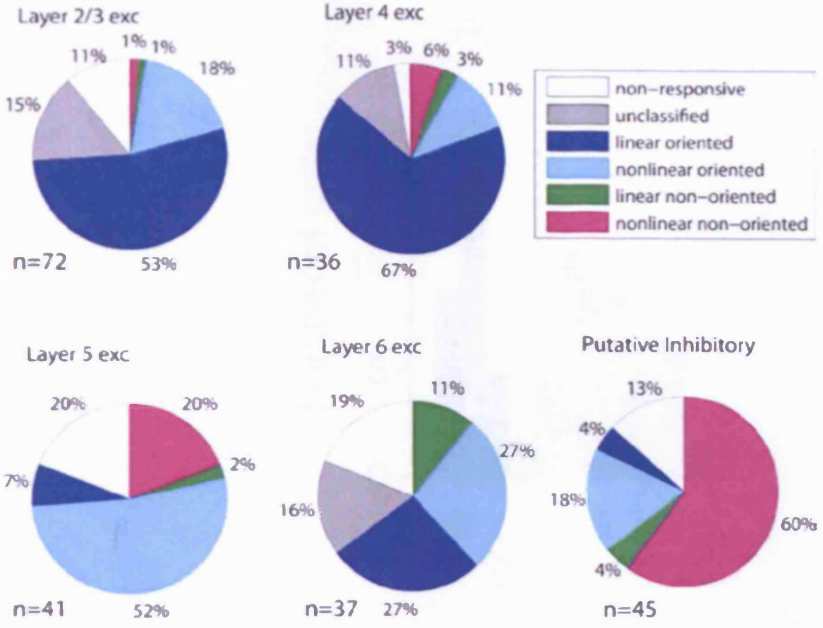

Figure 1.4 Laminar analysis of functional response characteristics (from Niell & Stryker, 2008).

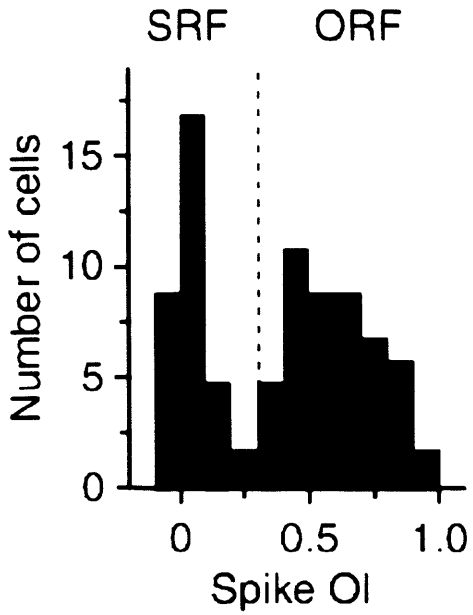

Figure 1.5 Dichotomy of simple and complex receptive fields in mouse V1 (from Liu *et al.*, 2010).
Distribution of ON/OFF subfield overlap indexes (OI) is bimodal. Liu et al. (2010) describe cells with non-overlapping RFs as simple (SRF) and cells with overlapping RFs as complex (ORF).

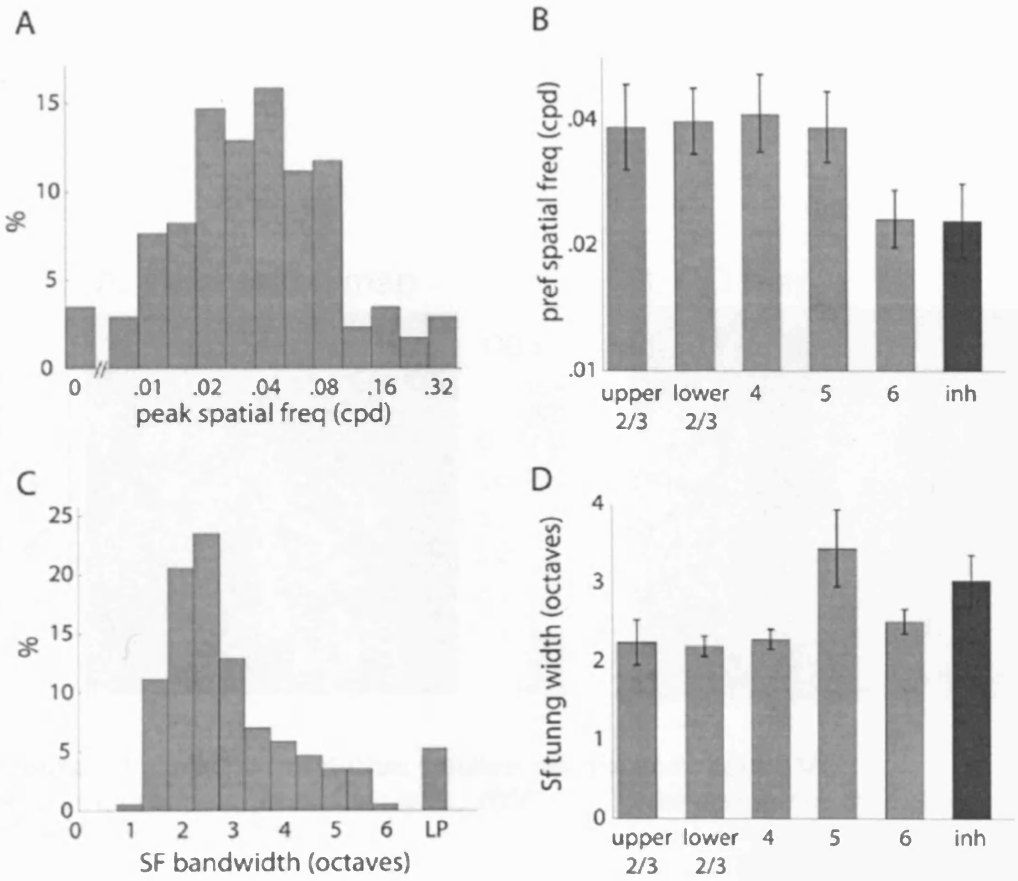

Figure 1.6 Spatial Frequency Tuning (adapted from Niell & Stryker, 2008). *A: Population distribution of spatial frequency preferences. B: Laminar distribution of spatial frequency preferences. C: Population distribution of spatial frequency tuning width. D: Laminar distribution of spatial frequency tuning widths.*

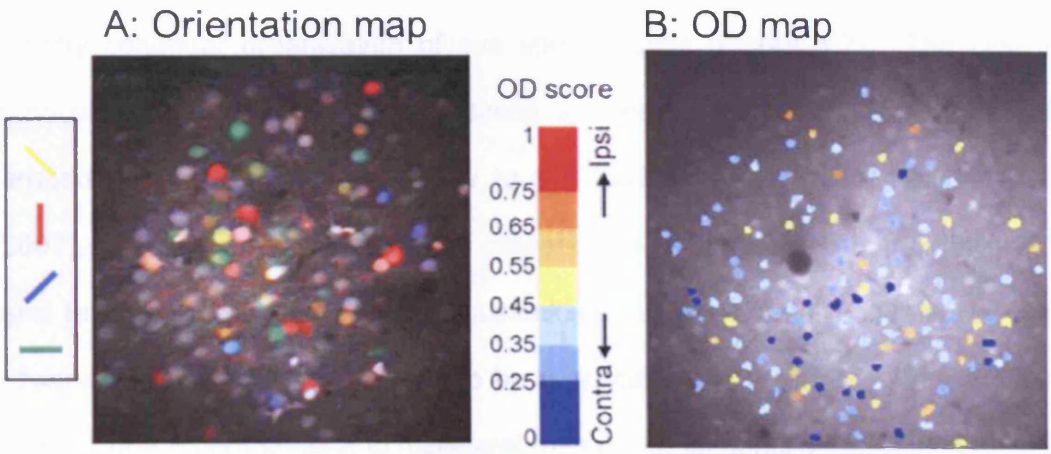

Figure 1.7 Cellular resolution calcium imaging of mouse V1
A: Orientation map (from Ohki et al., 2005). B: Ocular dominance map (from Mrsic-Flogel et al., 2007)

1.4 Ocular dominance

1.4.1 Binocular region

The central 30-40° of the mouse's visual field can be seen by both eyes and provides input to a binocular region of the primary visual cortex (Drager, 1975; Kalatsky & Stryker, 2003; Cang *et al.*, 2005). The binocular region of the visual cortex (Figure 1.8) makes up approximately one third of the total primary visual cortical area and unlike the cortices of many carnivores and primates it lacks a patchy columnar organisation of eye specific cells (Figure 1.7). The cells in binocular mouse visual cortex possess a strong contralateral bias, with only around 5% responding exclusively to the ipsilateral eye (Mrsic-Flogel *et al.*, 2007), and this contralateral bias is present to a similar degree both in layer 2/3 and layer 4 (Figure 1.9). As discussed above, the normal contralateral bias observed in the cortex is thought to be a product of a similar bias in the dLGN where the 9:1 contralateral to ipsilateral ratio of retinal ganglion cell innervation is transformed to a 2:1 ratio which is relayed to the binocular cortex (Coleman *et al.*, 2009). Convergent evidence of this contralateral bias in cortical ocular dominance has been obtained from electrophysiological single unit studies (Drager, 1975; Gordon & Stryker, 1996), cellular resolution calcium imaging (Mrsic-Flogel *et al.*, 2007), layer 4 VEP recordings (Sawtell *et al.*, 2003) and population level intrinsic signal imaging (Cang *et al.*, 2005; Hofer *et al.*, 2006).

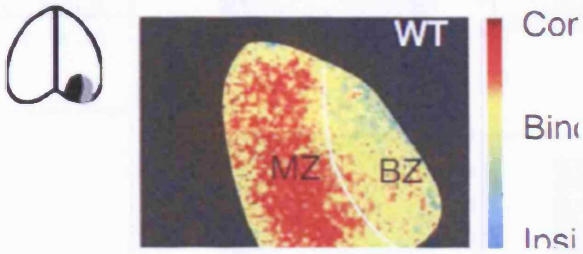

Figure 1.8 Intrinsic signal map of mouse V1 (from McCurry *et al.*, 2010)
To the left is the monocular zone (MZ) and to the right the binocular zone (BZ).

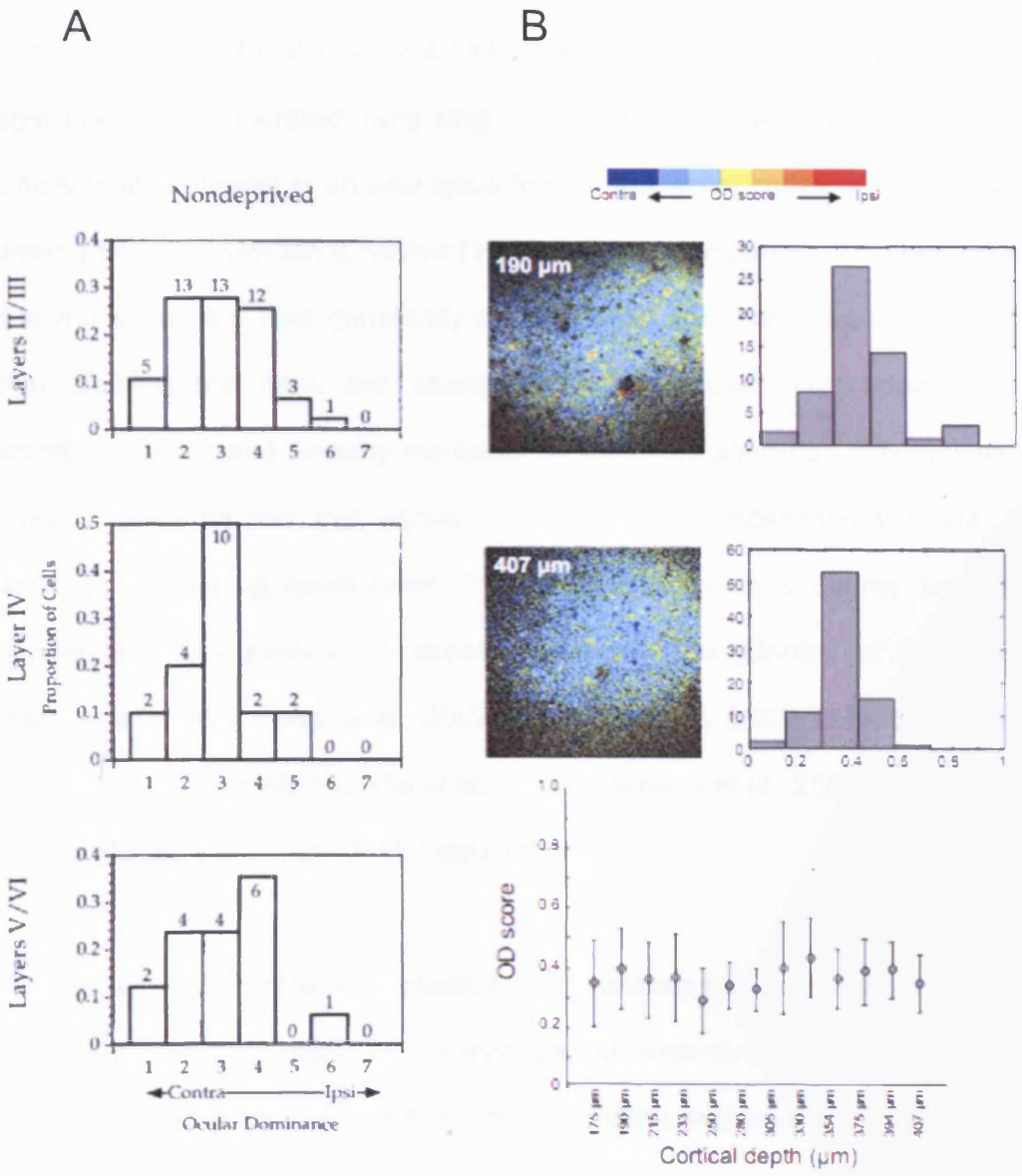

Figure 1.9 Laminar analysis of ocular dominance
A: Electrophysiologically determined OD distributions (adapted from Gordon & Stryker, 1996). Ocular dominance scale of 1-7 is that used by Hubel and Weisel (1962). B: OD distributions recorded by calcium imaging (from Mrsic-Flogel et al., 2007). OD score calculated by (Contra – Ipsi)/(Contra + Ipsi).

1.4.2 Ocular dominance plasticity in the mouse

As detailed in section 1.2 above, the phenomenon of ocular dominance plasticity was first described by Wiesel and Hubel in the developing cat cortex. Later Drager (1975) demonstrated using single unit recordings that ocular dominance plasticity is also present in an analogous form in the visual cortex of the mouse. Following this work Gordon & Stryker (1996), motivated in part by the emergence of the mouse as the best genetically characterised and manipulable mammal, further clarified the rules and characteristics of mouse ocular dominance plasticity. Genetic and sensory manipulation in combination has subsequently become a powerful tool that allows one to not only understand the role of experience in shaping development but additionally to some degree test the dependence of this process on specific gene products (Gordon *et al.*, 1996; Hensch *et al.*, 1998; Taha *et al.*, 2002a; Sawtell *et al.*, 2003; Taha & Stryker, 2005; Heimel *et al.*, 2008; Kaneko *et al.*, 2008a; Kaneko *et al.*, 2008b; Kaneko *et al.*, 2010; McCurry *et al.*, 2010; Morishita *et al.*, 2010).

As in the cat, ocular dominance plasticity in the mouse has been reported to be maximal during a brief postnatal sensitive period, extending in the mouse from postnatal day (P) 26 to P32 (Gordon & Stryker, 1996), with eye opening typically occurring at P10-13. During this critical period OD plasticity has been described as a two component process. First there is a reduction in responsiveness of the cortex to stimulation of the deprived eye which occurs within 1-3 days of eye closure (Frenkel & Bear, 2004b; Kaneko *et al.*, 2008a)(Figure 1.10A). Secondly after 5-7d MD there is an increase in responsiveness of the cortex to the non-

deprived eye and a small recovery of the deprived eye response which has been described as homeostatic (Frenkel & Bear, 2004b; Mrsic-Flogel *et al.*, 2007; Kaneko *et al.*, 2008b)(Figure 1.10B). As in the young cat, MD in mice results in a reduction in visual acuity although this impairment is considerably less severe than that observed in other species. The most comprehensive study of the degree of MD induced acuity impairment reported a reduction in the deprived eye acuity from 0.5 c/deg to 0.3 c/deg (Prusky & Douglas, 2003) (Figure 1.11). Similar degrees of plasticity have been reported using in vivo physiological methods during the critical period in the mouse cortex in both the primary thalamorecipient layer 4 and in layer 2/3 although they may occur by different molecular mechanisms (Gordon & Stryker, 1996; Frenkel & Bear, 2004; Cang *et al.*, 2005; Liu *et al.*, 2008). A recent imaging study has additionally provided an indication of what the stimulus for OD plasticity is by imaging cortical visual evoked responses through a closed eyelid revealing visually evoked activity but a loss of spatial information (Faguet *et al.*, 2009) (Figure 1.12).

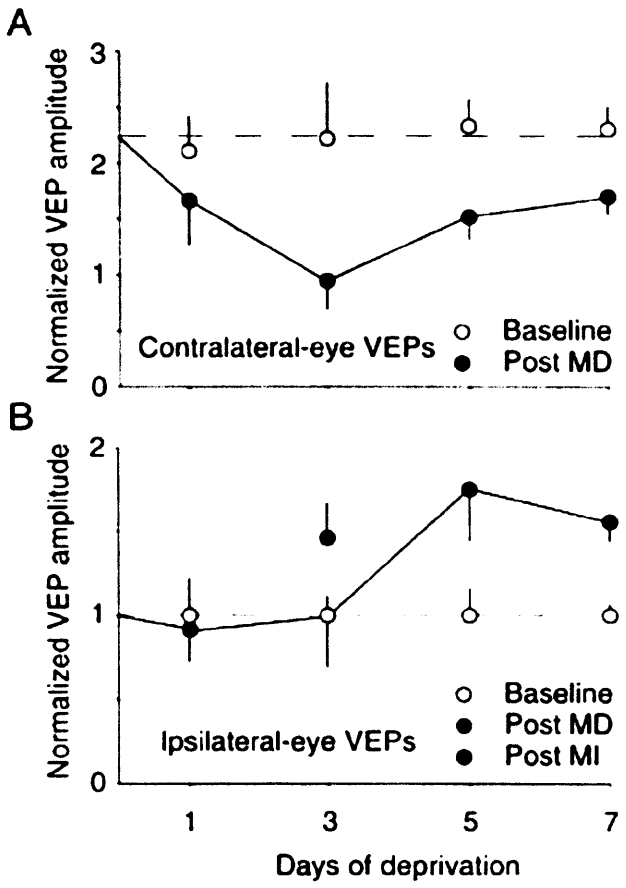

Figure 1.10 The effect of MD on L4 VEP magnitudes (adapted from Frenkel & Bear, 2004).
Cortical response to contralateral (A) and ipsi (B) eye stimulation after 1, 3 5 or 7 days of contralateral eye closure

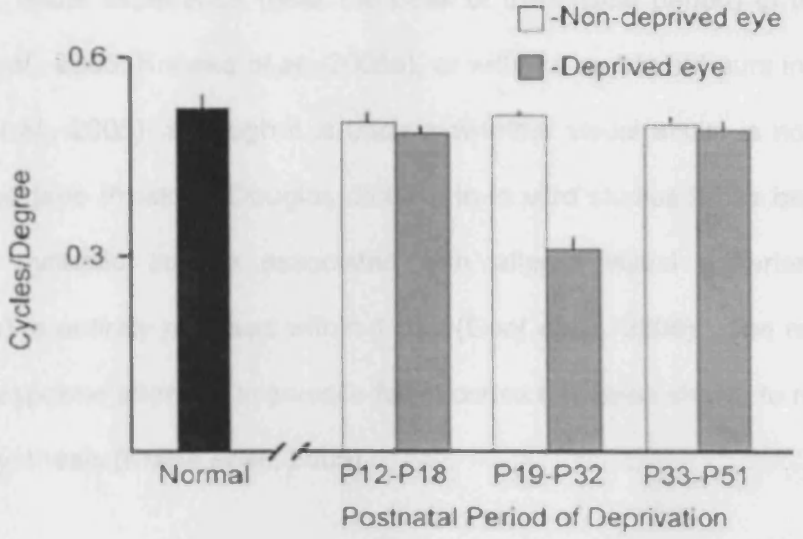

Figure 1.11 The effect of MD before, during and after the critical period on adult (P70-90) visual acuity (adapted from Prusky & Douglas, 2003).
Note that only MD during the critical period results in a long term reduction in impaired eye visual acuity.

A substantial capacity for OD plasticity is preserved into adulthood in the mouse with plasticity reported to still be present at P200 (Hofer *et al.*, 2006, although see Lehmann & Lowel, 2008). Adult plasticity induction requires 6-7 days of MD and has been consistently reported to be mediated by open eye potentiation (Sawtell *et al.*, 2003; Hofer *et al.*, 2006; Lehmann & Lowel, 2008; Sato & Stryker, 2008).

The mouse visual cortex also possesses a capacity for recovery of binocular responses during the critical period and adulthood after both critical period and adult monocular deprivation (Hofer *et al.*, 2006; Kaneko *et al.*, 2008a). Several studies have reported an apparent recovery of cortical responsiveness at the population level using intrinsic signal imaging after as little as 3 days of normal

binocular visual experience (near the peak of the critical period) in the mouse (Hofer *et al.*, 2006; Kaneko *et al.*, 2008a), or within a matter of hours in the ferret (Krahe *et al.*, 2005), although it is unclear whether visual acuity is normal after this period (see Prusky & Douglas, 2003). In in vitro studies it has been shown that the synaptic scaling associated with altered visual experience (dark exposure) is entirely reversed within 1 day (Goel *et al.*, 2006). The recovery of cortical response after MD in juvenile ferret cortex has been shown to not require protein synthesis (Krahe *et al.*, 2005).

Interestingly it has also been shown that having previous experience of ocular dominance plasticity and recovery facilitates subsequent episodes of ocular dominance plasticity (Hofer *et al.*, 2006, 2009). This was illustrated by comparing plasticity in either MD-naïve or MD-experienced adult mice. MD-naïve mice exhibited no OD shift after 3d monocular experience while MD-experienced mice exhibited a significant shift if the same eye that had previously been closed was deprived again. It has been proposed by Hofer et al. (2009) that this facilitation of adult plasticity occurs because structural changes from the first episode of monocular experience are conserved and provide a shortcut to plasticity during the second episode of monocular experience.

Longitudinal imaging of stretches of layer 5 cell dendrites has provided support for this idea in that the first and second episodes of monocular experience result in very different dendritic structural changes, even in age matched mice. The first episode of monocular experience results in a large increase in the density of

persistent new spines, while no such increase occurs during the second episode. There is also evidence that these new spines are being 'used' selectively during the second episode of MD as they increase in size, as reported by the integrated fluorescent brightness of thy1 driven GFP expression (Hofer *et al.*, 2009).

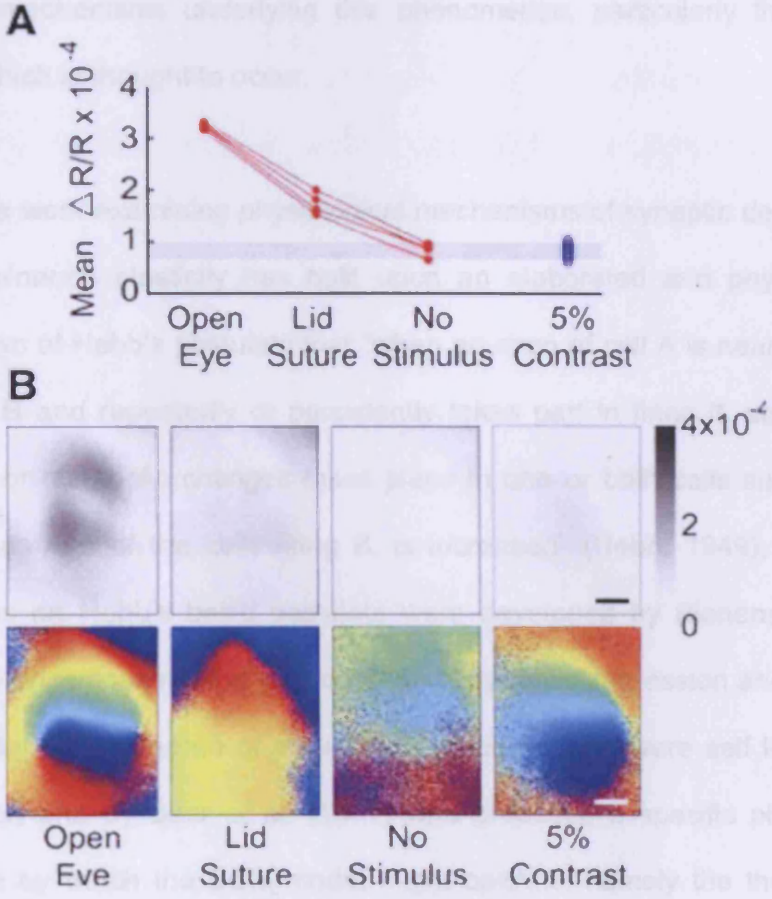

Figure 1.12 Intrinsic signal maps obtained through a closed eyelid. (adapted from Faguet *et al.*, 2009).
A: Intrinsic signal response magnitudes observed under various stimulation conditions within the same animal.
B: Response maps obtained under various stimulation conditions.

1.5 Synaptic models of ocular dominance plasticity in the rodent visual cortex

A large number of studies have explored the role that synaptic plasticity might play in mediating ocular dominance plasticity. The emergence of the mouse as a model of ocular dominance plasticity has prompted an exploration of the molecular mechanisms underlying this phenomenon, particularly the synaptic plasticity which is thought to occur.

Much of the work examining physiological mechanisms of synaptic depression in ocular dominance plasticity has built upon an elaborated and physiologically detailed form of Hebb's postulate that "when an axon of cell A is near enough to excite cell B and repeatedly or persistently takes part in firing it, some growth processes or metabolic changes takes place in one or both cells such that A's efficiency, as one of the cells firing B, is increased" (Hebb, 1949). Important elaborations on Hebb's basic postulate were developed by Bienenstock *et al.* (1982) who encompassed the phenomenon of synaptic depression and proposed a scheme by which degree of potentiation or depression were self limiting (the BCM model) and by Bear *et al.* (1987) who proposed a specific physiological mechanism by which the BCM model might operate, namely the then recently discovered NMDA receptor. In the BCM scheme, synaptic potentiation of a presynaptic input will occur if that input is active at a time when the postsynaptic cell is also active. Conversely if the presynaptic input arrives at a time of postsynaptic inactivity that input will be weakened. The level of activity required in the postsynaptic cell for potentiation to occur is referred to in the BCM scheme

as the modification threshold and is proposed to be dynamically modulated by the mean activity level of the cell (Bienenstock *et al.*, 1982). Bear *et al.* (1987) proposed that the recently discovered voltage gated nature of the NMDAR (Dingledine, 1983; Nowak *et al.*, 1984) may constitute a biological basis for the modification threshold and that the calcium influx following NMDAR activation may be a signal which indicates coincident pre- and postsynaptic activity and thus initiates plasticity processes. As empirical evidence accumulated it became apparent that the calcium signal may be graded and that modest calcium influxes may result in LTD while more substantial influxes result in LTP. Many studies have now empirically tested this idea.

Below I give an overview of relevant studies of both Hebbian like and non-Hebbian like synaptic plasticity in the rodent (mouse and rat) visual cortex which I have subdivided for the sake of clarity into phenomena which are considered to involve synaptic potentiation, synaptic depression and plasticity of inhibitory neurons.

1.5.1 Synaptic depression in the rodent visual cortex

An early description of electrically induced synaptic depression (LTD) in the rodent visual cortex was made by Kirkwood *et al.* (1993) using a stimulation protocol developed at the CA1 synapse by Dudek & Bear (1992). Depression of layer 3 field potentials was achieved by low frequency stimulation of layer 4 of the immature rat visual cortex and was shown to be NMDAR activation dependent by application of the NMDAR antagonist AP5. Additionally inhibition of protein

phosphatases 1 and 2a prevents this form of LTD suggesting that dephosphorylation might be an important step in the process of NMDAR dependent LTD (Kirkwood & Bear, 1994).

Further evidence has since accumulated supporting the idea that bidirectional alteration of the phosphorylation state of synaptic proteins is a significant mechanism of LTD and further that this mechanism might actually be recruited during OD plasticity. In the hippocampus inducing mass LTD by a "chemLTD" protocol (brief application of NMDA) results in a mass dephosphorylation of the Ser 845 site of the AMPAR subunit GluR1 as determined by antibodies which are specific to either the phosphorylated or dephosphorylated Ser 845 site (Lee *et al.*, 1998; Lee *et al.*, 2000)(see Figure 1.13). It was subsequently discovered that phosphorylation at the Ser 845 of GluR1 results in increased peak channel conductance and thus dephosphorylation might result in reduced peak channel conductance of the receptor (Banke *et al.*, 2000). That this dephosphorylation actually occurs in vivo was a relatively tractable problem in the visual cortex as after short MD a large number of synapses would be expected to contain GluR1 in the Ser 845 dephosphorylated state. This was found to be the case in rats by Heynen *et al* (2003) who showed that a 'molecular fingerprint' of low frequency stimulation (LFS) induced LTD, increased dephosphorylation of GluR1 at Ser 845, was present after 1d MD and additionally that a large reduction in surface AMPARs (both GluR1 and GluR2) could be observed. It has also been reported that V1 layer 2/3 LTD by low frequency stimulation is disrupted in mice lacking the GluR1 subunit (Iwai *et al.*, 2006). This idea is consistent with the impaired

depression reported in the somatosensory cortex of GluR1$^{-/-}$ mice after whisker deprivation (Wright *et al.*, 2008).

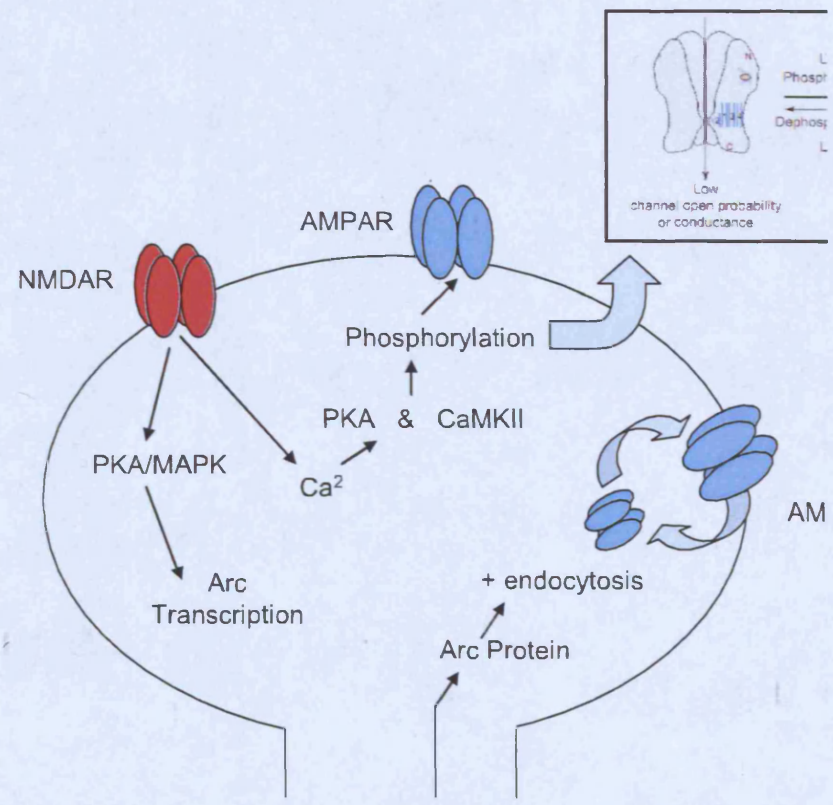

Figure 1.13 Pathways linking NMDAR activation to AMPAR mediated plasticity.

Additionally Heynen *et al* (2003) discovered that after 1d MD phosphorylation of GluR2 at Ser 880 was upregulated which some evidence suggests may increase likelihood of endocytosis of surface AMPARs receptors or internal retention of already internalised receptors (Chung *et al.*, 2000). The importance of GluR2 C-terminal interactions in receptor internalisation was directly tested by layer 4 viral

expression of a GluR2 C-terminal peptide which blocked OD plasticity in layer 4 but left plasticity in layer 2/3 intact (Yoon *et al.*, 2009). Recently it has also been shown that systemic treatment of critical period aged mice with the NMDAR antagonist CPP blocks closed eye depression after 4d MD although interpretation of this finding is complicated by the fact that this treatment reduces visual responsiveness of cortical neurons (Sato & Stryker, 2008).

As well as postsynaptic forms of synaptic plasticity, several studies have provided evidence that in layer 2/3 presynaptic forms of synaptic depression contribute to the loss of cortical responsiveness to a monocularly deprived eye. Crozier *et al.* (2007) provided evidence from slice recordings that LFS induced LTD proceeds by different mechanisms in layer 4 versus layer 2/3. LTD induction in L2/3 by LFS of layer 4 requires activation of cannabinoid receptors and does not require postsynaptic PKA activation, while the contrary is true of layer 4 LTD by white matter stimulation (Crozier *et al.*, 2007). Both forms of LTD are occluded by a period of monocular deprivation suggesting they both contribute to LTD normally. In vivo experiments further support the idea that laminar differences exist in cortical LTD mechanisms in that systemic application of the CB1 receptor antagonist AM251 blocks deprived eye depression in L2/3 but not in L4, although this work is complicated by the necessity of dissolving AM251 in DMSO which itself alters neuron firing rates (Liu *et al.*, 2008). This is consistent with anatomical observations that cannabinoid receptor expression is greater in L2/3 than L4 (Deshmukh *et al.*, 2007). Further observations which can be made of experiments in which depression is blocked specifically in layer 2/3

(Deshmukh *et al.*, 2007) or layer 4 (Yoon *et al.*, 2009) are that 1) OD plasticity in either layer 2/3 or layer 4 can occur independently of the other, and 2) that neither layer appears to have a determinative effect on the OD properties of the other.

Recently the importance in OD plasticity of the immediate early gene Arc (activity-regulated cytoskeletal associated protein) has been demonstrated using an $Arc^{-/-}$ mouse. Multiple forms of plasticity are disrupted in $Arc^{-/-}$ mice, amongst them depression of the closed eye response during OD plasticity (McCurry *et al.*, 2010). It is thought that Arc is an effector molecule that acts downstream of several convergent pathways to modulate AMPAR dynamics (Shepherd *et al.*, 2006; Waung *et al.*, 2008; McCurry *et al.*, 2010) (see Figure 1.13).

1.5.2 Synaptic potentiation in the rodent visual cortex

As described in section 1.4.2 longer periods (5-7d) of monocular deprivation result in potentiation of the open eye both in juvenile and adult mice. Two principle mechanisms have been proposed to account for spared eye potentiation; an LTP like process or homeostatic synaptic scaling.

Open eye potentiation by LTP

In the BCM scheme, reduced synaptic input due to deprived eye closure results in a reduction in the modification threshold for LTP. As a consequence the synapses relaying spared eye inputs, which have continued to transmit normally, become potentiated. There is ample evidence that LTP by theta burst stimulation

is possible in the visual cortex both in vitro (Kirkwood *et al.*, 1997) and in vivo (Heynen & Bear, 2001) and that following LTP induction cortical responses to visual stimulation are potentiated (Heynen & Bear, 2001; Cooke & Bear, 2010). There is also evidence that the ease with which LTP can be induced is increased by dark exposing animals before making brain slices (Kirkwood *et al.*, 1996). In the BCM framework, dark exposure reduces cortical firing rates resulting in a reduction in the LTP induction threshold. Potentiation of cortical responses can also be induced by exposure during wakefulness to a strong visual stimulus such as a contrast reversing grating (Frenkel *et al.*, 2006) and this form of plasticity is dependent upon interactions involving the C-terminal domain of GluR1 and occludes LTP (Cooke & Bear, 2010). There is no evidence however that an LTP like process occurs during ocular dominance plasticity. One of the earliest studies to explicitly test the LTP hypothesis used an αCaMKII knockout mouse which was known to have severe deficits in neocortical LTP (Gordon *et al.*, 1996). Around 50% of mice lacking αCaMKII were found to have a substantial deficit in OD plasticity while the other 50% appeared normal. The idea that CaMKII is required for LTP was further supported by the discovery that it directly phosphorylates the GluR1 AMPAR subunit which results in increased channel conductance (Lee *et al.*, 2000). This in part led to a further study examining mice possessing a mutated αCaMKII gene which was incapable of autophosphorylating, again only a partial plasticity deficit was observed (Taha *et al.*, 2002b). One caveat of these studies was that deprivations were possibly too short to see the maximum open eye potentiation which was more recently described to not be present until 5-6d MD (Frenkel & Bear, 2004a; Kaneko *et al.*,

2008b; McCurry *et al.*, 2010). The uncertainty of the dependence of visual cortex plasticity on CaMKII activity is in stark contrast to observations made of plasticity in mouse somatosensory cortex where a strong dependence on CaMKII auto phosphorylation has been reported (Glazewski *et al.*, 1996; Glazewski *et al.*, 2000). In contrast to studies examining the role of LTD in OD plasticity, no evidence of LTP occlusion has been described.

Open eye potentiation by homeostasis

Others have conceptualised open eye potentiation as a homeostatic response to reduced input to binocular neurons due to eye closure. This idea is supported by the otherwise paradoxical partial *closed eye* recovery that occurs after 5-6dMD (Frenkel & Bear, 2004a; Kaneko *et al.*, 2008b). In the homeostatic scheme synaptic gain at all synapses is increased in response to reduced neuronal activity, resulting in increased cortical responsiveness to both the deprived and spared eye.

In order for a homeostatic response to occur a mechanism for sensing neuronal activity levels is required. Broadly speaking two types of mechanism have been proposed. The first is cell autonomous whereby the each neuron is sensitive to it's own activity level and increases or decreases the weight of it's own synapses in order to keep it's firing rate within an optimum range. Another class of mechanism of homeostasis is non-cell autonomous and involves an extra-neuronal sensor which senses activity in it's vicinity and then signals to neurons to scale up or down their synaptic weights. Similarly multiple mechanisms of

effecting synaptic scaling have been proposed. Generally these converge upon modifications of AMPAR complement at synapses, although there is evidence that alteration of intrinsic neuronal excitability is another potential mechanism.

Homeostasis of neuronal excitability by synaptic scaling was first described in neuronal cultures where blockade of spiking activity results in scaling up of miniature excitatory post synaptic currents (mEPSCs), while acutely increasing activity by blocking inhibition results in scaling down of mEPSCs (Turrigiano *et al.*, 1998)(Figure 1.14). It was subsequently discovered that up-scaling could be induced in the intact brain by acute dark exposure and again measured ex-vivo in the form of mEPSC amplitude (Desai *et al.*, 2002). In rats, acute dark rearing for one week during the critical period results in synaptic scaling which is thought to be mediated by an increase in post synaptic density (PSD) GluR1 expression (Goel *et al.*, 2006).

Ex vivo measurements of neuronal excitability after monocular deprivation by eyelid closure or retinal inactivation by TTX, have yielded results which are more complex to interpret. Firstly studies have for the most part been limited to investigating synaptic scaling in the monocular cortex. This is because in the binocular area one would expect ambiguous results in that different degrees of synaptic scaling would be predicted depending upon the initial ocular dominance of each neuron. A second ambiguity arises due to the mixture of LTD like synaptic depression and homeostatic synaptic potentiation which occur even in the monocular area (Kaneko *et al.*, 2008b).

Reducing input to monocular cortex for two days by contralateral eye TTX injection in precritical period P14 mice results in synaptic scaling of mEPSCs in layer 4 star pyramid neurons, but not layer 2/3 pyramid neurons (Desai *et al.*, 2002). In contrast the same treatment at P23 results in mEPSC scaling in layer 2/3 but not in layer 4 indicating developmental regulation of the capacity for synaptic scaling which appears to progress through the cortical layers (Desai *et al.*, 2002).

Similarly 2d MD beginning at P14 results in an upscaling of spontaneous firing rates of layer 4 star pyramid neurons which is mediated by upscaling at excitatory synapses and downscaling at inhibitory synapses (Maffei *et al.*, 2004). Interestingly at the population level no homeostatic response has been observed in vivo in layer 4 after such a short period of MD although deprivations were begun in *in vivo* studies approximately two weeks later in development (Frenkel & Bear, 2004).

By P18 a 2d period of MD also results in an increase in spontaneous firing rates in layer 2/3 however paradoxically this occurs in parallel with a decrease in spontaneous excitatory currents and an increase in spontaneous inhibitory currents (Maffei & Turrigiano, 2008). The increased spontaneous firing rate in this case is explained by a change in the intrinsic excitability of neurons such that the action potential threshold is reduced (Desai *et al.*, 1999; Maffei & Turrigiano, 2008). Most recently it has been demonstrated that longer periods of MD (5-6d)

do result in scaling of mEPSCs in layer 2/3 of the binocular cortex (conference abstract, Lambo & Turrigiano, 2010).

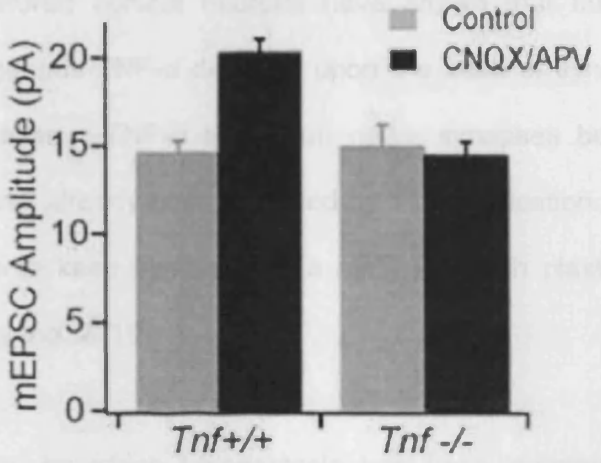

Figure 1.14 Synaptic scaling in organotypic cultured slices in response to CNQX and APV application is disrupted in mice lacking TNF- α (from Kaneko *et al.*, 2008b)

Other studies have attempted to measure and perturb homeostatic plasticity in vivo in response to MD. One proposed mechanism by which homeostatic plasticity may operate involves glial cells releasing the pro-inflammatory cytokine tumour-necrosis factor-alpha (TNF-α) in a manner which is modulated by local neuronal activity (Stellwagen & Malenka, 2006)(Figure 1.14). Application of TNF-α in neuronal cultures is known to increase surface expression of AMPARs and increase mEPSC amplitude (Beattie *et al.*, 2002; Kaneko *et al.*, 2008b; Steinmetz & Turrigiano, 2010). It has since been shown that disrupting the TNF-α signalling pathway, either by genetically deleting the gene which codes for TNF-α or by pharmacologically inhibiting endogenous TNF-α, specifically disrupts the open

eye potentiation observed after 5-6d MD (Kaneko *et al.*, 2008b). In contrast genetic deletion of TNF-α does not disrupt LTP induced by high frequency stimulation (Stellwagen & Malenka, 2006; Kaneko *et al.*, 2008b). Interestingly experiments in cultured cortical neurons have shown that the effect of the application of exogenous TNF-α depends upon the state of synaptic scaling at the time of application. TNF-α scales up naïve synapses but scales down synapses which have already been upscaled by TTX application. This suggests that TNF-α serves to keep synapses in a state in which plasticity can occur (Steinmetz & Turrigiano, 2010).

Another mechanism by which homeostasis has been proposed to occur at excitatory synapses involves activity dependent regulation of the immediate early gene Arc (or Arg3.1). Overexpression of high levels of Arc in neuronal cultures results in downscaling of synaptic strength by internalisation of AMPARs while genetic Arc knockout results in larger basal mEPSC amplitudes (Shepherd *et al.*, 2006). Arc induction has been proposed to be both the sensor and actuator of homeostatic plasticity and to work as a negative feedback system: activity induces Arc expression which reduces membrane AMPARs, while inactivity reduces Arc induction and promotes accumulation of membrane inserted AMPARs. This regulation of surface AMPAR expression is thought to be due to an interaction between Arc and the endocytotic machinery whereby Arc promotes endocytosis of AMPARs (Chowdhury *et al.*, 2006). Genetic knockout of Arc has been shown to have far reaching consequences for synaptic plasticity, indeed it has recently been described as a "master regulator of synaptic plasticity"

(Shepherd & Bear, 2011) and has been shown to be required for long-term memory formation in a range of animal behavioural tasks (Plath *et al.*, 2006). More recently Arc knockout has been shown to completely prevent spared eye potentiation during ocular dominance plasticity although it is unclear if this is due to a disruption of the previously hypothesised homeostatic mechanism (Shepherd *et al.*, 2006; McCurry *et al.*, 2010).

Increased postsynaptic expression of AMPA receptors has been associated with homeostatic plasticity in multiple studies (Goel *et al.*, 2006; Shepherd *et al.*, 2006; Hou *et al.*, 2008; Gainey *et al.*, 2009; Beique *et al.*, 2010). It appears specific subunits may have specific roles in mediating homeostasis at a more local versus more global scaling. Support for the importance of interactions involving GluR2 has been provided by inducing scaling in cultures with TTX and disrupting AMPAR subunit protein-protein interactions by expressing either GluR1 or GluR2 C-tail peptides. C-tail peptides disrupt protein-protein interactions in a dominant negative manner, occupying sites which normally interact with the endogenous receptor. Expression of GluR1-CT did not affect synaptic scaling while expression of GluR2-CT did (Gainey *et al.*, 2009). In contrast other studies have more locally disrupted presynaptic input to specific dendritic spines which also results in upscaling of local postsynaptic glutamate sensitivity and an insertion into the membrane of GluR2 lacking AMPARs. This local synaptic scaling was determined to be absent in mice lacking Arc (Hou *et al.*, 2008; Beique *et al.*, 2010). In agreement with the latter findings Goel et al

(2006) reported that 7d dark rearing resulted an increase in the ratio of GluR1 to GluR2 which was mediated entirely by increased expression PSD GluR1 levels.

Whatever the normal mechanism of open eye potentiation, Kaneko et al. *(2010)* found plasticity was accelerated in mice possessing a constitutively active form of H-ras , a protein known to be involved in activation of the ERC pathway. In these mice presynaptic release frequency was found to be lower at baseline, and in contrast to WT mice not to decrease after 3d MD (Kaneko *et al.*, 2010). The authors suggested that this may remove one step in the process of open eye potentiation (reduction in presynaptic release frequency) and thus accelerate plasticity in H-ras mice. It was additionally suggested that the lower basal presynaptic release frequency in H-ras mice allows more 'headroom' for presynaptic potentiation to occur.

The open eye potentiation which occurs in adult cortex after 6-7dMD has been less intensely studied. Current evidence suggests that disrupting NMDAR function either genetically by deletion of the NR1 NMDAR subunit (Sawtell *et al.*, 2003) or by systemic treatment with the NMDAR antagonist CPP (Sato & Stryker, 2008) abolishes adult OD plasticity. Additionally one study has shown an increased dependence on CaMKII in LTP induction in the aging visual cortex (Kirkwood *et al.*, 1997).

1.5.3 The role of inhibition in OD plasticity

Reducing production of the main inhibitory neurotransmitter in the brain, γ-aminobutyric acid (GABA) by genetic deletion of Gad65 prevents critical period ocular dominance plasticity while infusion of the GABA agonist benzodiazepine restores it (Hensch *et al.*, 1998). Similarly premature onset of the critical period can be induced by applying benzodiazepine at pre-critical period ages (Iwai *et al.*, 2003), and the effectiveness of this manipulation depends upon the modulation of the $GABA_A$ receptor α1 subunit (Fagiolini *et al.*, 2004).

These studies have prompted an interest in how the eye preference of inhibitory neurons is altered by MD. Recent advances have allowed recording of fluorescently labelled inhibitory neurons using calcium imaging (Ohki *et al.*, 2005). This has revealed that during MD inhibitory cells shift ocular dominance towards the open eye, but that this shift is delayed by ~2 days relative to excitatory cells (Gandhi *et al.*, 2008). In another study, in vivo intracellular recordings of fast spiking parvalbumin-positive large basket (FS) cells showed that in normal mice they can be driven equally well by input from either eye (Yazaki-Sugiyama *et al.*, 2009). Unexpectedly FS cells showed a shift to prefer the deprived eye after short MD, and subsequently a shift towards the open eye after longer MD. In the same study intracellular recordings from excitatory cells showed the expected initial contralateral bias which gradually reduced during the course of contralateral eye MD. Interestingly intracellular $GABA_A$ receptor blockade inverted the bias of deprived excitatory neurons. These findings together suggest that potentiation of excitatory deprived-eye synapses onto FS

cells may be one of the reasons for the OD shift away from the deprived eye after short MD (Yazaki-Sugiyama *et al.*, 2009).

1.6 The AMPA receptor

AMPA receptors are ligand gated ion channels named after their sensitivity to the synthetic glutamate analogue α-amino-3-hydroxyl-5-methyl-4-isoxazole-propionate which mediate the majority of fast excitatory transmission in the central nervous system (Dingledine *et al.*, 1999). Since much of the plasticity in the central nervous system is thought to occur as a result of alterations in the efficacy of transmission at excitatory synapses, modifications of synaptic AMPA receptor complement and constitution have been a major focus in studies of synaptic plasticity (Malenka & Nicoll, 1999). In previous sections I have described what is currently known about the role of AMPARs in ocular dominance plasticity. Here I will provide an overview of AMPAR function, composition and distribution in the cortex. As many studies described in this thesis make use of a GluR1 knockout mouse I will additionally detail what is known about the consequences during normal development of ablation of the GluR1 AMPAR subunit.

1.6.1 AMPAR structure

AMPA receptors are heteromeric tetrameric complexes made up of four homologous subunits GluR1-4 which combine in different stoichiometries to form functionally distinct receptors (Dingledine *et al.*, 1999)(Figure 1.15B). The

AMPAR subunits can be divided into those with or without long carboxyl-terminal (C-terminal) domains. The subunits GluR1, GluR4 and a splice variant of GluR2 (GluR2L) possess long cytoplasmic tails while GluR3 and a splice variant of GluR4 (GluR4S) have short cytoplasmic tails. The C-terminal tails determines in part how the receptors containing the subunits interact with other proteins such as scaffolding proteins and in what ways the channel kinetics can be post-translationally altered by phosphorylation (Song & Huganir, 2002). Long C-tailed subunit containing receptors (containing GluR1, GluR2L and GluR4) are driven into synapses during synaptic strengthening protocols such as LTP (Hayashi *et al.*, 2000; Shi *et al.*, 2001) and in response to sensory experience (Takahashi *et al.*, 2003), while receptors made up of short C-tailed subunits (containing GluR2 or GluR3) cycle in an activity independent manner in and out of the membrane and maintain synaptic transmission without altering synaptic strength (Luscher *et al.*, 1999; Shi *et al.*, 2001; Takahashi *et al.*, 2003; Zhu, 2009)

The typical subunit composition of an AMPAR varies between brain regions although in the most studied region, CA1 of the rodent hippocampus, around 80% of synaptic receptors are GluR1/GluR2 heteromers (Shepherd & Huganir, 2007; Lu *et al.*, 2009). The GluR2 subunit confers the important biophysical property of calcium impermeability upon the receptors into which it is incorporated and its presence is therefore crucial in

A

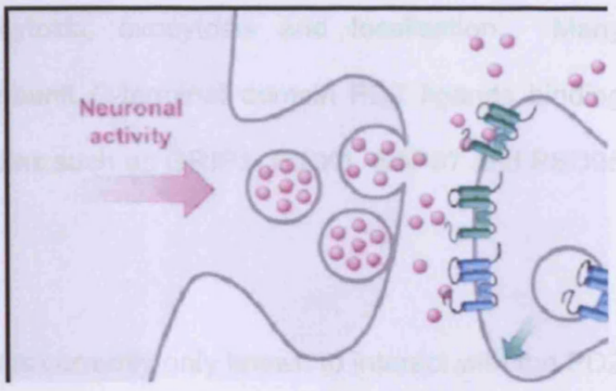

B

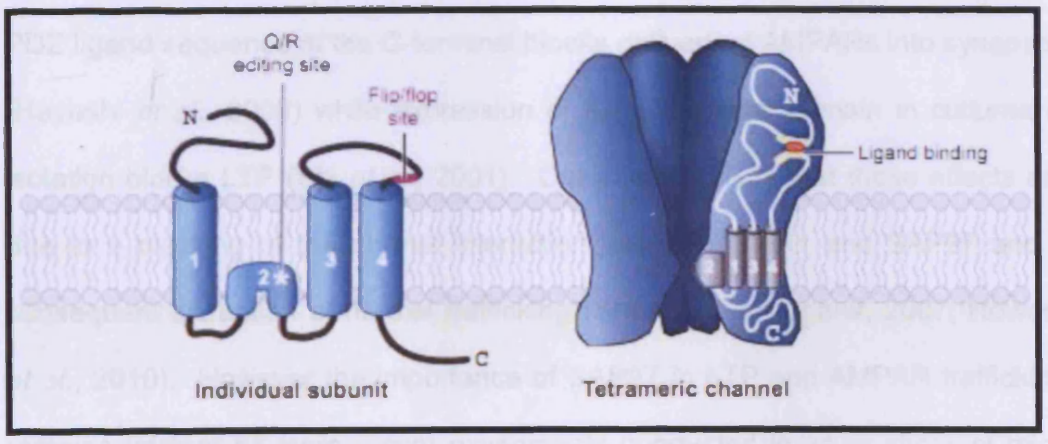

Figure 1.15 Schematics of an AMPAR containing synapse (adapted from Shepherd & Huganir, 2007).
A: Schematic of a synapse. B: Schematic of a tetrameric AMPAR channel.

preventing activation of calcium sensitive plasticity cascades. There is evidence that immediately following LTP induction, GluR2 lacking, calcium permeable

AMPARs are driven into the cell membrane and they may serve to consolidate LTP (Plant *et al.*, 2006).

The intracellular C-terminal domain of AMPARs interacts with many proteins in the process of receptor endocytosis, exocytosis and localisation. Many interactions occur via AMPAR subunit C-terminal domain PDZ ligands binding with PDZ domain containing proteins such as GRIP1, PICK1, SAP97 and PSD95 (Song & Huganir, 2002).

The GluR1 subunit's PDZ domain is currently only known to interact with the PDZ containing synapse associated protein SAP97 (Shepherd & Huganir, 2007). Expression in organotypic slice cultures of GluR1 containing a mutation of the PDZ ligand sequence of the C-terminal blocks delivery of AMPARs into synapses (Hayashi *et al.*, 2000) while expression of the C-terminal domain in cultures in isolation blocks LTP (Shi *et al.*, 2001). One hypothesis is that these effects are due to a blocking of the normal interaction between GluR1 and SAP97 and a subsequent disruption of normal trafficking (Shepherd & Huganir, 2007; Howard *et al.*, 2010). However the importance of SAP97 in LTP and AMPAR trafficking remains unclear as more recent experiments conducted in acute slices of mice carrying a modified PDZ domain lacking GluR1 receptor have found no baseline or LTP/LTD deficits in these animals (Kim *et al.*, 2005).

GRIP1 contains 7 PDZ domains and binds specifically to GluR2, GluR3 and GluR4c – the multiple PDZ domains are thought to promote association of the

AMPAR subunits with other anchored proteins (Dong *et al.*, 1997). Specific disruption of the GluR2 GRIP PDZ ligand disrupts synaptic accumulation of GluR2 containing receptors suggesting a role of GRIP1 in cytoskeletal anchoring of receptors (Song & Huganir, 2002). Overexpression of another PDZ domain containing protein, PICK1, results in reduced surface expression of GluR2 containing receptors, indicating a role for PICK1 in receptor internalization (Perez *et al.*, 2001). The GluR2 C-terminus also binds to N-ethylmaleimide-sensitive fusion protein (NSF) which is reported to positively regulate exocytosis of receptors (Beretta *et al.*, 2005).

1.6.2 Synaptic specificity of AMPAR subunit trafficking

A number of studies have sought to determine which AMPAR subunits are trafficked to which synapses in sensory circuits. Two key studies examined AMPAR trafficking at thalamocortical, intracortical, corticogeniculate and retinogeniculate synapses (Kielland *et al.*, 2009; Zhu, 2009). Thalamocortical synapses on layer 4 stellate neurons were found to generate faster synaptic responses than intracortical synapses and to have GluR4 containing receptors more heavily trafficked into them in a manner dependent upon spontaneous synaptic activity (Zhu, 2009). In contrast, layer 4 stellate neuron's intracortical synapses have GluR1 containing receptors selectively trafficked into them in a manner dependent upon sensory experience (Zhu, 2009). GluR2 containing receptors were trafficked into both types of synapse and, consistent with previous reports, in a sensory activity-independent manner (Shi *et al.*, 2001; Takahashi *et al.*, 2003; Zhu, 2009). Synaptic incorporation of GluR1 was also

examined at retinogeniculate vs. corticogeniculate synapses onto the same thalamic relay cells, where GluR1 was found to be selectively recruited at retinogeniculate synapses over corticogeniculate synapses (Kielland *et al.*, 2009).

1.6.3 AMPARs in spine growth and stabilization

As well as their function in altering synaptic efficacy, there is evidence that AMPARs have a permissive role in stabilisation of structural changes to dendrites (Lamprecht & LeDoux, 2004; Kopec *et al.*, 2007). Dendritic spines initially appear as thin protrusions without synapses, and persistence of newly formed spines is associated with the presence of synapses and spine volume enlargement (Holtmaat *et al.*, 2005; Knott *et al.*, 2006). Similarly, induction of chemical LTP, a protocol which produces LTP at a majority of synapses, results first in spine volume increases followed by increased surface expression of AMPARs (Kopec *et al.*, 2006). The increased surface expression of AMPARs which follows dendritic spine enlargement is largely due to increased exocytosis of GluR1 containing receptors (Kopec *et al.*, 2006). It seems that membrane incorporation of GluR1 containing AMPARs is not however sufficient in itself to drive spine enlargement – an LTP like stimulus is also required – although expression of a GluR1-C-tail peptide in combination with an LTP stimulus is sufficient to permit spine enlargement (Kopec *et al.*, 2007). This indicates that the ion channel function of GluR1 is not critical to stabilising spines and has prompted the hypothesis that instead the C-terminus of GluR1 serves a stabilising function through interactions with other proteins (Kopec *et al.*, 2007).

Further evidence for the idea of a stabilising role of GluR1 in new spine formation has come from behavioural studies which examined mice which carried a mutation of the PKA and CaMKII phosphorylation sites of GluR1 (Esteban *et al.*, 2003). This mutation results in normal task learning, but impaired task retention suggesting a deficit in the process of long-term consolidation of memories, a mechanism which is hypothesised to in part depend upon formation and stabilisation of new spines (Esteban *et al.*, 2003; Lee *et al.*, 2003; Lamprecht & LeDoux, 2004).

1.6.4 AMPAR receptor function in the absence of the GluR1 subunit

Many of the experiments described in this thesis make use of a previously generated mutant mouse which possesses a germline knockout of the GRIA1 gene which codes for the GluR1 (also referred to in the literature as GluRA and GluA1) AMPAR subunit (Zamanillo *et al.*, 1999). Next I will describe what is known about AMPAR function in the absence of GluR1.

In the GluR1 lacking mouse there is no evidence of upregulation of other AMPAR subunits at the protein level (Zamanillo *et al.*, 1999) or the mRNA level (Wright *et al.*, 2008) in basal conditions. Although it is known that GluR2 homomers can form in the absence of other subunits, and that GluR2 also forms heteromers with GluR3 (Lu *et al.*, 2009), some evidence suggests disrupted dendritic targeting of GluR2 containing AMPARs in GluR1$^{-/-}$ mice in the hippocampus (Zamanillo *et al.*, 1999). This was indicated by increased somatic GluR2 localisation and decreased dendritic localisation.

Investigations of the normality of AMPAR mediated currents in GluR1$^{-/-}$ mice have produced conflicting results. One consistent finding is that GluR1$^{-/-}$ mice exhibit a dramatic reduction in CA1 cells' somatic AMPAR mediated currents (extrasynaptic currents) with reductions of approximately 95% reported (Zamanillo *et al.*, 1999; Andrasfalvy *et al.*, 2003; Jensen *et al.*, 2003). In contrast synaptic currents measured by fEPSP recordings in GluR1$^{-/-}$ mice were initially reported to be normal as were tetanic stimulation evoked dendritic calcium influxes suggesting that this element of the signalling cascade for LTP is functional (Zamanillo *et al.*, 1999). These findings are consistent with Phillips *et al.* (2008) who observed no baseline differences in fEPSP slope in 8-9 week old GluR1$^{-/-}$ mice relative to WTs and Wright *et al.* (2008) who observed normal spiking rates in vivo in somatosensory cortex in response to whisker stimulation in GluR1$^{-/-}$ mice. However other studies have reported that the ratio of synaptic AMPAR to NMDAR currents rises during development in WT but not GluR1$^{-/-}$ mice (Jensen *et al.*, 2003) and that the fEPSC magnitude is significantly reduced in adult GluR1$^{-/-}$ mice relative to WTs (Romberg *et al.*, 2009), indicating a deficit in synaptic efficacy in GluR1$^{-/-}$ mice. GluR1$^{-/-}$ mice have also been shown to have impaired distance dependent scaling of synaptic currents; in WT mice mEPSC amplitude increases as a function of distance from the soma (Smith *et al.*, 2003) whereas no significant distance dependent scaling was observed in GluR1$^{-/-}$ mice (Andrasfalvy *et al.*, 2003).

Only a very limited published analysis has been conducted of dendritic spine morphology in GluR1$^{-/-}$ mice which found no differences in dendritic spine density of CA1 pyramidal neurons (Zamanillo *et al.*, 1999). However preliminary observations from our own laboratory have suggested a phenotype of abnormal spine morphology may exist in the mature somatosensory cortex of GluR1$^{-/-}$ mice.

1.7 Aims of this study

The aim of this study is to examine the extent to which specific plasticity phenomena which have been described in vitro are utilised in the living brain in vivo during experience dependent development and adult plasticity of cortical circuits. I have done this by asking the simple question of whether manipulations which are known to disrupt plasticity in vitro also disrupt well characterised developmental plasticity phenomena in the visual cortex in vivo. The present studies use the mouse visual system as a model and examine ocular dominance plasticity and retinotopic map refinement using in vivo functional imaging, in vivo electrophysiology, and ex vivo electrophysiology.

Chapters 3 to 5 examine the importance of interactions involving the AMPAR subunit GluR1 in various in vivo visual cortex plasticity events in both the juvenile and adult brain. Chapter 3 includes experiments which probe the normality of baseline visual responses in GluR1$^{-/-}$ mice relative to their WT littermates. This includes measurements of retinotopic map scatter, cortical response magnitudes and ocular dominance. Additionally in this chapter the intrinsic signal methodology of assessing map organisation in mice is examined. In Chapter 4 the importance of interactions involving GluR1 in critical period ocular dominance plasticity is explored. This includes analysis of GluR1's role in deprived eye depression and open eye homeostatic potentiation. In Chapter 5 the role of GluR1 in a number of adult plasticity phenomena is tested. These include

monocular deprivation induced spared eye potentiation, recovery after MD and facilitation of plasticity due to prior experience.

Chapter 6 explores a dramatic homeostatic plasticity deficit which was serendipitously discovered in a commonly used C57BL/6J mouse strain (C57BL/6JOlaHsd) during the course of other experiments in this thesis. This discovery permits the probing of a mechanistic link between homeostatic plasticity described during monocular deprivation and synaptic scaling described in response to acute dark exposure. It also allows some examination of the degree of similarity of mechanisms of adult and juvenile plasticity.

A brief summary of key findings is presented at the end of each experimental chapter and an in depth discussion of all results is presented in Chapter 7.

Chapter 2. Materials and methods

2.1 Animals

All surgical procedures were performed in accordance with the UK Animals (Scientific Procedures) Act 1986. Specific details of animals used are provided in the methods section at the start of each results chapter.

2.2 Intrinsic signal imaging

Optical imaging of intrinsic signals (OI) was pioneered as a means by which to map on a gross scale regions of cortex which respond to a specific stimuli (Grinvald *et al.*, 1986). The technique is based upon the principle that a decrease in light reflectance is observable in active regions of cortex which correlates well with the electrical signal measurable using voltage sensitive dyes (Grinvald *et al.*, 1986). The three major causes of variation in light reflected by the cortex and consequently sources of intrinsic optical signals are thought to be 1) changes in blood volume, 2) changes in concentration of deoxy-hemoglobin vs. oxy-haemoglobin molecules and 3) changes in the light scattering properties of the tissue (Zepeda *et al.*, 2004). Varying the wavelength of tissue illumination results in intrinsic signals of different origins. For example illuminating at 570nm (an isosbestic wavelength for oxy/deoxy-haemoglobin, that is a wavelength at which both molecules are equally absorbent) results in a relatively non-spatially specific signal dominated by changes in blood volume (Frostig *et al.*, 1990). In contrast illuminating at longer wavelengths such as that employed in this study (700nm) results in a signal which is shorter latency, more transient, more

spatially specific, and thought to reflect blood oxygenation state as well as changes in light scattering (Frostig *et al.*, 1990., see Figure 2.1).

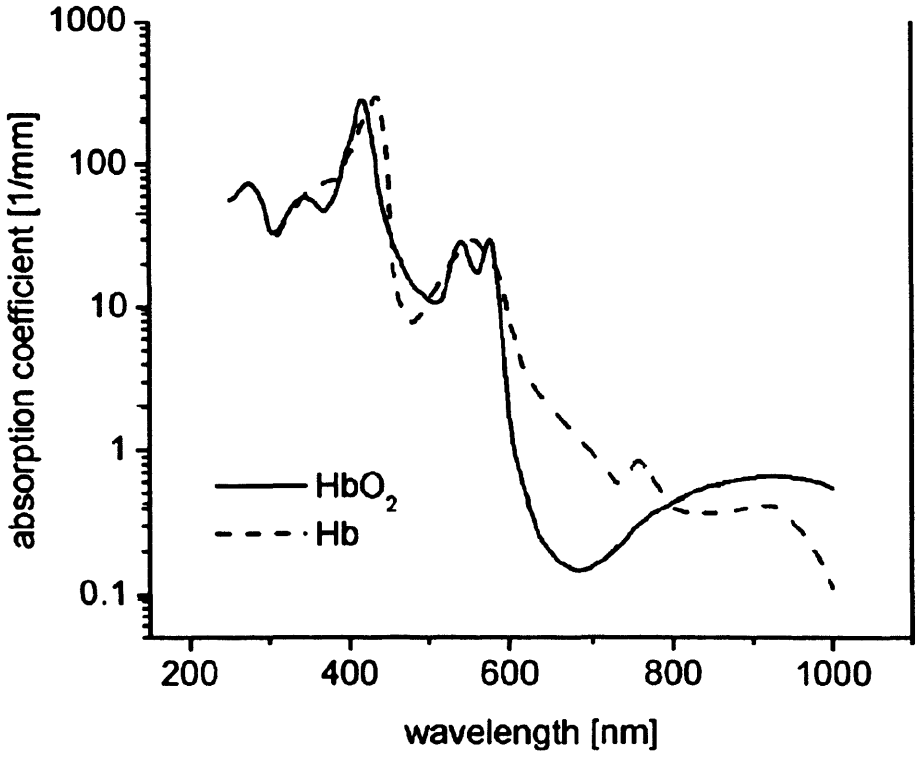

Figure 2.1 Absorption spectra of Hb and HbO2 (adapted from Faber *et al.*, 2003)
The absorption spectra of Hb and HbO_2, note the difference in absorption at 700nm

The optical imaging methodology has been used extensively to map cortical sensory areas and subsequently to measure development and plasticity of these sensory areas (Zepeda *et al.*, 2004). In the case of the visual cortex, structures observable in many higher mammals such as ocular dominance and orientation columns have been imaged during development in order to understand the role

of nature (i.e. genetic factors) vs. nurture (i.e. visual experience) in the formation of mature visual cortex circuits (Godecke & Bonhoeffer, 1996; Crair *et al.*, 1998; Sengpiel *et al.*, 1998).

More recently the focus has shifted towards investigation of the molecular mechanisms by which experience alters the physiology of the brain. This has resulted in a large number of studies of the mouse visual system due largely to the fact that the mouse is the best genetically described and currently the most genetically manipulable mammal (Gordon *et al.*, 1996; Hensch *et al.*, 1998; Taha *et al.*, 2002a; Sawtell *et al.*, 2003; Taha & Stryker, 2005; Heimel *et al.*, 2008; Kaneko *et al.*, 2008a; Kaneko *et al.*, 2008b; Kaneko *et al.*, 2010; McCurry *et al.*, 2010; Morishita *et al.*, 2010). In higher mammals such as cats and monkeys ocular dominance plasticity can be examined by quantifying alterations in ocular dominance column territory dominated by either eye. In contrast in the mouse binocular visual cortex does not possess distinct clusters of contra/ipsi eye domains and is instead made up of a relatively noncompartmentalised collection of cells of varying responsiveness to left and right eye, commonly referred to as a salt and pepper distribution (see the overview of mouse visual cortex in chapter 1 and Mrsic-Flogel *et al.*, 2007). For this reason the ratio of responsiveness of a patch of the binocular region as a whole to left eye versus right eye stimulation has been used as a measure of ocular dominance shift (Cang *et al.*, 2005a; Heimel *et al.*, 2007). This has additionally allowed an absolute magnitude of response to be calculated and consequently a teasing apart of potentiation of

spared eye from the depression of deprived eye response (Cang *et al.*, 2005a; Hofer *et al.*, 2006; Heimel *et al.*, 2007). Additionally the non-clustered nature of mouse visual cortex neuron receptive field properties results in a smooth progression of retinotopy across the approximately 3x3mm^2 of V1.

2.3 General surgical preparation for imaging

Mice were first sedated with Chlorprothixene (Sigma, 1mg/kg, i.m.) after which anaesthesia was induced with 3-4% Isoflurane in oxygen in an induction chamber. Mice were then placed on a homeostatic heating blanket (Harvard Apparatus, UK) and secured in a custom made stereotaxic frame. Anaesthesia was maintained during surgery with 1.8-2% Isoflurane in oxygen administered via a nose cone, and reduced to 0.8-1.1% during imaging. Depth of anaesthesia was continually assessed by monitoring heart rate (maintained in the range 350-550 bpm) and hind limb withdrawal reflex. The eyes were next protected with an eye cream (Isoptomax) and a local anaesthetic was administered subcutaneously to the scalp. The scalp and periosteum was then resected above the visual cortex and the skull was cleared of connective tissue and covered with a 2% agarose solution and sealed with a 10mm diameter glass coverslip.

2.4 General description of imaging apparatus

Intrinsic signal imaging was carried out using an Imager 3001 imaging system (Optical Imaging Inc, Mountainside, NJ) with the CCD camera focussed ~200um

below the cortical surface. A macroscope tandem lens was used, constructed from two front to front photographic lenses (50mm, f1.2). This arrangement provides a high numerical aperture and a low depth of field resulting in a blurring of large cortical blood vessels when focussed below the surface thus a minimisation of the image artefacts associated with them. During acquisition of cortical surface vasculature maps, the brain was illuminated via fibre optic light guides with green light of wavelength 546nmn generated by a halogen light box, using a band pass interference filter. This maximised the contrast of blood vessels as haemoglobin is highly absorbent of light of this wavelength. During intrinsic signal acquisition the cortex was illuminated via fibre optic light guides with red light of wave length 700nm which was filtered upon leaving the halogen light box. Incident light reflected by the cortex was then further filtered prior to entering the objective by a 700nm±30nm bandpass filter, in order to prevent stray light in the room (in particular from the stimulus monitor) reaching the camera. Video frames are captured by a CCD camera at a rate of 25Hz (40.3 ms/frame). The video frames are then temporally binned in software such that a typical data frame represents 120.9ms. The CCD camera acquires images at a spatial resolution of 748x572 pixels which are then down sampled in software to a resolution of 250x191 pixels. After down sampling a single pixel represents 20um x 20um.

2.5 Episodic intrinsic signal imaging paradigm

Episodic imaging was the first paradigm developed to measure intrinsic signals in the visual cortex (Grinvald et al., 1986). In this scheme an activity map is generated by first collecting an image of the 'inactive' cortex in response to a blank stimulus and subsequently an image of the 'active' cortex during visual stimulation. The active image is then divided by the inactive image resulting in a map in which pixel values which deviate from 1 indicate a difference between the maps and thus neuronal activity in the area of cortex to which the pixels corresponds (see Figure 2.3).

2.6 Periodic intrinsic signal imaging paradigm

An alternative paradigm of intrinsic signal imaging was developed by Kalatsky and Stryker (2003) whereby the visual system is presented periodically with a stimulus at a specific temporal frequency thus generating a periodic pattern of cortical activation (see Figure 2.4B) which can be extracted by transforming the signal from the time to the frequency domain by Fourier decomposition (Figure 2.6A). If the stimulus is suitably designed a periodic intrinsic optical signal can be recorded and extracted at the frequency of stimulation. In the experiments described we followed Kalatsky and Styker (2003) in using a stimulus with a temporal repetition period of 8 seconds, thus stimulating at 0.125Hz. For the most part the stimulus consisted of a white horizontal bar of diameter one degree and width 30-60 degrees drifting vertically on a black background with a period of 8 seconds (see Figure 2.2A). The signal was acquired at a rate of 8.33Hz.

2.7 Quantification of intrinsic signal ocular dominance

Ocular dominance was quantified in a similar manner for maps collected using both the episodic and periodic imaging paradigms. Firstly two maps were produced by the procedures described above, having stimulated the binocular area of the visual cortex by presenting a visual stimulus to either the contralateral or ipsilateral eye (Figure 2.7A and B). Stimuli were generated using a VSG5 (Cambridge Research Systems, UK) and presented to either eye in isolation with the aid of computer controlled eye shutters (custom build in house). Having obtained activity maps, a region of interest (ROI) was determined by thresholding the ipsilateral map at 60% of the maximum ipsilateral pixel value (Figure 2.7C). The average pixel value was then calculated within this ROI of both the ipsilateral and contralateral maps (Figure 2.7C). This average pixel value provided an absolute measure of cortical response to contralateral and ipsilateral eye stimulation. In addition an ocular dominance index (ODI) was calculated using the formula:

ODI = (Contralateral – Ipsilateral)/(Contralateral + Ipsilateral)

2.8 Quantification of intrinsic signal map scatter

The periodic imaging paradigm has been used as a means by which to measure the degree of organisation of retinotopic cortical maps (Smith & Trachtenberg,

2007). The principal of this analysis is that in a well organised map one should observe a spatially smooth progression of phase values. The phase value of each pixel is thus compared with the phase values of its closest neighbours and the degree of discrepancy calculated.

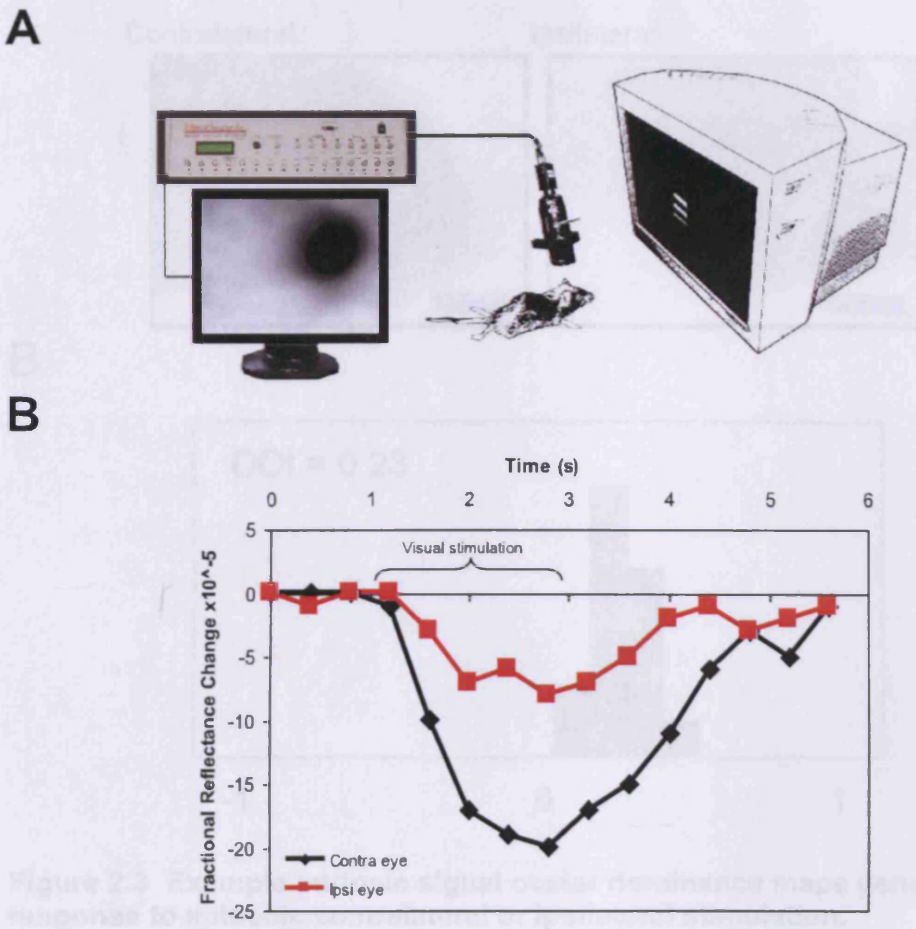

Figure 2.2 Imaging of intrinsic signals in the visual cortex using episodic stimulation paradigm.
A: Schematic of recording setup.
B: Example of the signal observed in the activated area of visual cortex in response to contralateral versus ipsilateral eye stimulation.

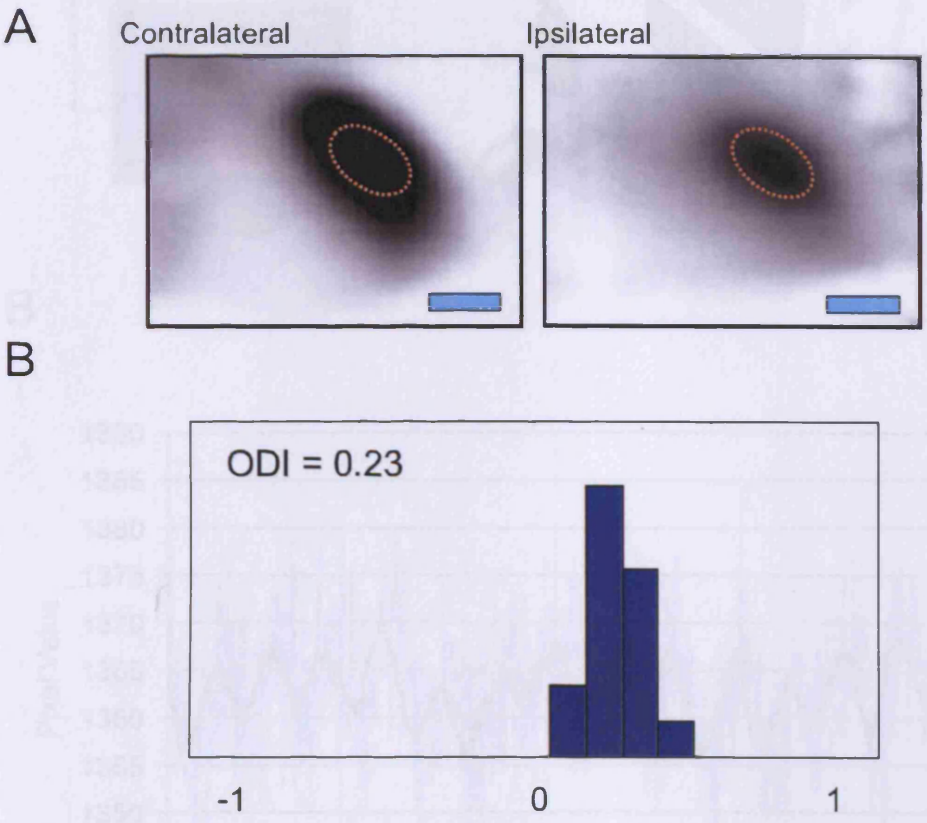

Figure 2.3 Example intrinsic signal ocular dominance maps generated in response to episodic contralateral or ipsilateral stimulation.
A: Magnitude maps of response to contralateral (left) or ipsilateral (right) eye stimulation using a 30x30 degree drifting grating.
B: Histogram of ocular dominance scores of each pixel in the above 60% threshold active area of the visual cortex indicated by orange dotted line in A. Scale bar 500μm.

A

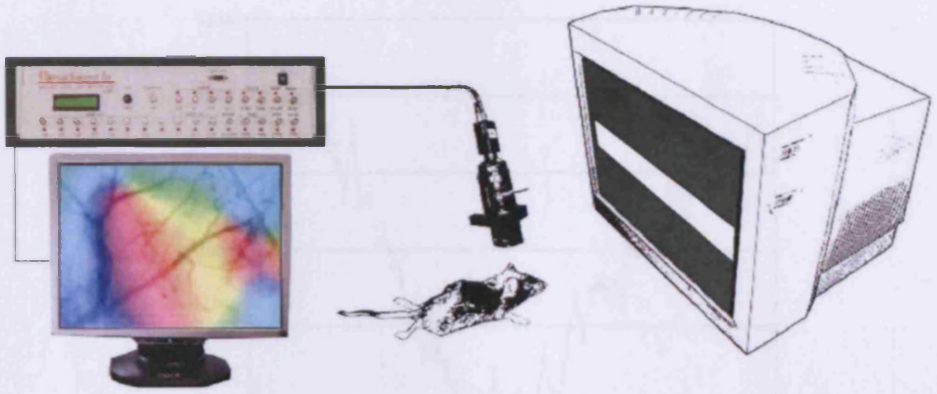

B

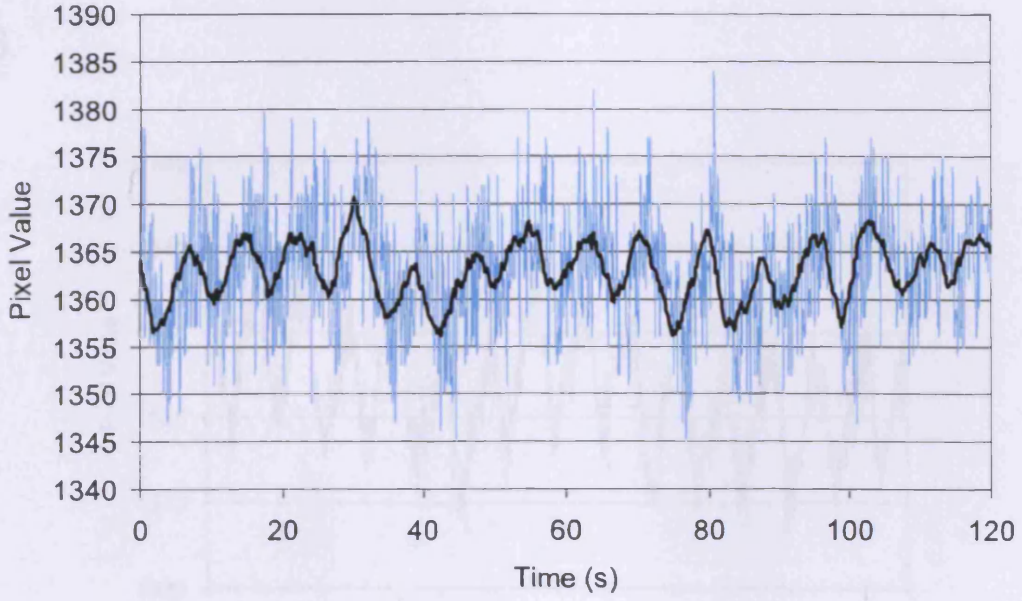

Figure 2.4 Imaging of intrinsic signals in the visual cortex using a periodic stimulation paradigm.
A: Schematic of intrinsic signal recording setup.
B: Example of the raw signal observed for one pixel (light blue) and 20 data point (2.3 sec) moving average, note 8 sec periodicity.

A

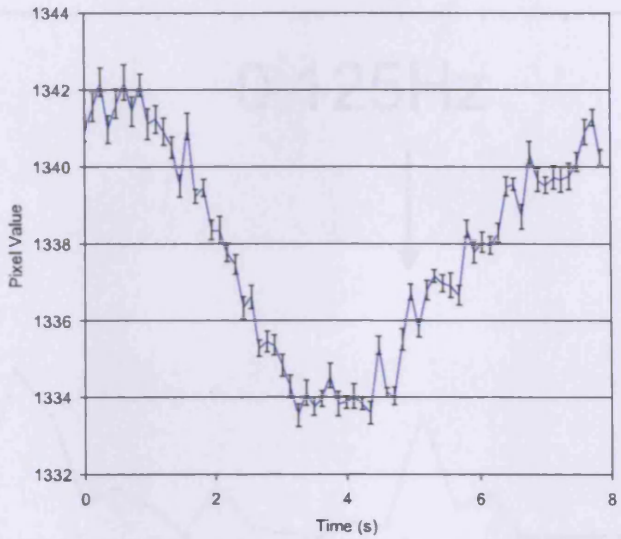

B

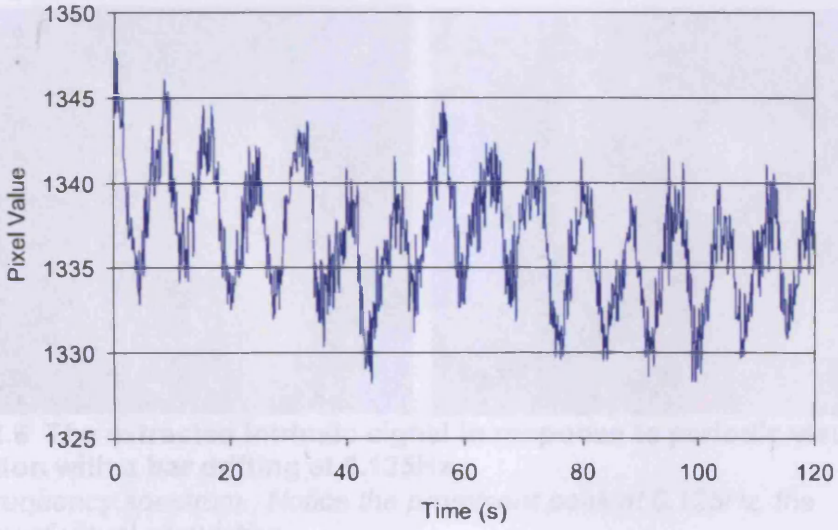

Figure 2.5 The cyclical signal elicited by a periodic stimulus.
A: Example average of 20 single 8 sec cycles of intrinsic signal.
B: Example averaged time course of 25 neighbouring pixels (a 5x5 bin) with similar phase values over one 120 sec block of periodic stimulation.

A

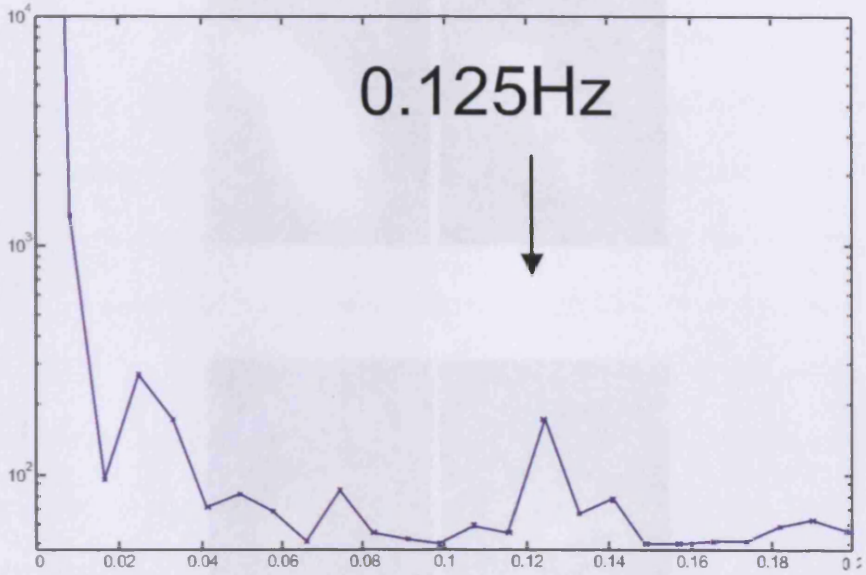

B

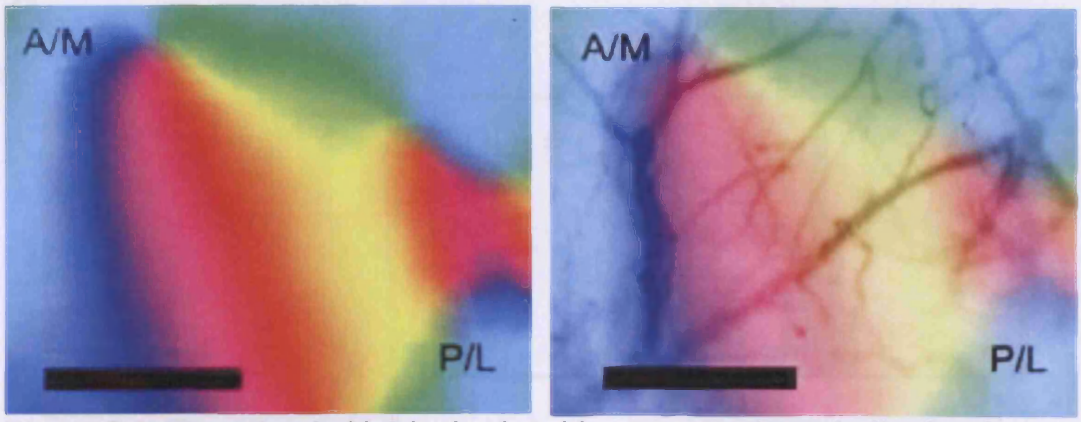

Figure 2.6 The extracted intrinsic signal in response to periodic visual stimulation with a bar drifting at 0.125Hz.
A: The frequency spectrum. Notice the prominent peak at 0.125Hz, the frequency of visual stimulation.
B: Lowpass filtered phase maps of extracted intrinsic signal retinotopic map and the same map overlaid on cortical surface vasculature map. Note the inversion of direction of phase transition to the right of the map in the V2 area.
Scale bar = 1mm. A/M, anterior medial; P/L, posterior lateral.

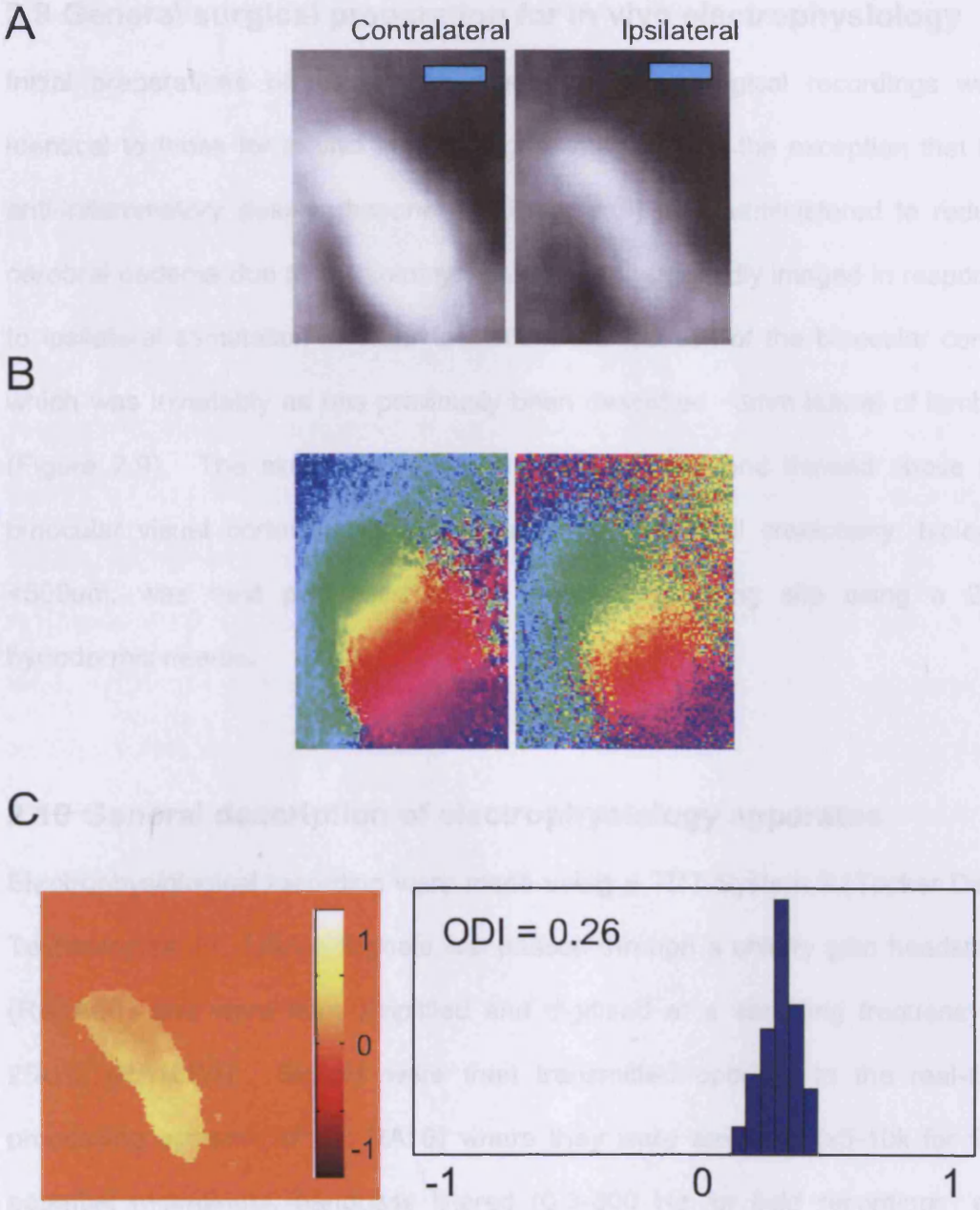

Figure 2.7 Example intrinsic signal ocular dominance maps generated in response to periodic contralateral or ipsilateral stimulation.
A, B: Magnitude and phase maps respectively of response to contralateral (left) or ipsilateral (right) eye stimulation. C: Spatial map and histogram of ocular dominance scores of each pixel in the above 60% active threshold. Scale bar 500μm.

2.9 General surgical preparation for in vivo electrophysiology

Initial preparations of mice for in vivo electrophysiological recordings were identical to those for in vivo intrinsic signal imaging with the exception that the anti-inflammatory dexamethasone (0.05 mg, s.c.) was administered to reduce cerebral oedema due to craniotomy. Mice were then rapidly imaged in response to ipsilateral stimulation in order to confirm the location of the binocular cortex which was invariably as has previously been described ~3mm lateral of lambda (Figure 2.9). The skull was then cleared of agarose and thinned above the binocular visual cortex using a surgical blade. A small craniotomy, typically <500um, was next performed at the desired recording site using a 24G hypodermic needle.

2.10 General description of electrophysiology apparatus

Electrophysiological recording were made using a TDT System 3 (Tucker Davis Technologies, FL, USA). Signals first passed through a unitary gain headstage (RA4AC1) and were then amplified and digitised at a sampling frequency of 25kHz (RA16PA). Signals were then transmitted optically to the real-time processing system (RP2.1, RA16) where they were amplified (x5-10k for field potential recordings), bandpass filtered (0.3-300 Hz for field recordings) and notch filtered at 50 Hz using a program designed in RPvdsEx (also Tucker Davis Technologies, FL, USA). The signal was then relayed onwards to a desktop PC running Brainware v9.07 (also Tucker Davis Technologies, FL, USA) which recorded at a rate of 25kHz either field potential waveforms or spikes above an

adjustable threshold and additionally output TTL pulses used for stimulus and recording synchronisation.

2.11 Visually evoked potentials

2.11.1 Recording protocol

Visual evoked potentials (VEPs) were recorded using 0.1MΩ impedance Parylene-C insulated tungsten microelectrodes (Intracel, UK) and a silver wire served as a reference electrode. As detailed above, signals were acquired at 25kHz, bandpass filtered (0.3-300Hz) and amplified (x5-10k). The silver wire reference electrode was positioned in electrode gel which was in contact with the skull. After the recording site was prepared (see section 1.9), the recording electrode was lowered by visual guidance to the cortical surface. The electrode was then gradually lowered a further 50μm at a time while the animal was being visually stimulated until a short latency (approximately 60ms latency, see Figure 2.8) maximally negative going field potential was observed – invariably this was at a depth of 400-450μm which corresponds to layer 4 (Porciatti *et al.*, 1999; Sawtell *et al.*, 2003). The electrode was then allowed to settle for 10 minutes at this location after which a further recording was made to confirm the stability of the response. Stimulus triggered recordings were then made of VEPs in response to an contrast reversing grating presented to the binocular visual field of each eye individually using computer controlled eye shutters. Each eye was stimulated 40-80 times, divided into alternating eye blocks of 20 stimulations per eye.

2.11.2 Stimulus

Square wave horizontal gratings and of spatial frequency 0.06c/deg were presented in the central 30 degrees of the visual field and occupied -20 to +30 degrees of visual space in elevation. The grating contrast reversed abruptly at a frequency of 1Hz and field potential recording onset was synchronised to contrast reversal. The stimulus was generated with a VSG Series 5 stimulus generator (Cambridge Research Systems, Rochester, UK) and presented on a 21 inch monitor positioned at a distance of 20 cm.

2.11.3 Analysis

Field potential recordings were first downsampled from 25kHz to 1kHz. Averaged VEPs were calculated for the response to independent contralateral and ipsilateral eye stimulation and response magnitude was quantified by measuring the maximum negative point of the VEP waveform relative to the prestimulus period. All data analysis was conducted with custom software written in MatLab v7.0 (MathWorks).

A

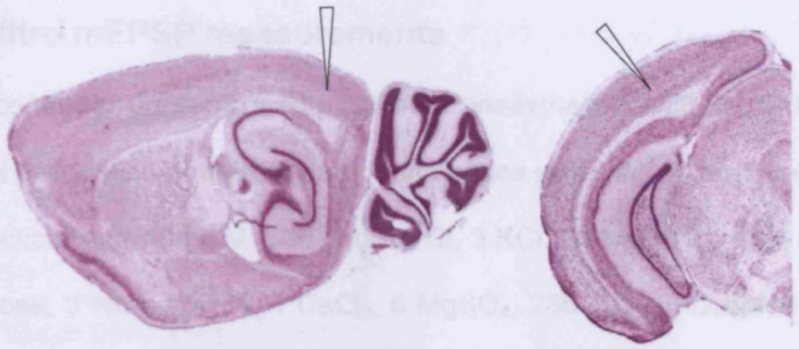

B

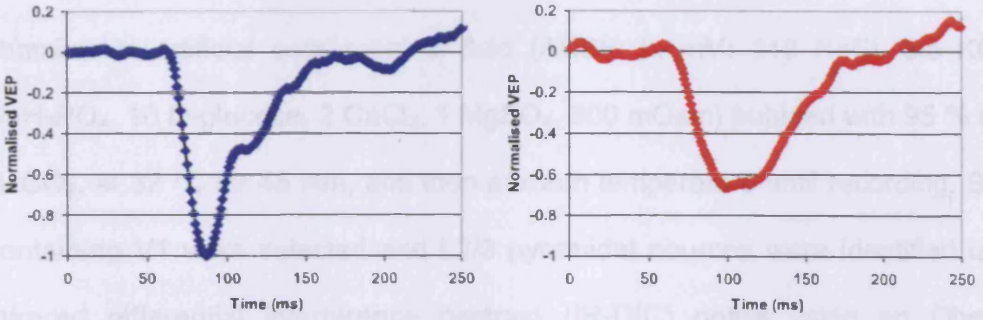

Figure 2.8 Visually evoked potential recording
A: Visually evoked potential recording site illustrated in a sagittal (left) and coronal (right) section (adapted from Franklin & Paxinos, 2008).
B: Examples of visually evoked potentials elicited by contralateral (left) and ipsilateral (right) visual stimulation normalised to contralateral response.

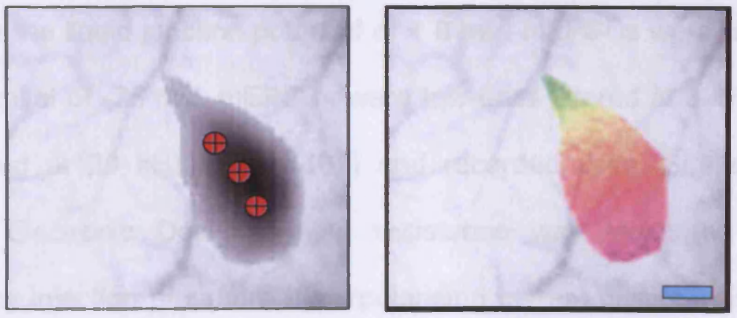

Figure 2.9 Example intrinsic signal targeted VEP recording sites.
Recording sites marked with red crossed circles. Scale bar 500μm.

2.12 In Vitro mEPSP measurements

P28-P31 control or dark-exposed mice were anaesthetised with isoflurane, killed by cervical dislocation and decapitated, and brains were rapidly removed into ice-cold dissection buffer (in mM: 108 choline-Cl, 3 KCl, 26 $NaHCO_3$, 1.25 NaH_2PO_4, 25 D-glucose, 3 Na-pyruvate, 1 $CaCl_2$, 6 $MgSO_4$, 285 mOsm) bubbled with 95% O_2/5% CO_2. 400 µm thick coronal slices were cut through V1 using a VT1000S microtome (Leica Microsystems). Brain slices were incubated in a submerged chamber in artificial cerebrospinal fluid (ACSF; in mM: 119 NaCl, 3.5 KCl, 1 NaH_2PO_4, 10 D-glucose, 2 $CaCl_2$, 1 $MgSO_4$, 300 mOsm) bubbled with 95 % O_2/ 5 % CO_2, at 32 °C for 45 min, and then at room temperature until recording. Slices containing V1 were selected and L2/3 pyramidal neurons were identified under infrared differential interference contrast (IR-DIC) optics using an Olympus BX50WI microscope. Whole cell recordings were made at 35 – 37 °C. Recording pipettes (4 – 6 MΩ) contained in mM: 130 $KMeSO_4$, 8 NaCl, 2 KH_2PO_4, 2 D-glucose, 10 HEPES, 4 Mg-ATP, 7 phosphocreatine, 0.3 GTP, 0.5 ADP, pH 7.30, 285 mOsm. Recorded neurons had resting membrane potentials ≤ -70 mV, not corrected for the liquid junction potential of + 8 mV. mEPSCs were recorded at a holding potential of -75 mV. mEPSCs were low-pass filtered at 3 kHz, and data were digitised at 20 kHz (micro1401) and recorded using Signal v.4.05 (all Cambridge Electronic Design). Input resistance was monitored throughout recordings by injection of square hyperpolarising current pulses. mEPSCs were isolated with 1 µM tetrodotoxin, 100 µM picrotoxin and 50 µM D-AP5 (all Tocris).

Action potential blockade was confirmed by injection of square depolarising current pulses (1 nA, 500 ms). ≥100 mEPSCs per cell were detected and measured using MiniAnalysis (Synaptosoft), using previously described shape and amplitude threshold criteria.

2.13 Immunohistochemistry

Mice were anaesthetised with sodium pentobarbital and transcardially perfused first with phosphate-buffered saline (PBS, 0.1M) followed by 4% paraformaldehyde in PBS for 10 mins, and then post-fixed for 2 hours. Brains were then removed and rinsed thoroughly with PBS containing 0.2% Tween 20. Coronal sections (50-60μm) were then cut using a vibrotome. Sections were then incubated for one hour in a blocking solution of 5% normal chicken serum/PBS and 0.2% Tween 20, followed by 22 hours incubation in GluR1 C3T antibody (05-855, Millipore) in 0.1% normal chicken serum containing 0.2% Tween 20; 2 hours at room temperature followed by 20 hours at 4^0C. Sections were next washed 3 times in PBS and then incubated in the secondary antibody, Alexa488 chicken anti-rabbit in 0.1%PBS, for three hours at room temperature. Sections were then washed again with PBS and aqueous mounted in ProLong Gold (Invitrogen).

2.14 Monocular Deprivation

Animals were monocularly deprived during the critical period for ocular dominance plasticity (beginning typically at postnatal day 25-27). Anaesthesia was induced in a chamber with 4% isoflurane in oxygen and maintained with 1-2% isoflurane breathed spontaneously via a nose cone. All hair surrounding the eye was first removed using fine scissors, the area was cleaned using an ethanol wipe, and the eye was treated with an ophthalmic cream (Isoptomax). The extreme margins of the eyelids were then trimmed then sutured shut by placing 2 mattress stitches using 6-0 silk suture material (Ethicon). The sutured lids were then treated with a small amount of antibiotic cream (Chloramphenicol, Medicon) and checked daily for any sign of opening or infection in which case animals were excluded from the study. Before physiological recordings were made the eye was examined closely under a microscope to ensure clarity of the optic medium.

2.15 Dark exposure

For dark exposure animals were reared for 3-5 days during the critical period for ocular dominance plasticity (beginning typically at postnatal day 25-27) in a double doored light impermeable room and cleaned and fed with the aid of infrared goggles. Prior to imaging or in vitro electrophysiology, animals were anaesthetised before leaving the dark room in a chamber containing 2-3% isoflurane.

2.16 Anaesthesia

In all terminal assessments a combination of the sedative Chlorprothixene (Sigma, UK) and Isoflurane was employed. Pre-treatment of animals with Chlorprothixene significantly reduced the concentration and degree of modulation of Isoflurane required to achieve a satisfactory depth of anaesthesia. Minimising the variation in Isoflurane concentration was found to be critical to reducing inter-animal variability in the absolute response magnitudes of both intrinsic signals and VEPs as both were modulated almost linearly within a range of Isoflurane concentrations from 0.7-1.3% (see Figure 2.10).

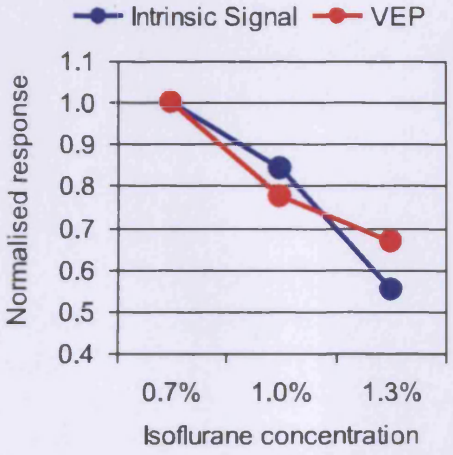

Figure 2.10 Modulation of both intrinsic signal and layer 4 visual evoked potential magnitude by isoflurane concentration.

2.17 Statistics

All statistical tests were performed using SPSS 16. For all data sets normality of distribution was assessed using the Kolmogorov-Smirnov test and equality of variance tested using Levene's test for equality of variance. In the case of

normality, parametric tests were selected appropriately depending upon the outcome of the equality of variance test (typically t-tests) and values were quoted as means ± standard error of the mean (S.E.M.). Non-normally distributed datasets were compared using the non-parametric Kolmogorov-Smirnov test and medians and interquartile range (I.Q.R.) were quoted.

Chapter 3. Basal cortical visual responses of the GluR1 knockout mouse

3.1 Introduction

A large number of the studies in this thesis make use of the GluR1$^{-/-}$ mouse generated by Zamanillo et al (1999). This is a germline knockout animal which results in some strengths and weaknesses in the data. The major strength of the germline knockout approach is that one can be certain that the gene of interest is not expressed.

However a significant weakness of using a germline knockout animal is the absence of both spatial and temporal specificity of gene expression disruption. This can result in some ambiguity of results. For example in brain plasticity experiments the lack of spatial specificity of a germline knockout can make it ambiguous whether a phenotype is due to the absence of a gene in the area in which you are interested or in another brain region which might innervate the area which you intend to investigate. Similarly the lack of temporal specificity renders it ambiguous whether a phenotype is due to a knockout induced developmental abnormality or a disruption of the specific process in which one is interested. In this chapter I describe findings which are relevant to the question of the basal normality of GluR1$^{-/-}$ animals (relative to their WT littermates).

3.2 Methods

3.2.1 Animals

The GluR1 knockout mouse colony was maintained as heterozygous GluR1$^{+/-}$ mutants and heterozygote x heterozygote crosses were used to generate homozygous mutant animals lacking GluR1 and WT littermates. Animals were obtained from Rolf Sprengel (Max Plank Institute, Heidelberg) via the Rawlins lab (Oxford) and were periodically out bred into a C57BL/6JOlaHsd background (Harlan, UK). The number of animals used in experiments are detailed in each section.

3.2.2 Data acquisition

Intrinsic signal imaging (episodic) and recordings of visually evoked potentials were carried out as described in Chapter 2.

3.3 Intrinsic signal visual cortical responses

Mice lacking GluR1 and their littermates were first analysed during the critical period using intrinsic signal imaging. Mice were visually stimulated as described in the general methods and intrinsic signals were recorded. This allowed quantification of the binocular visual cortical response to contralateral and ipsilateral eye stimulation and quantification of the monocular visual cortical response to contralateral eye stimulation. All response magnitudes are

presented as $\Delta R/R \times 10^{-4}$. The number of animals used in experiments in this section were as follows: WT = 8, GluR1$^{-/-}$ = 9.

Response magnitudes were observed to be broadly depressed by approximately 30% in GluR1$^{-/-}$ mice relative to WT littermates (Figure 3.1): contralateral monocular cortex response WT = 1.9 ± 0.24, GluR1$^{-/-}$ = 1.3 ± 0.13 ($P < 0.05$, t-test), a 32% reduction; contralateral binocular cortex response WT = 1.7 ± 0.18, GluR1$^{-/-}$ = 1.2 ± 0.16 ($P < 0.05$, t-test), a 29% reduction; ipsilateral binocular cortex response WT = 1.1 ± 0.18, GluR1$^{-/-}$ = 0.7 ± 0.19 ($P = 0.07$, t-test), a 36% reduction.

From the contralateral and ipsilateral response magnitudes an ODI was calculated as described in the general methods. This allowed quantification of the degree of contralateral eye dominance in the binocular cortex irrespective of absolute response magnitude. The ODI of GluR1$^{-/-}$ and WT littermates was statistically indistinguishable with GluR1$^{-/-}$ mice ODI = 0.28 ± 0.04 and WT mice ODI = 0.26 ± 0.05 ($P = 0.69$, t-test, Figure 3.2).

These results indicate that although GluR1$^{-/-}$ intrinsic signal response amplitudes are depressed relative to WT littermates, a normal balance of responsiveness between the two eyes develops. As I am postulating a role for GluR1 in OD plasticity an abnormal balance of OD in GluR1$^{-/-}$ mice would not have been surprising. Indeed a recent study of the role of Arc in OD plasticity found just such a basal OD index abnormality in Arc$^{-/-}$ animals (McCurry *et al.*, 2010).

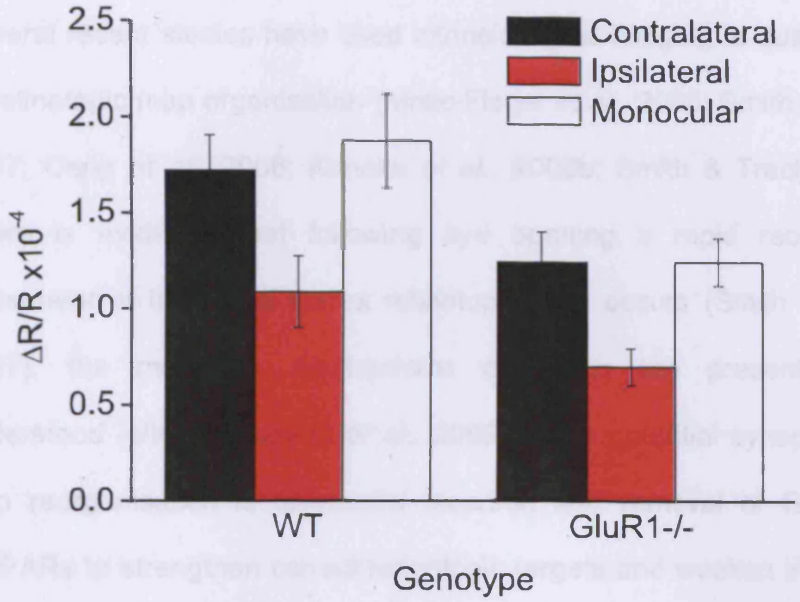

Figure 3.1 Absolute intrinsic signal response magnitudes in the primary visual cortex.

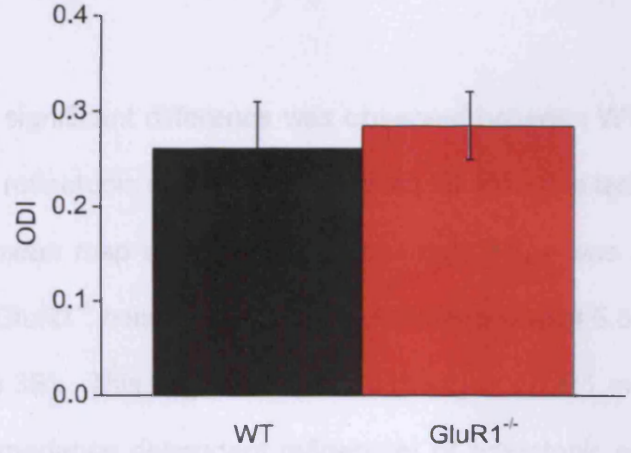

Figure 3.2 Baseline WT and GluR1$^{-/-}$ ocular dominance index.

3.4 Intrinsic signal retinotopic map scatter

Several recent studies have used intrinsic signal imaging to quantify the degree of retinotopic map organisation (Mrsic-Flogel *et al.*, 2005; Smith & Trachtenberg, 2007; Cang *et al.*, 2008; Kaneko *et al.*, 2008b; Smith & Trachtenberg, 2010). There is evidence that following eye opening a rapid reorganisation and refinement of the visual cortex retinotopic map occurs (Smith & Trachtenberg, 2007), the molecular mechanisms of which are presently incompletely understood (although see Li *et al.*, 2009). One potential synaptic substrate for map reorganisation is differential insertion and removal of GluR1 containing AMPARs to strengthen correct retinotopic targets and weaken incorrect ones. I therefore examined retinotopic map scatter in GluR1$^{-/-}$ and WT mice at an age at which this process is reported to have normally concluded (P32, as reported by Smith & Trachtenberg, 2007). The number of animals used in experiments in this section were as follows: WT = 6, GluR1$^{-/-}$ = 6.

At this age a significant difference was observed between WT and GluR1$^{-/-}$ mice such that the retinotopic maps of mice lacking GluR1 were less organised (Figure 3.3A). The mean map scatter of WT retinotopic maps was 3.0 ± 0.64 degrees while that of GluR1$^{-/-}$ mice was almost double this value at 5.8 ± 0.67 ($P = 0.02$, t-test, Figure 3.3B). This suggests that trafficking of GluR1 may normally have a role in the experience dependent refinement of retinotopic maps in the primary visual cortex.

There is some uncertainty about the methodology of periodic intrinsic signal imaging as a measure of visual cortex retinotopic map organisation. If the intrinsic signal is weak it is more likely to be contaminated by biological noise resulting in inappropriate phase values being assigned to pixels of the functional map. Although previous studies have shown that low scatter maps can be recorded despite low signal magnitude (Smith & Trachtenberg, 2007) signal magnitude is clearly a contributing factor. In order to examine in a more controlled manner the relationship between intrinsic signal magnitude and map scatter, the contrast of visual stimulus was systematically varied and the scatter of the resultant retinotopic maps examined within the same animal. A linear relationship was observed between response magnitude and stimulus contrast (Figure 3.4A). A strong relationship was also observed between map scatter and response magnitude whereby maps with greater response magnitude appeared more organised (Figure 3.4B; Figure 3.5).

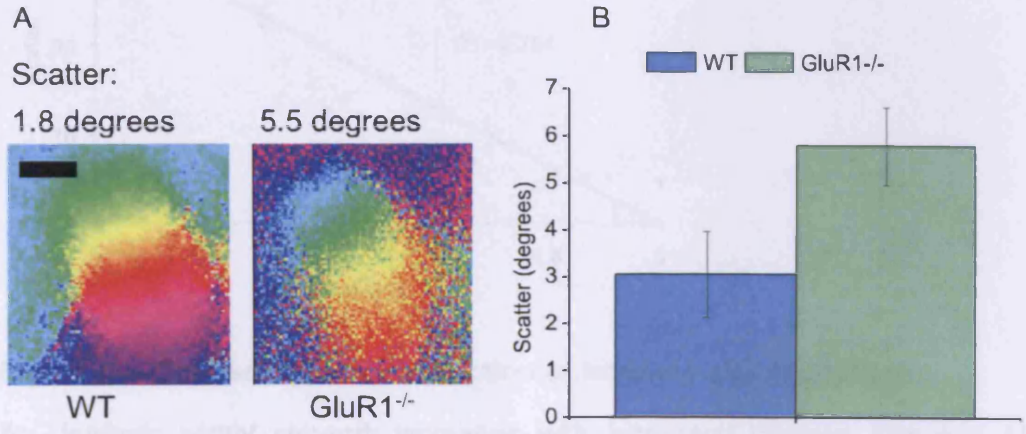

Figure 3.3 Retinotopic map scatter
A: Examples of V1 retinotopic maps recorded from WT and GluR1$^{-/-}$ mice. The map from the GluR1$^{-/-}$ mouse (right) is visibly less organised. B: Average map scatter values from WT and GluR1$^{-/-}$ mice. Scale bar 500μm.

A

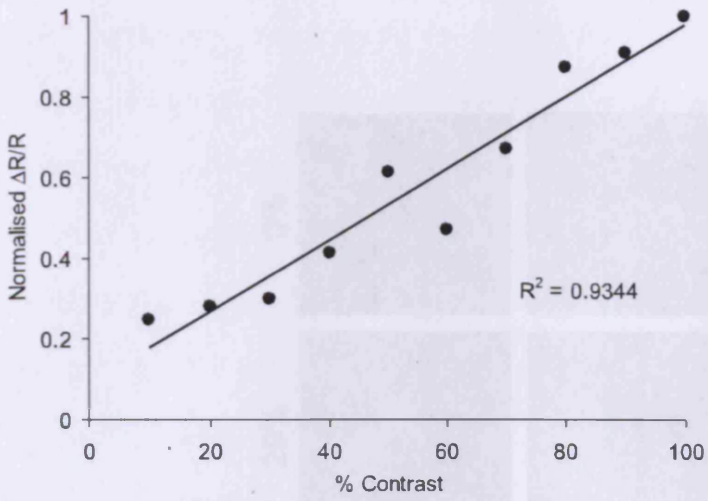

B

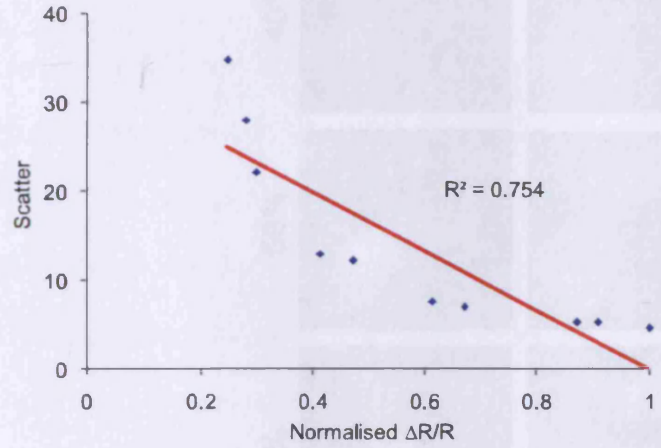

Figure 3.4 Scatter varies as a function of intrinsic signal strength.

A: Intrinsic signal strength increases with increased contrast stimulus. Line indicates linear fit. B: Map scatter decreases with increased intrinsic signal magnitude. Line indicates linear fit.

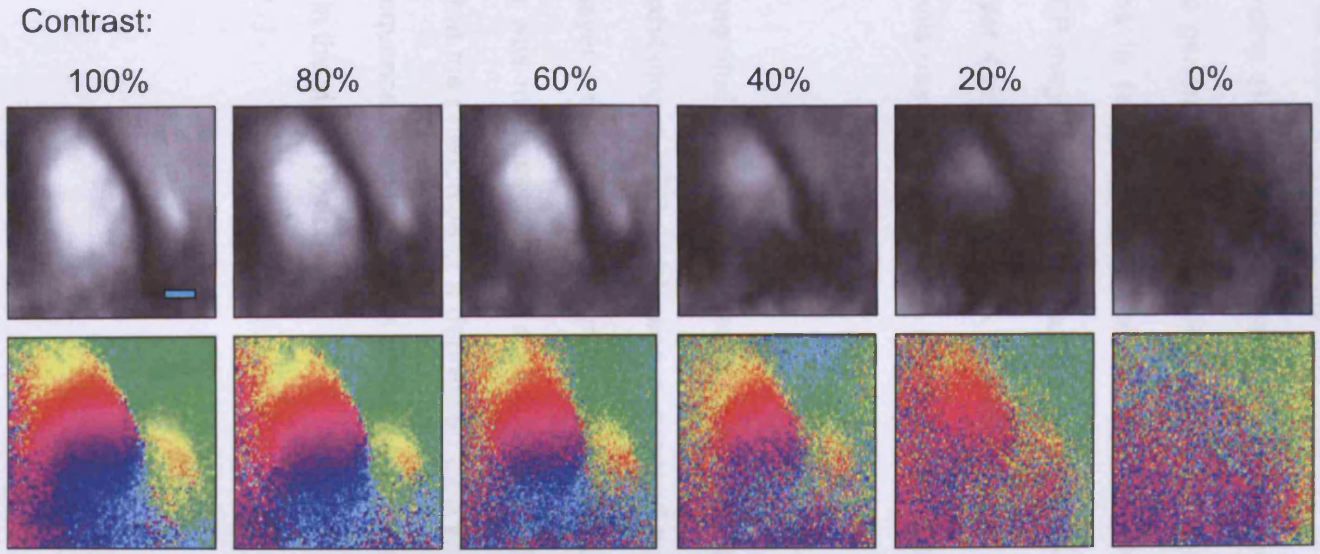

Figure 3.5 Retinotopic maps collected at different stimulus contrasts by periodic intrinsic signal imaging. Scale bar 500μm.

3.5 Laminar analysis of visually evoked field potentials (VEPs)

Having observed a difference in intrinsic signal magnitude between WT and GluR1$^{-/-}$ animals I next sought to determine if this difference could be more directly measured electrophysiologically and localised to either L2/3 or L4. A 0.1MOhm recording electrode was advanced into the primary visual cortex as described in the general methods. VEPs were then recorded at 50μm spaced recording depths in response to visual stimulation with a contrast reversing grating. The VEP magnitude was measured relative to the pre-stimulus voltage. The depth of layer 4 was determined as described in the general methods. The number of animals used in experiments in this section were as follows: WT = 6, GluR1$^{-/-}$ = 3.

Layer 4 VEP magnitudes were consistent with intrinsic signal magnitudes, with GluR1$^{-/-}$ mice exhibiting a VEP which was depressed by 36.2% relative to WT littermates. In layer 4 the WT VEP magnitude was 325 ± 26.9 μV while GluR1$^{-/-}$ VEP magnitude was measured as 207 ± 14.0 μV ($P < 0.05$, t-test, Figure 3.6). This suggests that the phenotype of a depressed L2/3 intrinsic signal magnitude may be a consequence of abnormalities at the L4 thalamocortical synapse or at an earlier point in the visual system.

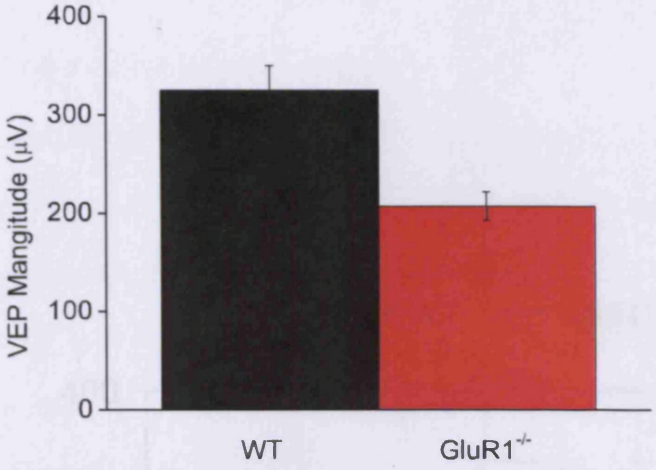

Figure 3.6 VEP magnitude is depressed at baseline in GluR1$^{-/-}$ mice relative to WT littermates.

Figure 3.7 Baseline ODI is identical in GluR1$^{-/-}$ mice and WT littermates

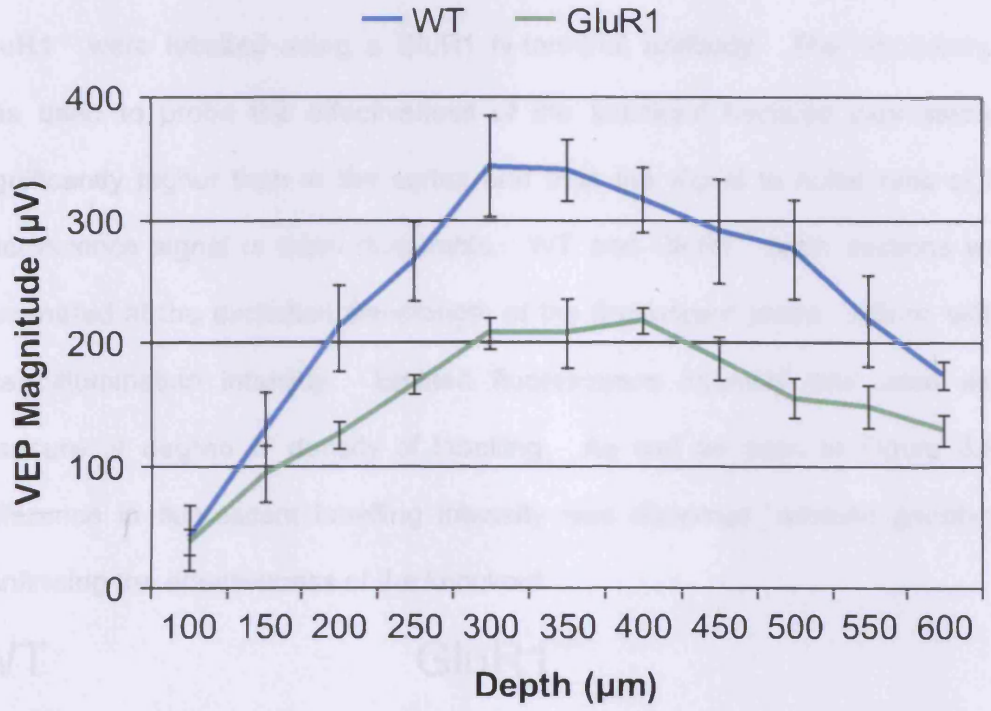

Figure 3.8 VEPs recorded at different depths throughout the primary visual cortex in response to binocular visual stimulation.

3.6 Immunohistochemistry

In addition to the genotyping procedure described in the general methods, the effectiveness of GluR1 ablation in the GluR1$^{-/-}$ animal was further confirmed by fluorescence immunohistochemitry. Coronal brain sections from a WT and GluR1$^{-/-}$ were labelled using a GluR1 N-terminal antibody. The hippocampus was used to probe the effectiveness of the knockout because expression is significantly higher than in the cortex and thus the signal to noise ratio of the fluorescence signal is more favourable. WT and GluR1$^{-/-}$ brain sections were illuminated at the excitation wavelength of the fluorescent probe, 395nm, with a fixed illumination intensity. Emitted fluorescence intensity was used as a measure of degree of density of labelling. As can be seen in Figure 3.9 a difference in fluorescent labelling intensity was observed between genotypes confirming the effectiveness of the knockout.

WT GluR1$^{-/-}$

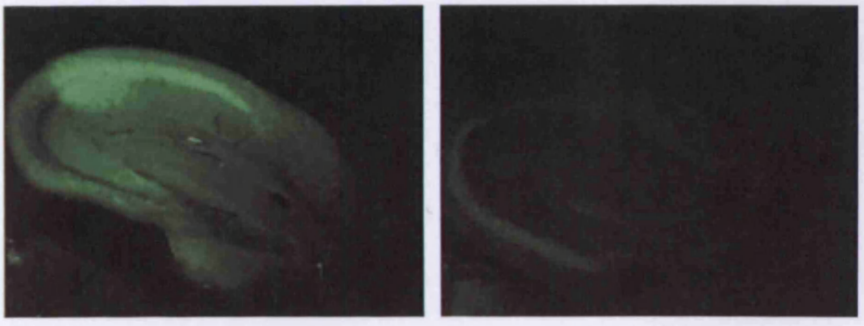

Figure 3.9 Immunohistochemistry
Fluorescent immunohistochemical labelling of the GluR1 protein N-terminal illustrating effectiveness of the knockout.

3.7 Summary of findings

The aim of the experiments presented in this chapter was to examine the potential effect of knockout of the GluR1 receptor on basal primary visual cortex responses. The key findings were:

1. Baseline intrinsic signal response magnitudes are depressed in GluR1$^{-/-}$ mice relative to WT littermates in both binocular and monocular cortex.
2. Baseline VEP magnitudes are depressed in GluR1$^{-/-}$ mice relative to WT littermates in the binocular area to the same extent as intrinsic signal magnitudes in layer 2/3.
3. The ratio of contralateral to ipsilateral response magnitude in binocular cortex is normal in GluR1$^{-/-}$ mice.
4. The primary visual cortex retinotopic map appears less organised in GluR1$^{-/-}$ mice than WT littermates.
5. Intrinsic signal map scatter is confounded with intrinsic signal magnitude indicating caution is necessary in the interpretation of map scatter values.

Chapter 4. GluR1 as a substrate of critical period experience dependent plasticity

4.1 Introduction

As described in detail in the general introduction, closing one eye during the critical period for ocular dominance plasticity in the mouse results in an ocular dominance shift whereby, upon eye reopening, neurons in the binocular cortex are found to have shifted ocular dominance preference from the deprived eye towards the spared eye (Gordon & Stryker, 1996). Subsequently developed methodologies which provided absolute quantification of responsiveness to the deprived and spared eye (as opposed to a ratio of responsiveness of the two eyes) permitted the ocular dominance shift to be dissected into two phases; an initial depression of responsiveness to the closed eye followed by a delayed potentiation of responsiveness to the spared eye (Frenkel & Bear, 2004; Mrsic-Flogel *et al.*, 2007; Kaneko *et al.*, 2008a; Kaneko *et al.*, 2008b). Other work has provided evidence that ocular dominance plasticity occurs by different molecular mechanisms in different cortical layers (Crozier *et al.*, 2007; Liu *et al.*, 2008).

This chapter addresses both the initial depression of responsiveness of neurons to the deprived eye which occurs over 1-3 days after eye closure and the delayed potentiation of responsiveness of neurons to the spared eye which occurs over 5-6 days. Specifically, this chapter examines the dependence of these plasticity processes on interactions involving the AMPAR subunit GluR1. Additionally the question of whether the role of GluR1 in OD plasticity is layer specific is addressed by contrasting data acquired using optical intrinsic signal imaging (a signal thought to be dominated by activity in L2/3), visually evoked potentials

(recorded in L4) and multiunit recordings made in both cortical layers. An attempt is also made at confirming the assumption of the layer 2/3 laminar origin of the intrinsic signal.

4.2 Methods

4.2.1 Animals

For experiments examining the depression phase of OD plasticity the mouse colony was maintained as heterozygous GluR1-/- mutants and heterozygote x heterozygote crosses were used to generate homozygous mutant animals lacking GluR1 and WT littemates. Animals were obtained from Rolf Sprengel (Max Plank, Heidelberg) via the Rawlins lab (Oxford) and were periodically out bred into a C57BL/6JOlaHsd background (Harlan, UK).

As described in Chapter 7, C57BL/6JOlaHsd mice exhibit impaired homeostatic plasticity thus to test the role of GluR1 in this process required that the GluR1 mutation was bred into a different background. After determining that the C57BL/6J background (Jackson, UK) exhibited homeostatic plasticity (see Chapter 7) we proceeded to backcross the C57BL/6JOlaHsdGluR1$^{+/-}$ into this background. This was done for two generations, after which GluR1 heterozygous offspring were crossed to generate animals lacking GluR1 and WT littermates. The numbers of animals used in experiments are detailed in each section.

4.2.2 Monocular deprivation

Animals were monocularly deprived under isoflurane anaesthetic as described in Chapter 2. Monocular deprivation began at postnatal day 26-28 and lasted for either 3 or 5-6 days, thus physiological recordings were made between postnatal days 29-34. Wherever possible the knockout and WT animals within a litter were distributed between the experimental conditions evenly.

4.2.3 Data acquisition and analysis

Intrinsic signal imaging (episodic) and visually evoked potential recordings were conducted as described in Chapter 2. All intrinsic signal response magnitudes are presented as $\Delta R/R \times 10^{-4}$.

4.2.4 Cortical L2/3 muscimol inactivation

A craniotomy was performed above the primary visual cortex. Electrodes were then positioned either in layer 4 on the cortical surface as described in Chapter 2. The intrinsic signal capture system was then positioned as normal. A 2% warm agarose solution containing 1000μM muscimol was then applied and sealed with a glass coverslip before recording commenced. Back to back alternating recordings of VEPs and intrinsic signal were made as frequently as possible during the 40-60 minute recording session with an average cycle of VEP and intrinsic signal recording taking around 7 minutes.

4.3 Results

4.3.1 Effect of short monocular deprivation (3d) on intrinsic signal magnitudes

Juvenile mice were monocularly deprived for three days during the critical period followed by intrinsic signal imaging of the contralateral hemisphere. As described in Chapter 3 the baseline intrinsic signal magnitude of mice lacking GluR1 differed from that of their wild type littermates. Thus the data could be interpreted in at least two ways; 1) relative to the genotypic baseline and 2) in terms of absolute signal magnitude. The numbers of animals used in experiments in this section were as follows: control WT = 8, control GluR1$^{-/-}$ = 9, 3dMD WT = 7, 3dMD GluR1$^{-/-}$ = 7.

4.3.2 Ocular dominance shift: calculated relative to genotypic baseline

As described in Chapter 3 the ODI of GluR1$^{-/-}$ mice and their WT littermates was statistically indistinguishable in control animals (WT ODI = 0.26 ± 0.05, GluR1$^{-/-}$ = 0.28 ± 0.04, P = 0.69, t = 0.41, t-test). After three days of MD both WT and GluR1$^{-/-}$ mice exhibited a highly significant shift of ODI (deprived WT ODI = -0.04 ± 0.03, $p < 0.01$, t = 5.3; deprived GluR1$^{-/-}$ ODI = 0.01 ± 0.02, $P < 0.01$, t = 6.2, t-test; Figure 4.1). Both WT and GluR1$^{-/-}$ ODIs shifted to a similar degree and thus remained statistically indistinguishable (P = 0.22, t = 1.28, t-test).

As has previously been reported, the cause of the ODI shift after three days of monocular deprivation was a depression of deprived eye response magnitude in

CARDIFF UNIVERSITY
PRIFYSGOL CAERDYDD

WT animals (a 42% reduction, control = 1.74 ± 0.18, deprived = 0.99, P < 0.01, t = 3.86, t-test; Figure 4.2A). After 3d MD a near identical percentage change in

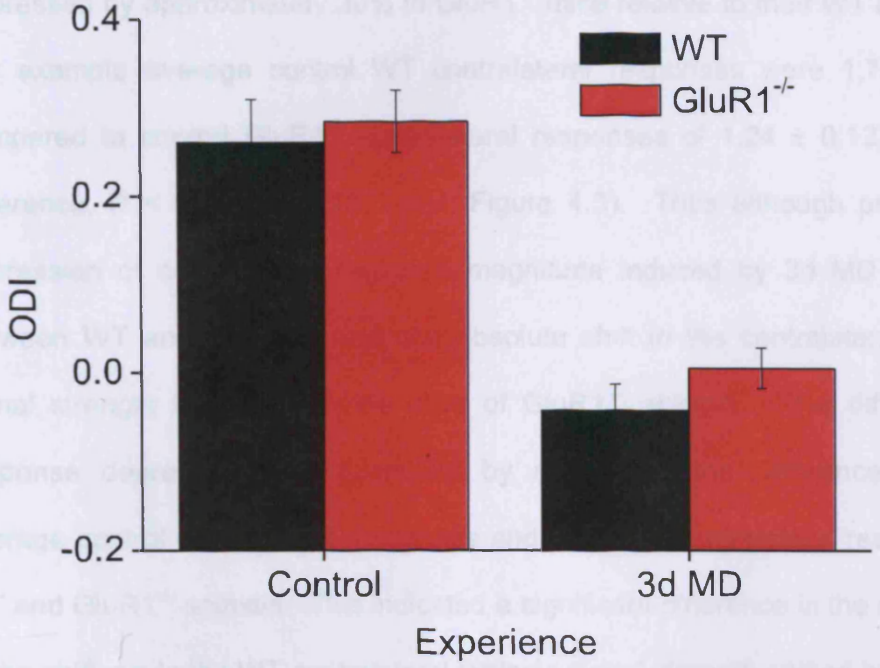

Figure 4.1 ODI shift measured using intrinsic signal imaging.

contralateral response magnitude was observed in GluR1$^{-/-}$ mice (a 40% reduction, control = 1.24 ± 0.12, deprived = 0.74 ± 0.06, P < 0.05, t = 2.56, t-test; Figure 4.2B). Consistent with previous studies no plasticity of ipsilateral response magnitudes was observed after 3d MD (WT 1% change, WT control = 1.08 ± 0.18, WT deprived = 1.07 ± 0.64, P = 0.99, t = 0.018, t-test; GluR1$^{-/-}$ 6% change, GluR1$^{-/-}$ control = 0.70 ± 0.09, GluR1$^{-/-}$ deprived = 0.74 ± 0.08, P = 0.68, t = 0.43, t-test; Figure 4.2).

4.3.3 Ocular dominance shift: calculated by absolute intrinsic signal magnitude

As described in Chapter 3 the intrinsic signal response magnitude is basally depressed by approximately 30% in GluR1$^{-/-}$ mice relative to their WT littermates (for example average control WT contralateral responses were 1.74 ± 0.18, compared to control GluR1$^{-/-}$ contralateral responses of 1.24 ± 0.12, a 28.7% difference, $P < 0.05$, $t = 2.15$, t-test; Figure 4.3). Thus although proportional depression of contralateral response magnitude induced by 3d MD is similar between WT and GluR1$^{-/-}$ mice, the absolute shift in the contralateral intrinsic signal strength is smaller in the case of GluR1$^{-/-}$ animals. This difference in response depression was quantified by calculating the difference between average control contralateral responses and deprived contralateral responses in WT and GluR1$^{-/-}$ animals. This indicated a significant difference in the magnitude of the shift: while the WT contralateral intrinsic signal strength shifted by 0.73, the shift in GluR1$^{-/-}$ animals was 0.50 ($P < 0.05$, $t = 2.48$, t-test; Figure 4.4). In summary while WT and GluR1$^{-/-}$ animals exhibit a comparable fractional depression of deprived eye responses, in absolute intrinsic signal terms GluR1$^{-/-}$ mice depress less.

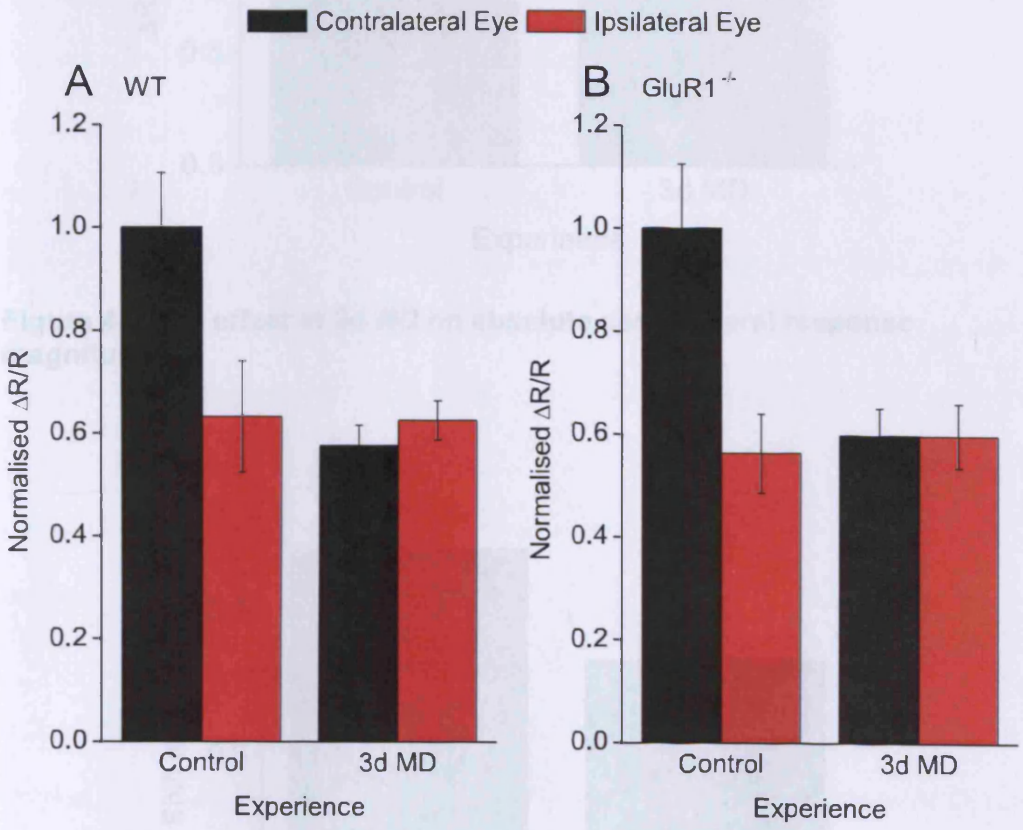

Figure 4.2 Depression of contralateral response following 3d MD measured by intrinsic signal imaging in A: WT mice and B: GluR1$^{-/-}$ mice.

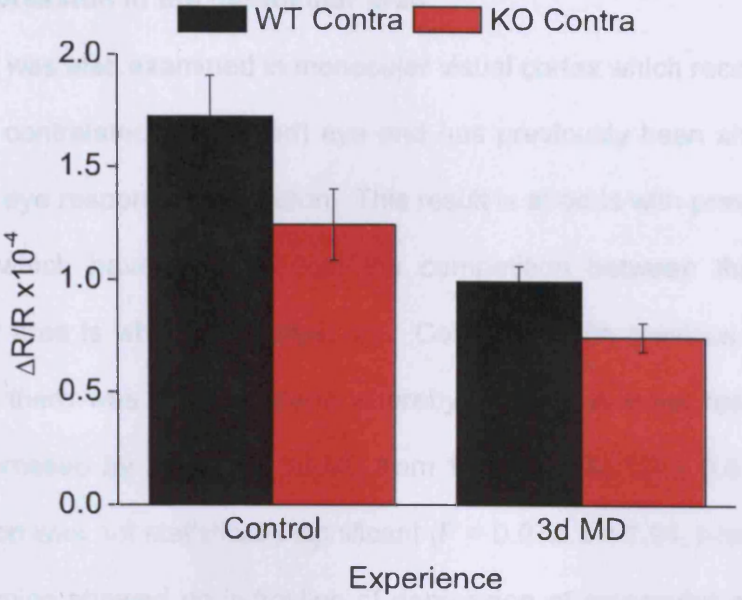

Figure 4.3 The effect of 3d MD on absolute contralateral response magnitude

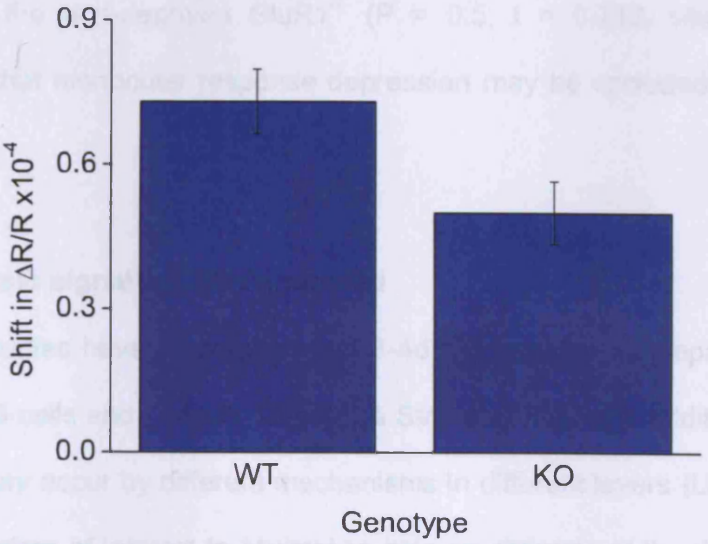

Figure 4.4 Comparison of absolute contralateral intrinsic signal magnitude shift in WT and GluR1-/- mice following 3dMD

4.3.4 Depression in the monocular area

Plasticity was also examined in monocular visual cortex which receives input only from the contralateral (deprived) eye and has previously been shown to exhibit deprived eye response depression. This result is at odds with previous studies in the cat which have reported that the competition between the eyes in the binocular area is what drives plasticity. Consistent with previous findings in the literature there was a strong trend whereby mean monocular responses of WT mice depressed by 26% after 3d MD from 1.9 ± 0.24 to 1.4 ± 0.07 however this depression was not statistically significant ($P = 0.072$, $t = 1.94$, t-test). In contrast $GluR1^{-/-}$ mice showed no indication of depression of monocular area responses (3% depression; control = 1.27 ± 0.13, deprived = 1.24 ± 0.17, $P = 0.91$, $t = 0.12$, t-test). Interestingly the deprived WT monocular response magnitude was close to that of the non-deprived $GluR1^{-/-}$ ($P = 0.5$, $t = 0.712$, t-test) raising the possibility that monocular response depression may be occluded in the $GluR1^{-/-}$ animal.

4.3.5 Intrinsic signal is L2/3 dominated

Previous studies have established that 3-4d MD induces a comparable OD shift in both L2/3 cells and L4 cells (Gordon & Stryker, 1996) and additionally that OD plasticity may occur by different mechanisms in different layers (Liu *et al.*, 2008). It was therefore of interest to attempt to gain an estimate of the degree to which the intrinsic signal is contributed to by layer 2/3 activity vs. layer 4 activity. In a pilot study the visual cortex was gradually deactivated from the surface

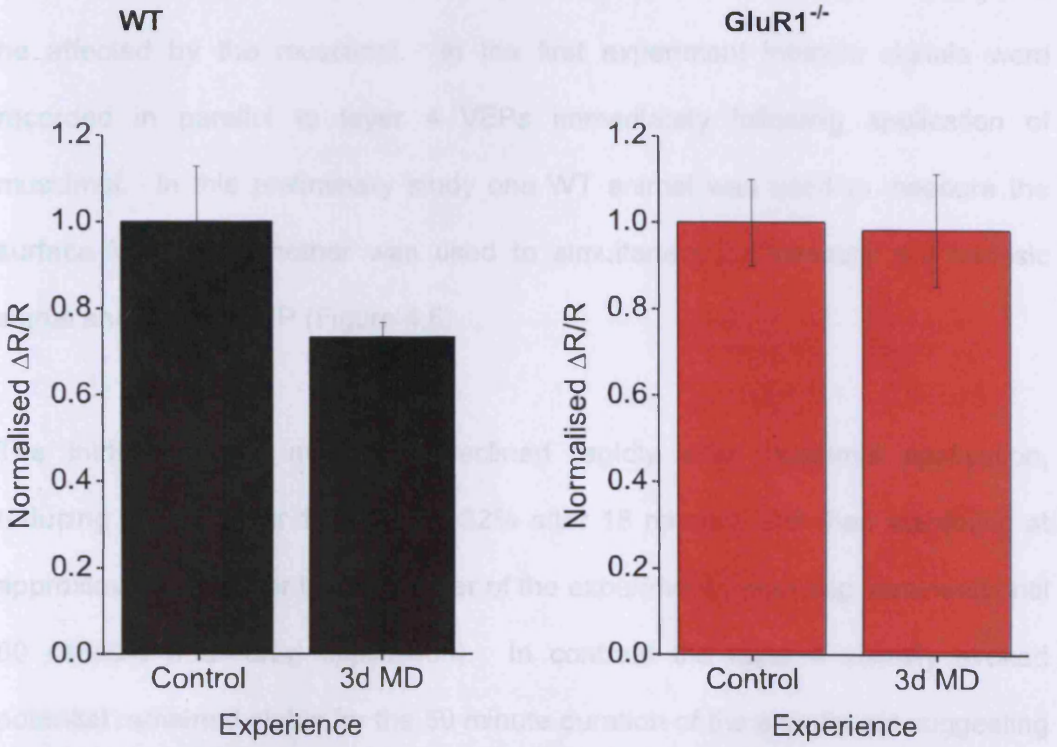

Figure 4.5 3dMD induced depression of closed eye response is absent in the monocular cortex of GluR1$^{-/-}$ mice.

downwards by direct application of the $GABA_A$ agonist muscimol (1000μM) while simultaneously monitoring field potentials in layer 4 or at the surface and recording the intrinsic optical signal. This allowed the intrinsic signal to be recorded in the absence of L2/3 activity with a confidence that layer 4 was yet to be affected by the muscimol. In the first experiment intrinsic signals were recorded in parallel to layer 4 VEPs immediately following application of muscimol. In this preliminary study one WT animal was used to measure the surface VEP and another was used to simultaneously measure the intrinsic signal and layer 4 VEP (Figure 4.6).

The intrinsic signal magnitude declined rapidly after muscimol application, reducing to 58% after 11 minutes, 32% after 18 minutes and then stabilising at approximately 25% for the remainder of the experiment (recording continued until 60 minutes after drug application). In contrast the layer 4 visually evoked potential remained stable for the 60 minute duration of the experiment suggesting that the muscimol did not reach the cells in layer 4. In another experiment the VEP was recorded from the cortical surface and declined in magnitude in a manner very similar to the intrinsic signal, reducing to 59% after 12 minutes, 14% after 18 minutes and then stabilising at approximately 15-20%. This data indicates that the intrinsic signal is dominated by the activity of cells in the superficial layers of the cortex and that an apparently normal level of activity in layer 4 accounted for ~25% of the control intrinsic signal magnitude. This interpretation is strengthened by the strong correlation between the time courses

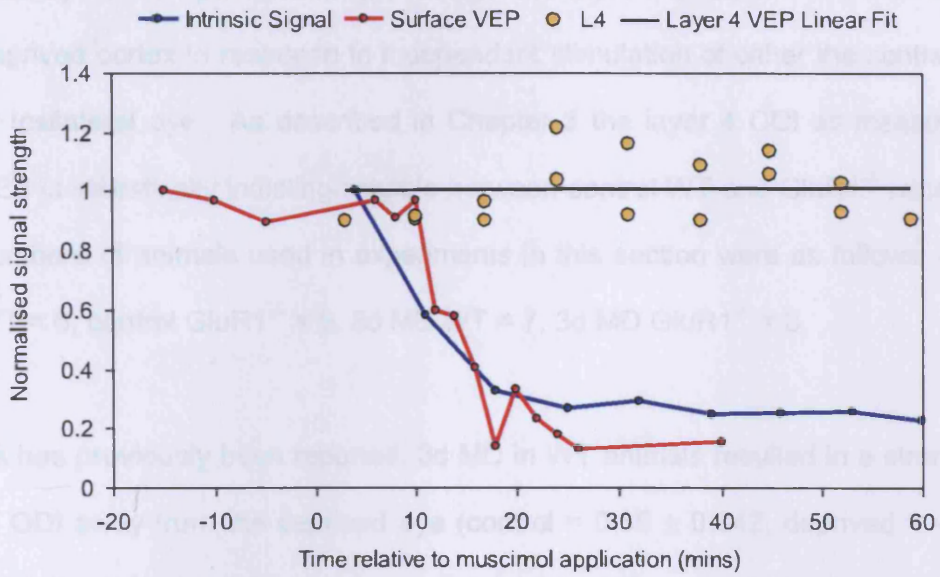

Figure 4.6 Isolation of layer 4 intrinsic signal by surface Muscimol application.

of muscimol inactivation of superficial layer electrical activity and muscimol inactivation of intrinsic signals.

4.3.6 Effect of short monocular deprivation (3d) on layer 4 visually evoked potentials

Visually evoked potentials were recorded in layer 4 of control and monocularly deprived cortex in response to independent stimulation of either the contralateral or ipsilateral eye. As described in Chapter 3 the layer 4 ODI as measured by VEP is statistically indistinguishable between control WT and GluR1$^{-/-}$ mice. The numbers of animals used in experiments in this section were as follows: control WT = 6, control GluR1$^{-/-}$ = 5, 3d MD WT = 7, 3d MD GluR1$^{-/-}$ = 8.

As has previously been reported, 3d MD in WT animals resulted in a strong shift of ODI away from the deprived eye (control = 0.35 ± 0.042, deprived = -0.07 ± 0.08, $P < 0.01$, $t = 4.37$, t-test). In contrast this shift was entirely absent in GluR1$^{-/-}$ littermate mice (control = 0.34 ± 0.05, deprived = 0.32 ± 0.03, $P = 0.71$, $t = 0.38$, t-test). This argues for a role of GluR1 specifically in layer 4 ocular dominance plasticity.

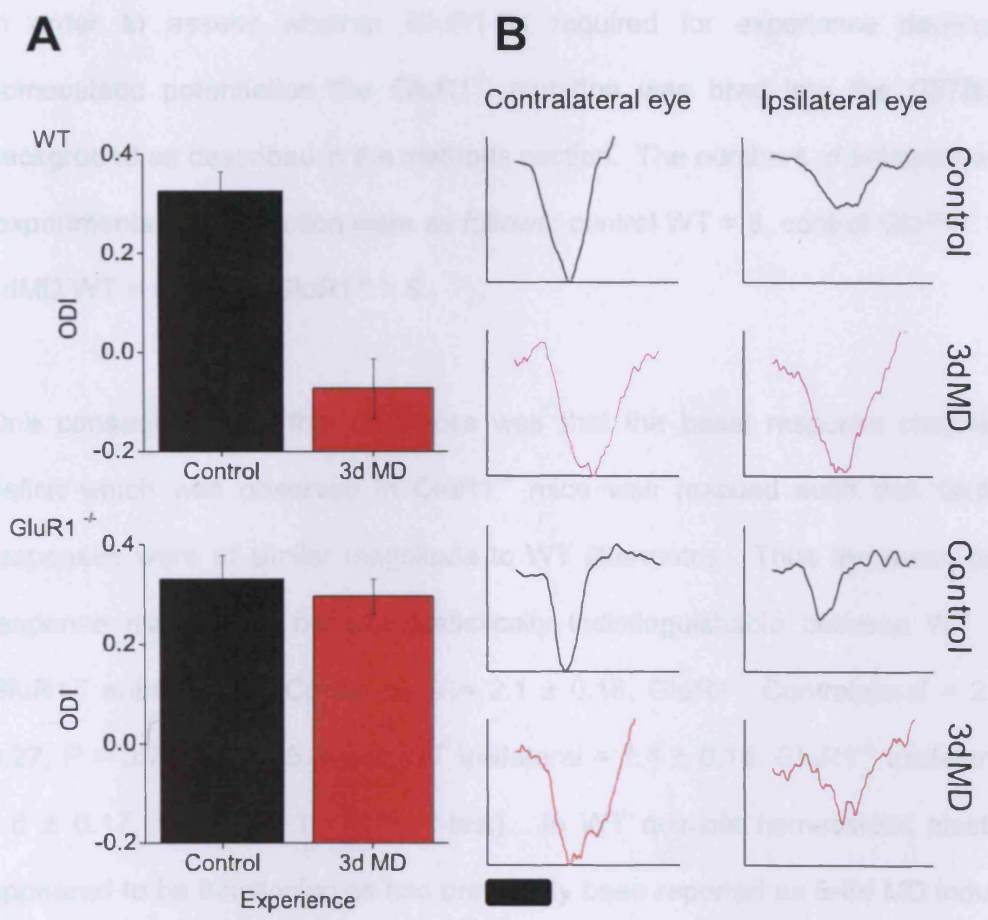

Figure 4.7 Layer 4 ocular dominance plasticity measured with VEPs.
A: ODI shift observed after 3d MD in WT (top) is completely absent in GluR1$^{-/-}$ mice (bottom). B: Example VEP traces normalized to contralateral response. Time scale bar, 50ms.

4.3.7 Effect of long monocular deprivation (5-6d) on intrinsic signal response magnitudes.

In order to assess whether GluR1 is required for experience dependent homeostatic potentiation the GluR1$^{-/-}$ mutation was bred into the C57BL/6J background as described in the methods section. The numbers of animals used experiments in this section were as follows: control WT = 8, control GluR1$^{-/-}$ = 8, 3dMD WT = 6, 3dMD GluR1$^{-/-}$ = 6.

One consequence of this backcross was that the basal response magnitude deficit which was observed in GluR1$^{-/-}$ mice was rescued such that GluR1$^{-/-}$ responses were of similar magnitude to WT littermates. Thus the mean basal response magnitudes became statistically indistinguishable between WT and GluR1$^{-/-}$ animals (WT Contralateral = 2.1 ± 0.18, GluR1$^{-/-}$ Contralateral = 2.2 ± 0.27, P = 0.73, t = 0.35, t-test; WT Ipsilateral = 1.4 ± 0.14, GluR1$^{-/-}$ Ipsilateral = 1.6 ± 0.17, P = 0.39, t = 0.89, t-test). In WT animals homeostatic plasticity appeared to be functioning as has previously been reported as 5-6d MD induced approximately a 40% increase in spared eye response ($P < 0.05$, t = 2.3, t-test) while the closed eye depressed by 10% (post 5d MD: contralateral = 1.8 ± 0.18, ipsilateral = 2.0 ± 0.23,). In contrast GluR1$^{-/-}$ mice exhibited no spared eye potentiation and the closed eye depressed by around 35% (P = 0.06, t = 2.0, t-test). These findings indicate that this form of homeostatic plasticity is impaired in animals lacking GluR1 (Figure 4.8).

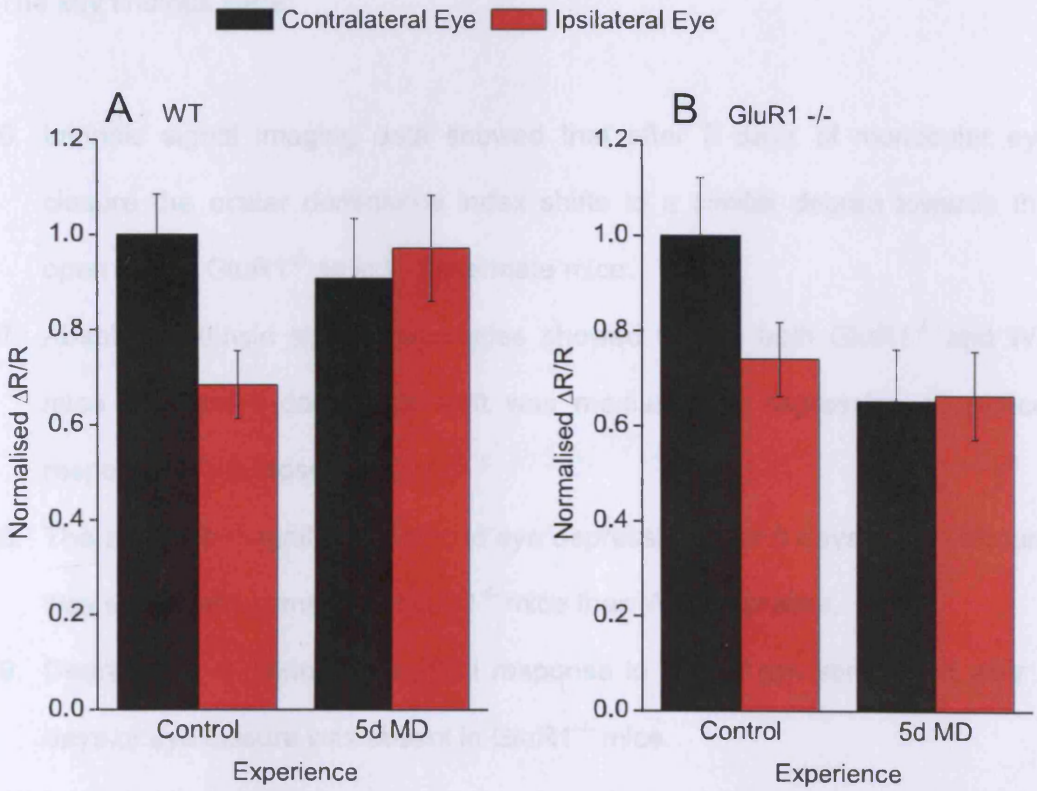

Figure 4.8 Impaired open eye potentiation in GluR1 lacking mice after 5d MD.

4.4 Summary of findings

The aim of the experiments presented in this chapter was to examine the effect of knockout of the GluR1 receptor on critical period ocular dominance plasticity. The key findings were:

6. Intrinsic signal imaging data showed that after 3 days of monocular eye closure the ocular dominance index shifts to a similar degree towards the open eye in GluR1$^{-/-}$ as in WT littermate mice.
7. Absolute intrinsic signal magnitudes showed that in both GluR1$^{-/-}$ and WT mice the ocular dominance shift was mediated by depression of cortical response to the closed eye.
8. The absolute magnitude of closed eye depression after 3 days of eye closure was significantly smaller in GluR1$^{-/-}$ mice than WT littermates.
9. Depression of monocular cortical response to closed eye stimulation after 3 days of eye closure was absent in GluR1$^{-/-}$ mice.
10. Intrinsic signal imaging was shown to reflect predominantly activity in the superficial layers of the cortex.
11. Layer 4 VEP recordings were used to show that ocular dominance plasticity in response to 3 days eye closure is absent in GluR1$^{-/-}$ mice.
12. Intrinsic signal imaging was used to show that homeostatic plasticity after 6 days of eye closure is absent in mice lacking GluR1.

Chapter 5. GluR1 as a substrate of adult plasticity

5.1 Introduction

Although early work on rodent visual cortex ocular dominance plasticity suggested that it was limited to a postnatal critical period (Gordon & Stryker, 1996) subsequent studies demonstrated that the capacity for a form of OD plasticity persists into (at least early) adulthood (Sawtell *et al.*, 2003; Lehmann & Lowel, 2008; Sato & Stryker, 2008). Studies of adult OD plasticity are in broad agreement that it requires a longer 5-7d period of deprivation, is mediated solely by potentiation of the spared eye response (see Figure 5.2) and is blocked by systemic application of the NMDAR antagonist CPP. One aim of the work in this chapter was to determine if GluR1 is a necessary substrate of adult open eye potentiation.

In addition to the plasticity inducible by MD, further adult plasticity occurs in the event of restoration of normal binocular input. After deprived eye reopening a recovery of the normal ocular dominance ratio takes place over a period of <4d in juvenile animals (Kaneko *et al.*, 2008a) and over a period of <8d in adults (Hofer *et al.*, 2006). This recovery process, at least in critical period animals, is known to be dependent upon Trk-B signaling and be mediated by a reversal of the MD induced potentiation of the spared eye. We tested here if GluR1 removal might be one downstream target of this Trk-B dependent recovery process.

Although 3d MD has been repeatedly demonstrated to be insufficient to induce

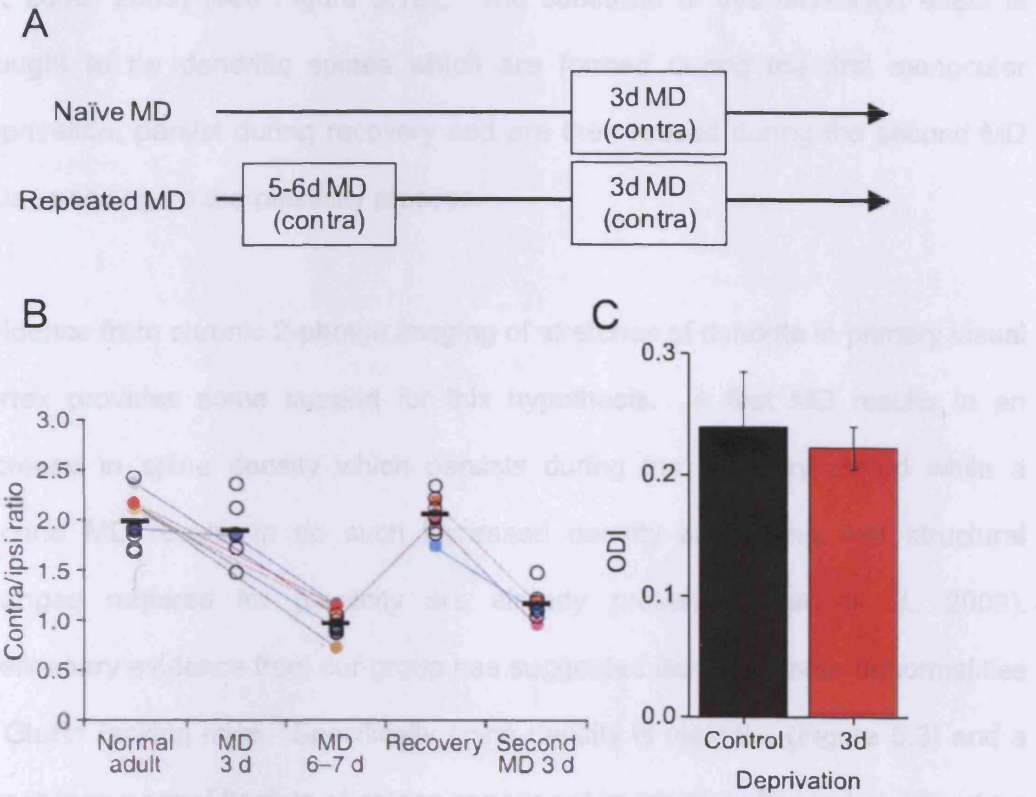

Figure 5.1 The prior experience paradigm.
A:Schematic of prior experience paradigm. B: The plasticity observed at different stages of the prior experience paradigm (adapted from Hofer et al., 2006). Coloured lines represent individual animals. C: The effect of 3d MD on adult mice, note no OD shift is apparent.

an OD shift in adult mice (Sawtell *et al.*, 2003; Hofer *et al.*, 2006; Sato & Stryker, 2008) two studies have shown that if a mouse has prior experience of having undergone an OD shift (either during the critical period or during adulthood) then this facilitates adult plasticity and permits an OD shift to occur after 3d (Hofer *et al.*, 2006, 2009) (see Figure 5.1B). The substrate of this facilitation effect is thought to be dendritic spines which are formed during the first monocular deprivation, persist during recovery and are then reused during the second MD thus speeding up the plasticity process.

Evidence from chronic 2-photon imaging of stretches of dendrite in primary visual cortex provides some support for this hypothesis. A first MD results in an increase in spine density which persists during the recovery period while a second MD results in no such increased density suggesting that structural changes required for plasticity are already present (Hofer *et al.*, 2009). Preliminary evidence from our group has suggested dendritic spine abnormalities in GluR1 lacking mice. Specifically spine density is elevated (Figure 5.3) and a larger than normal fraction of spines appear not to progress beyond an immature filopodia like state and are thus likely to be unstable (these observations were made by Dr Claire Cheetham). We hypothesized that if the substrate of the facilitation effect of prior experience is dendritic spines then we might see some expression of the GluR1 spine phenotype in the prior experience paradigm; that is the benefit of prior experience might be disrupted.

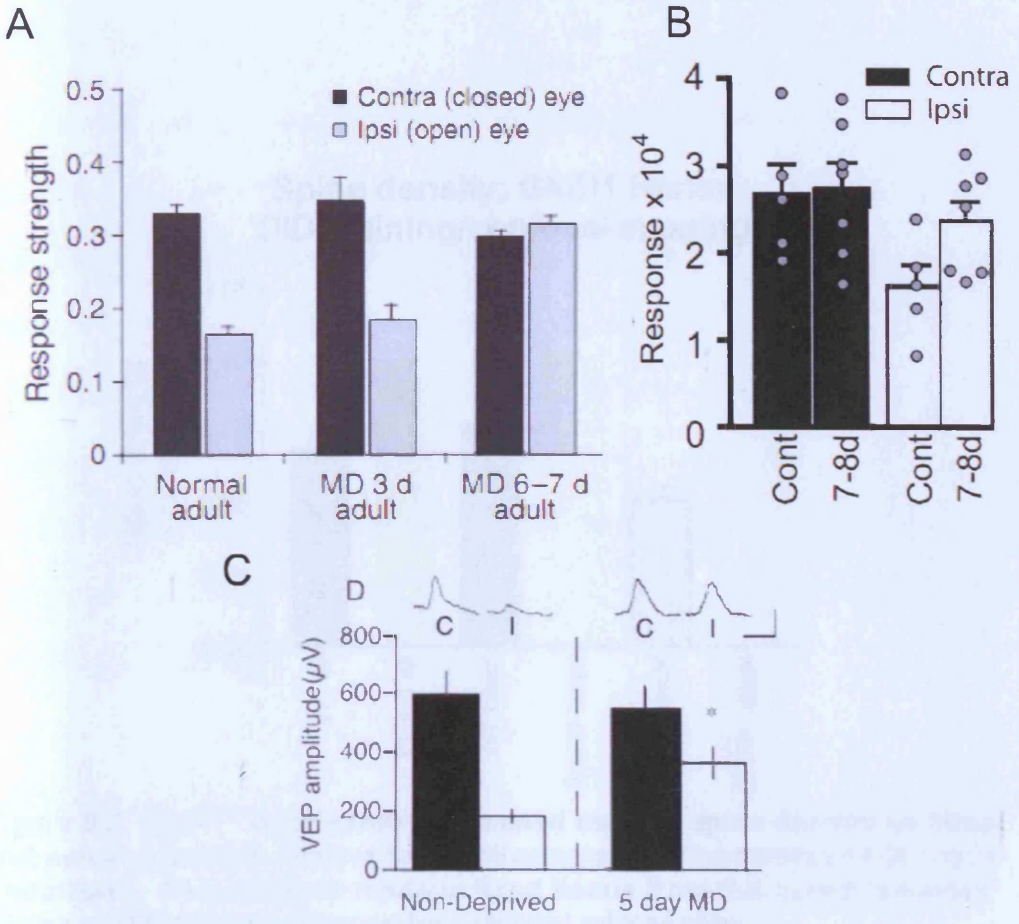

Figure 5.2 Consensus in the literature on the cause of adult OD shift
A consensus exists that adult OD plasticity is due to potentiation of the spared (ipsilateral) eye.
A: Intrinsic signal data reproduced from Hofer et al. (2006). B: Intrinsic signal data from Sato and Stryker (2008). C: VEP data from Sawtell et al. (2003).

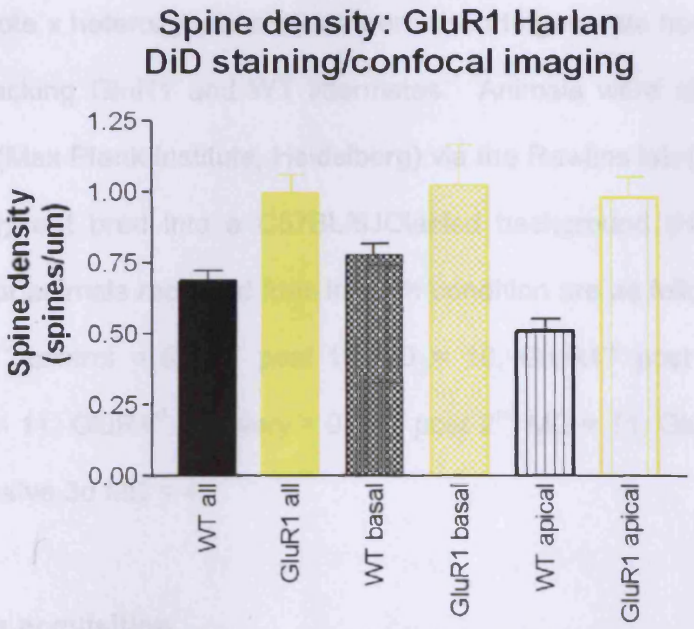

Figure 5.3 GluR1$^{-/-}$ mice exhibit increased cortical spine density on basal and apical dendrites relative to WT littermates (data courtesy of Dr Claire Cheetham). Observations made in fixed tissue from the somatosensory cortex of DiD labeled neurons by confocal microscopy.

5.2 Methods

5.2.1 Animals

The mouse colony was maintained as heterozygous GluR1-/- mutants and heterozygote x heterozygote crosses were used to generate homozygous mutant animals lacking GluR1 and WT littermates. Animals were obtained from Rolf Sprengel (Max Plank Institute, Heidelberg) via the Rawlins lab (Oxford) and were periodically out bred into a C57BL/6JOlaHsd background (Harlan, UK). The numbers of animals recorded from in each condition are as follows: WT control = 5, GluR1$^{-/-}$ control = 5, WT post 1st MD = 10, GluR1$^{-/-}$ post 1st MD = 8, WT recovery = 11, GluR1$^{-/-}$ recovery = 9, WT post 2nd MD = 11, GluR1$^{-/-}$ post 2nd MD = 8, WT naïve 3d MD = 4.

5.2.2 Data acquisition

Intrinsic signal imaging was carried out as described in Chapter 2.

5.2.3 Monocular deprivation

Monocular deprivation was carried out as described in the general methods. In the longitudinal imaging experiments (see Figure 5.1 The prior experience paradigm.) animals experienced an initial 6d MD during adulthood (at around P90) after which they were imaged to confirm an OD shift had occurred. Mice then experienced binocular vision for approximately 4 weeks after which recovery of a normal ODI was confirmed by imaging. Mice were then redeprived for a

further 3d and finally imaged to assess OD. A further group of animals experienced 3d MD at P120, after which they were imaged to confirm that this short MD is insufficient to induce OD plasticity in adults.

5.3 Results

5.3.1 3d MD is insufficient to induce an OD shift in adult animals

Previous studies have reported 3d MD is insufficient to induce an OD shift in adult animals (Sawtell *et al.*, 2003; Hofer *et al.*, 2006). This finding was confirmed by depriving a group of mice aged P120 for 3d and then imaging to measure OD. A 3d MD resulted in no significant alteration of ODI with control ODI = 0.24 ± 0.05 and 3d MD ODI = 0.22 ± 0.02 (Figure 5.1A).

5.3.2 6d MD results in a GluR1 independent OD shift in adult animals

A longer MD has been reported to induce OD plasticity in adult animals which is mediated by potentiation of the open eye (see Figure 5.2). We sought to confirm this by depriving WT mice for 6d at approximately P90 (mean age = 88.8 ± 3.75 days). This resulted in a strong OD shift from a control ODI of 0.24 ± 0.05 to a deprived ODI of 0.03 ± 0.01 ($P < 0.01$, t-test). To test whether this shift requires insertion GluR1 containing AMPARs a similar deprivation was conducted in mice lacking GluR1. GluR1$^{-/-}$ mice underwent an OD shift indistinguishable from WT, with ODI moving from 0.26 ± 0.09 to 0.03 ± 0.01 ($P < 0.01$, t-test), indicating that adult MD induced open eye potentiation occurs in the absence of GluR1 (Figure 5.4).

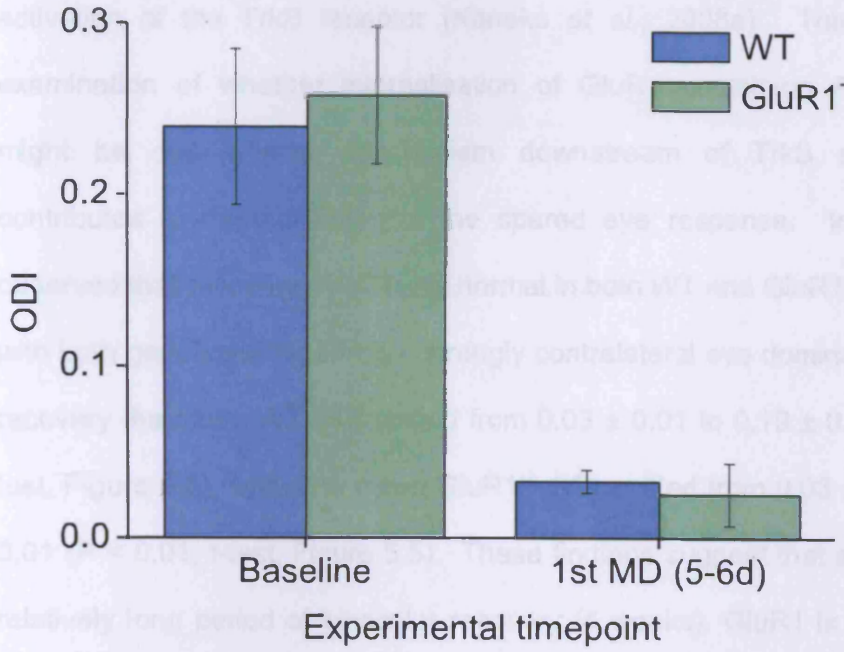

Figure 5.4 5-6d MD results in a robust OD shift in adult mice.

5.3.3 Role of GluR1 in the recovery from MD

A period of binocular visual experience after an OD shift has occurred has been reported to result in a recovery of a normal ODI in both juvenile (Hofer *et al.*, 2006; Kaneko *et al.*, 2008a) and adult mice (Hofer *et al.*, 2006). In juvenile mice it has been reported that recovery of normal ODI occurs over <4d and requires activation of the TrkB receptor (Kaneko *et al.*, 2008a). This study allowed examination of whether internalisation of GluR1 containing AMPA receptors might be one effector mechanism downstream of TrkB signaling which contributes to depotentiation of the spared eye response. In this study we observed that recovery of ODI was normal in both WT and GluR1 lacking animals with both genotypes regaining a strongly contralateral eye dominance. Following recovery the mean WT ODI shifted from 0.03 ± 0.01 to 0.19 ± 0.02 ($P < 0.01$, t-test, Figure 5.5), while the mean GluR1$^{-/-}$ ODI shifted from 0.03 ± 0.02 to 0.19 ± 0.01 ($P < 0.01$, t-test, Figure 5.5). These findings suggest that at least over this relatively long period of binocular recovery (4 weeks), GluR1 is not required for recovery. There is considerable variability in the ODI observed basally in both WT and GluR1$^{-/-}$ mice and it has been reported that the ODI of individual animals remains stable over time (Kaneko *et al.*, 2008b). In order to ascertain whether the ODI of individual animals recovers to their pre-MD balance, pre-MD ODI was plotted against post-recovery ODI. There was no significant correlation observed between these two measures (Figure 5.6).

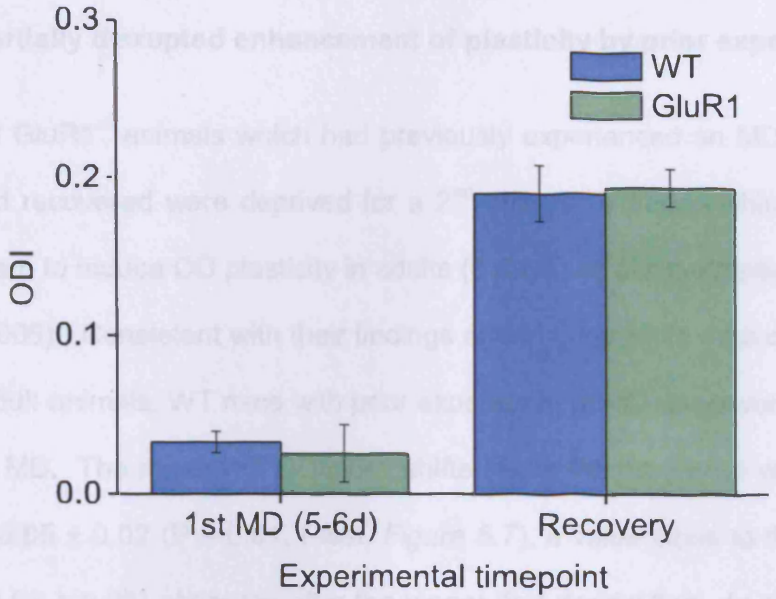

Figure 5.5 Recovery from MD in adulthood does not require GluR1.

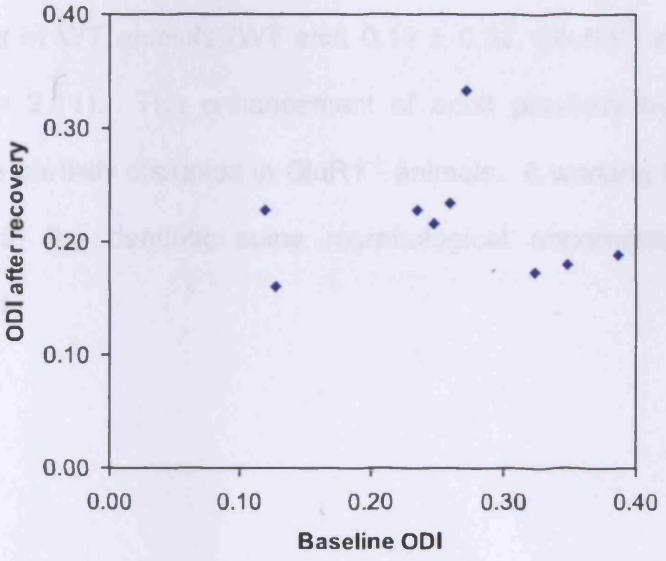

Figure 5.6 Individual mouse's ODI after recovery is uncorrelated with baseline ODI ($R^2 = 0.005$).

5.3.4 Partially disrupted enhancement of plasticity by prior experience

WT and GluR1$^{-/-}$ animals which had previously experienced an MD-induced OD shift and recovered were deprived for a 2nd time for a period which is normally insufficient to induce OD plasticity in adults (3 days) as per the paradigm of Hofer et al. (2006). Consistent with their findings and in contrast to data collected from naïve adult animals, WT mice with prior experience of MD underwent an OD shift after 3d MD. The mean WT OD index shifted from the recovered value of 0.19 ± 0.02 to 0.05 ± 0.02 ($P < 0.01$, t-test, *Figure 5.7*), a value close to the mean ODI value (0.03 ± 0.01) observed after the longer first deprivation. In contrast, while GluR1$^{-/-}$ mice underwent a significant OD shift from 0.19 ± 0.01 to 0.12 ± 0.02 ($P < 0.01$, t-test, *Figure 5.7*), the size of the shift was significantly smaller than that observed in WT animals (WT shift 0.14 ± 0.02, GluR1$^{-/-}$ shift 0.08 ± 0.02, $P < 0.05$, $t = 2.11$). The enhancement of adult plasticity by prior experience is therefore partially disrupted in GluR1$^{-/-}$ animals. A working hypothesis is that this is due to the dendritic spine morphological abnormalities which we have observed.

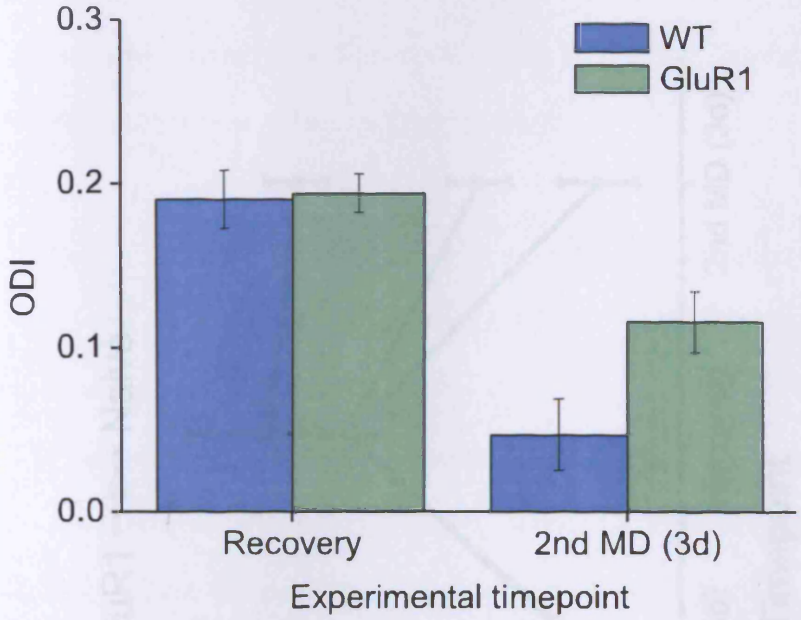

Figure 5.7 Plasticity enhancement due to prior experience is reduced in mice lacking GluR1 relative to age matched WT littermates.

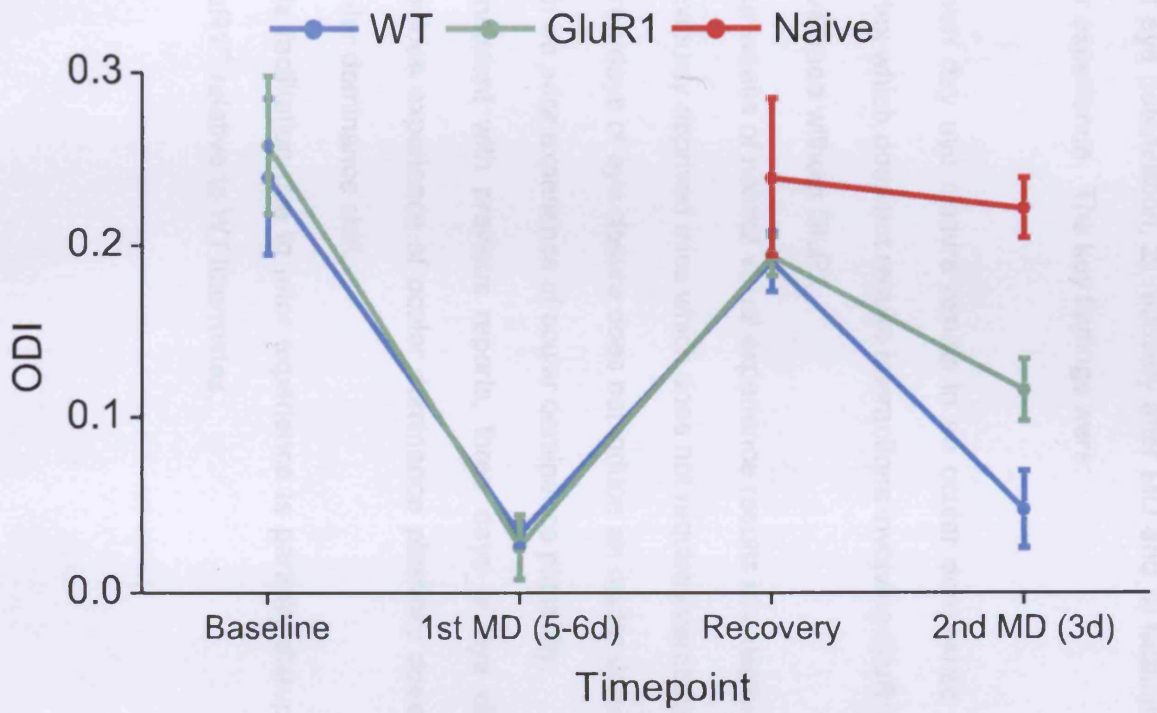

Figure 5.8 The timecourse of the complete prior experience paradigm in WT and GluR1$^{-/-}$ mice. ***A subset of mice was imaged at each of the four time points. Other time points are constituted of mice which had been exposed to the same visual experience but only imaged at 1-2 time points.***

5.4 Summary of findings

The aim of the experiments presented in this chapter was to examine the importance of interactions involving the GluR1 receptor during adult visual cortex plasticity. Three processes were investigated: 1) monocular eye closure induced spared eye potentiation, 2) recovery after MD and 3) facilitation of plasticity due to prior experience. The key findings were:

1. Seven day eye closure results in an ocular dominance shift in adult visual cortex which does not require interactions involving GluR1 in mice which have developed without GluR1.
2. Four weeks of normal visual experience results in a recovery of binocularity in previously deprived mice which does not require interactions involving GluR1.
3. Three days of eye closure does not induce an ocular dominance in adult mice with no prior experience of ocular dominance plasticity.
4. Consistent with previous reports, three days of eye closure in mice with previous experience of ocular dominance plasticity does result in a reliable ocular dominance shift.
5. This facilitation due to prior experience is partially disrupted in mice lacking GluR1$^{-/-}$ relative to WT littermates.

Chapter 6.Strain differences in plastic response to monocular deprivation and dark exposure

6.1 Introduction

A serendipitous discovery during studies of the GluR1$^{-/-}$ mouse was that the inbred C57BL/6J substrain on which it was generated (C57BL/6JOlaHsd, Harlan UK) had a severe plasticity deficit when compared to other C57BL/6 substrains (for example C57BL/6J, Charles River, UK).

The C57BL/6JOlaHsd is the default C57BL/6J mouse supplied by Harlan in much of Europe. It was identified in 2001 that the C57BL/6J mice being sold by Harlan carried a chromosomal deletion of a 365kb locus which includes the genes Sncg (coding the presynaptic protein α-synuclein) and Mmrn2 (coding the protein multimerin-1) (Specht & Schoepfer, 2001, 2004). As this strain had been used by many neuroscience experimenters interchangeably with other C57BL/6J mice acquired from other companies (which did contain the locus deleted in C57BL/6JOlaHsd), and because α-synuclein is a synaptically localised protein, some research effort was directed towards determining if the strain expressed a plasticity phenotype. One study found no plasticity deficits in spatial learning in the C57BL/6JOlaHsd strain (Chen et al., 2002). Another series of experiments found no differences in fear conditioning induction while extinction of conditioned fear occurred more slowly in the C57BL/6JOlaHsd mouse relative to C57BL/6J (Stiedl et al., 1999; Siegmund et al., 2005).

In the course of the experiments described in Chapters 3 and 4 an ocular dominance plasticity deficit was observed in the WT littermates of GluR1$^{-/-}$ mice.

Specifically I observed that the delayed homeostatic plasticity reported in the literature was absent. One possibility was that the plasticity deficits we observed could be due to inadvertent contamination of the genetic background of our GluR1 knockout mouse colony with genetic material from another knockout strain. For the experiments described in this chapter I therefore purchased C57BL/6JOlaHsd mice directly from Harlan and compared them unless otherwise stated to mice of the C57BL/6J strain purchased directly from Charles River. In this chapter I describe a number of experiments designed to further probe this homeostatic plasticity deficit. Monocular deprivation and dark rearing were used to induce a homeostatic plastic response which was then measured in vivo using functional imaging of intrinsic signals and in vitro by measuring spontaneous miniature excitatory postsynaptic potentials (mEPSPs). As α-synuclein is one protein absent in C57BL/6JOlaHsd animals, homeostasis was assessed in animals of another strain which had α-synuclein deliberately knocked out. Additionally in this chapter I provide evidence that supports a dissociation of critical period versus adult mechanisms of open eye potentiation.

6.2 Methods

6.2.1 Animals

Almost all studies in this chapter compare the spontaneous mutation carrying C57BL/6JOlaHsd mouse strain (Harlan, UK) with the C57BL/6J mouse strain (provided under licence from Jackson Laboratories, USA by Charles River, UK). In this chapter I have abbreviated the Harlan strain (C57BL/6JOlaHsd) to

"6JOlaHsd" and the Jackson strain (C57BL/6J) to "6J". All animals were bought specifically for the experiments.

One exception is the studies conducted on α-synuclein knockout mice which were performed on homozygous knockout animals and WT animals of a matched genetic background (C57BL/6JCrl, Charles River, UK) provided by Prof Vladimir Buchman, Cardiff University School of Biosciences.

In the in vivo experiments described the following numbers of animals were used in the various conditions: MD studies - control 6J = 10, 3d MD 6J = 8, 5-6d MD 6J = 9, control 6JOlaHsd = 21, 3d MD 6JOlaHsd = 6, 5d MD 6JOlaHsd = 11; DR studies - control 6J = 16, 3d DR 6J = 6, control 6JOlaHsd = 16 , 3d DR 6JOlaHsd = 7; scatter comparisons – 6J = 5, 6JOlaHsd = 5; α-synuclein studies – control WT = 9, 5d MD WT = 6, control $\alpha^{-/-}$ = 6, 5d MD $\alpha^{-/-}$ = 5. In the in vitro synaptic scaling studies the following numbers of mice were used: control 6J = 6, 3d DR 6J = 6, control 6JOlaHsd = 6, 3d DR 6JOlaHsd = 6.

6.2.2 Monocular deprivation

Animals were monocularly deprived under isoflurane anaesthetic by the protocol described in Chapter 2. Critical period monocular deprivations began at postnatal day 26-28 and lasted for either 3 or 5-6 days, thus physiological recordings were made between postnatal days 29-34. Adult deprivations began around P90 and lasted for 6 days.

6.2.3 Dark exposure

Animals were dark exposed by being placed in a light isolated antechambered room. Animals were cared for with the aid of infrared goggles under infrared illumination. Dark exposure lasted for 3 days after which animals were anaesthetized in the room before being exposed to light.

6.2.4 Data acquisition

Intrinsic signal imaging was carried out as described in Chapter 2.

6.2.5 Ex vivo assay of homeostatic plasticity. Written by CC.

P28-P31 control or dark-exposed mice were anaesthetised with isoflurane, killed by cervical dislocation and decapitated, and brains were rapidly removed into ice-cold dissection buffer (in mM: 108 choline-Cl, 3 KCl, 26 NaHCO3, 1.25 NaH2PO4, 25 D-glucose, 3 Na-pyruvate, 1 CaCl2, 6 MgSO4, 285 mOsm) bubbled with 95% O2/5% CO2. 400 µm thick coronal slices were cut through V1 using a VT1000S microtome (Leica Microsystems). Brain slices were incubated in a submerged chamber in artificial cerebrospinal fluid (ACSF; in mM: 119 NaCl, 3.5 KCl, 1 NaH2PO4, 10 D-glucose, 2 CaCl2, 1 MgSO4, 300 mOsm) bubbled with 95 % O2/ 5 % CO2, at 32 °C for 45 min, and then at room temperature until recording. Slices containing V1 were selected by observation of anatomical landmarks and L2/3 pyramidal neurons were identified under infrared differential interference contrast (IR-DIC) optics using an Olympus BX50WI microscope. Whole cell recordings were made at 35 – 37 °C. Recording pipettes (4 – 6 MΩ)

contained in mM: 130 KMeSO4, 8 NaCl, 2 KH2PO4, 2 D-glucose, 10 HEPES, 4 Mg-ATP, 7 phosphocreatine, 0.3 GTP, 0.5 ADP, pH 7.30, 285 mOsm. Recorded neurons had resting membrane potentials ≤ -70 mV, not corrected for the liquid junction potential of + 8 mV. mEPSCs were recorded at a holding potential of -75 mV. mEPSCs were low-pass filtered at 3 kHz, and data were digitised at 20 kHz (micro1401) and recorded using Signal v.4.05 (all Cambridge Electronic Devices). Input resistance was monitored throughout recordings by injection of square hyperpolarising current pulses. mEPSCs were isolated with 1 µM tetrodotoxin, 100 µM picrotoxin and 50 µM D-AP5 (all Tocris). Action potential blockade was confirmed by injection of square depolarising current pulses (1 nA, 500 ms). ≥100 mEPSCs per cell were detected and measured using MiniAnalysis (Synaptosoft), using previously described shape and amplitude threshold criteria.

6.3 Results

6.3.1 Between-strain basal responses

The intrinsic signal responses of control 6J and 6JOlaHsd animals were first examined. All absolute intrinsic signal response magnitudes are presented as $\Delta R/R \times 10^{-4}$. In the monocular cortical area response magnitudes between the two strains were statistically indistinguishable (Figure 6.1A). The mean 6J response magnitude was 1.34 ± 0.16 and the mean 6JOlaHsd was 1.47 ± 0.11 ($P = 0.5$, t-test). In contrast in the binocular area a basal difference in OD index was observed between strains with the mean 6J ODI measured as 0.31 ± 0.03 and the mean 6JOlaHsd ODI measured as 0.21 ± 0.03 ($P < 0.05$, t-test, Figure

6.1B). Both contralateral and ipsilateral binocular response magnitudes were observed to differ between strains with both being marginally larger in 6JOlaHsd than 6J animals. The mean 6J contralateral response was 1.2 ± 0.13 while the mean 6JOlaHsd contralateral response was 1.4 ± 0.07 (Figure 6.1A). The mean 6J ipsilateral response was 0.6 ± 0.06 while the mean 6JOlaHsd ipsilateral response was 1.0 ± 0.07. The difference in ipsilateral response magnitude was statistically significant ($P < 0.01$, t-test) and accounted for the most part of the differences in ODI between the strains.

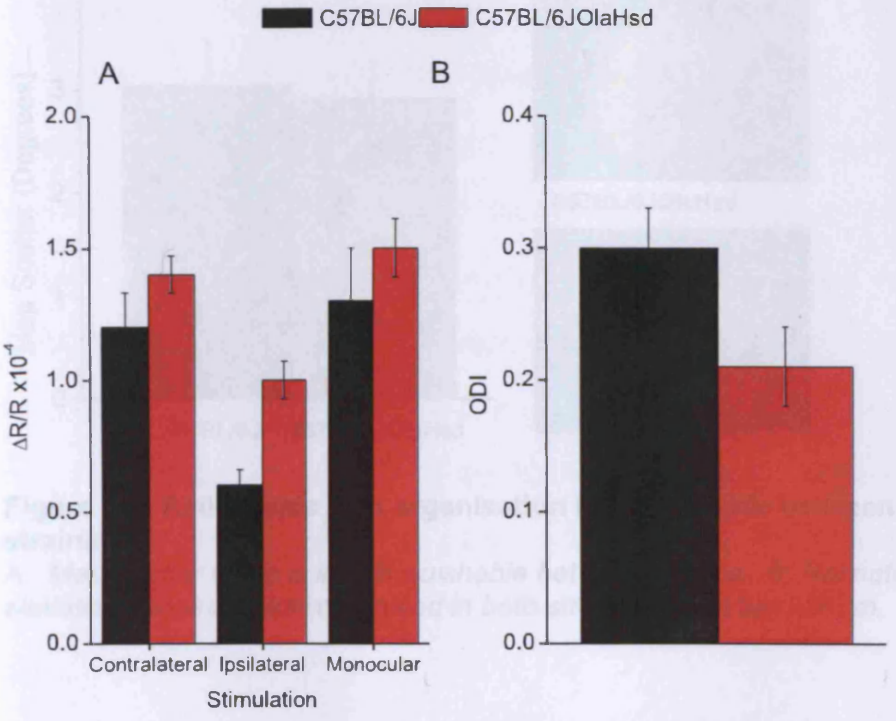

Figure 6.1 Comparison of basal responses in C57BL/6J and C57BL/6JOlaHsd mice.
A: Absolute intrinsic signal magnitudes. Note the significantly larger ipsilateral response magnitude observed in the C57BL/6JOlaHsd strain. B: Ocular Dominance Index (ODI) as measured using intrinsic signal imaging. Binocular cortex in C57BL/6J mice is significantly more contralateral eye dominated.

In a subset of juvenile animals the scatter of cortical maps was compared between the two strains in order to assess if there were any gross differences in retinotopic organisation. The mean scatter values for C57BL/6J and C57BL/6JOlaHsd animals were 3.0 ± 0.44 degrees and 2.9 ± 0.37 degrees respectively (P = 0.87, t-test, Figure 6.2).

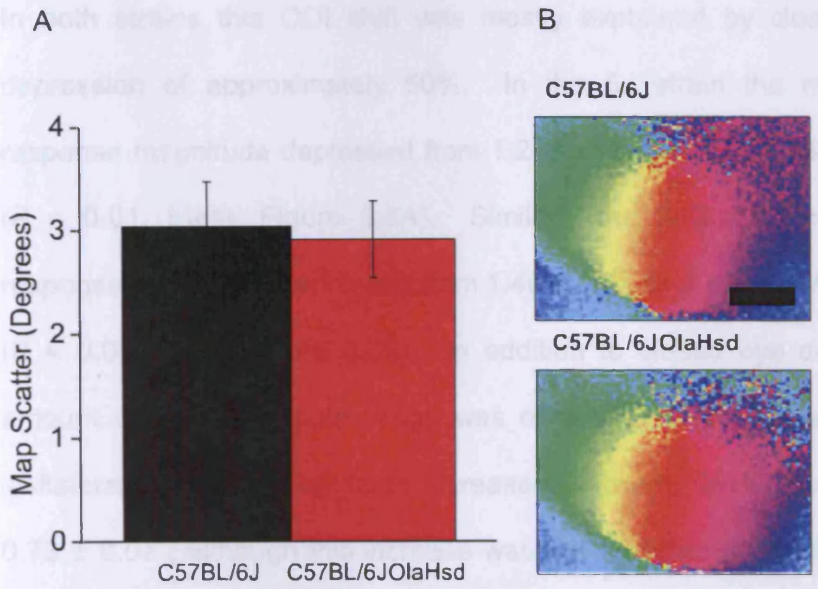

Figure 6.2 Retinotopic map organisation is comparable between the two strains.
A: Map scatter value is indistinguishable between strains. B: Retinotopic elevation maps are well organised in both strains. Scale bar 500μm.

6.3.2 MD induced closed eye depression

Animals of both strains were monocularly deprived for 3d in order to examine if there was a strain difference in closed eye depression. Both strains expressed a strong ODI shift towards the open eye. Mice of the 6J strain shifted from 0.31 ± 0.03 to -0.13 ± 0.05 ($P < 0.001$, t-test) while mice of the 6JOlaHsd strain shifted from 0.21 ± 0.03 to -0.11 ± 0.05 ($P < 0.001$, t-test).

In both strains this ODI shift was mostly explained by closed eye response depression of approximately 50%. In the 6J strain the mean contralateral response magnitude depressed from 1.2 ± 0.13 to 0.58 ± 0.06, a 52% decrease ($P < 0.01$, t-test, Figure 6.3A). Similarly the 6JOlaHsd mean contralateral response magnitude depressed from 1.40 ± 0.07 to 0.75 ± 0.07, a 46% decrease ($P < 0.01$, t-test, Figure 6.3B). In addition to closed eye depression a small amount of open eye potentiation was observed in the 6J strain such that the ipsilateral response magnitude increased following 3dMD from 0.60 ± 0.06 to 0.73 ± 0.07 , although this increase was not statistically significant ($P = 0.15$, t-test, Figure 6.3A). In contrast in the 6JOlaHsd strain the ipsilateral response magnitude remained stable with a control mean of 0.96 ± 0.07 and a deprived mean of 0.97 ± 0.08 ($P = 0.98$, t-test, Figure 6.3B).

The monocular cortex contralateral to the deprived eye was also examined after 3dMD in the two strains. Although both exhibited a similar percentage depression in monocular response, only the depression measured in the 6J strain was statistically significant. The monocular response in the 6J strain depressed

from 1.34 ± 0.16 to 0.83 ± 0.81 ($P < 0.05$, t-test) while in the 6JOlaHsd strain the monocular response decreased from 1.5 ± 0.11 to 1.07 ± 0.13 ($P = 0.09$, t-test).

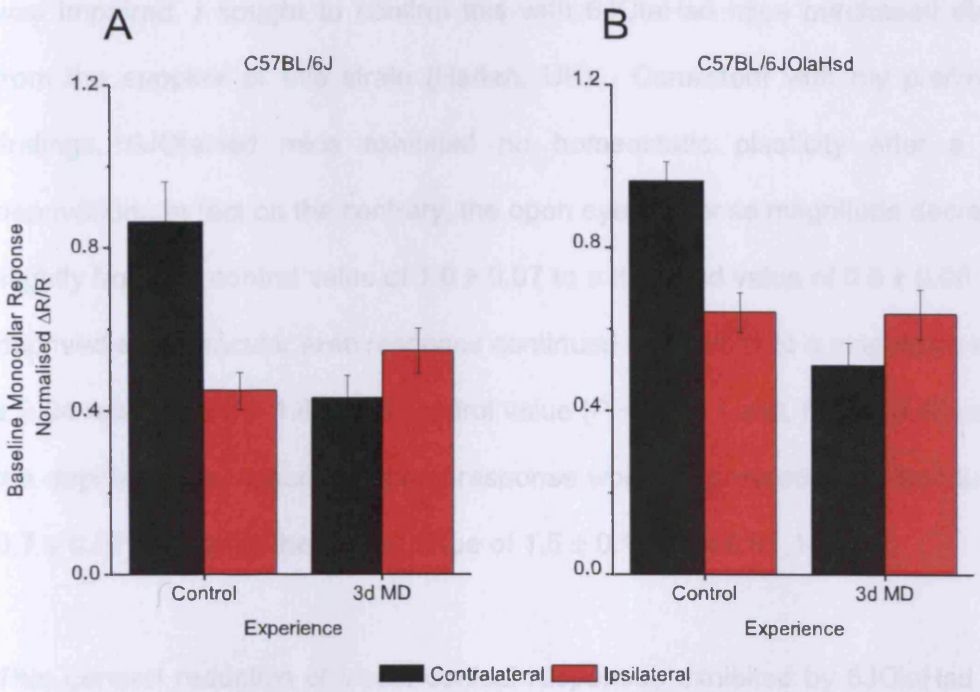

Figure 6.3 Effects of short (3d) monocular experience.
A & B: Closed eye depression is normal in both strains during the critical period. Values are normalised to the genotypic baseline monocular response.

6.3.3 MD induced open eye homeostatic potentiation

Although preliminary work with WT littermates of GluR1$^{-/-}$ animals (on a 6JOlaHsd background) had indicated that critical period open eye potentiation was impaired, I sought to confirm this with 6JOlaHsd mice purchased directly from the supplier of this strain (Harlan, UK). Consistent with my preliminary findings, 6JOlaHsd mice exhibited no homeostatic plasticity after a 5-6d deprivation. In fact on the contrary, the open eye response magnitude decreased slightly from the control value of 1.0 ± 0.07 to a deprived value of 0.8 ± 0.08. The deprived eye binocular area response continued to depress to a magnitude of 0.5 ± 0.04 relative to the 1.4 ± 0.07 control value ($P < 0.01$. t-test, Figure 6.4B) as did the deprived eye monocular cortex response which depressed to a magnitude of 0.7 ± 0.07 relative to the control value of 1.5 ± 0.11 ($P < 0.01$, t-test).

This general reduction of visual cortical responses exhibited by 6JOlaHsd mice was in marked contrast to the plasticity profile of the 6J strain. The profile of plasticity in the 6J strain was consistent with previously published work on the effects of 5-6dMD during the critical period in that an apparently homeostatic plastic response was observed. In the 6J strain the response magnitude of the open eye increased significantly to 0.9 ± 0.08 from the control mean of 0.6 ± 0.06 ($P < 0.05$, t-test, Figure 6.4A). A hallmark that suggests a homeostatic plastic mechanism is engaged is the otherwise paradoxical increase in the response magnitude of the closed eye reported after longer deprivations. This was observed in the 6J strain in both binocular and monocular cortex as has

previously been described (Kaneko *et al.*, 2008b). The closed eye binocular cortex response increased from the 3d MD mean of 0.6 ± 0.08 to a 5-6dMD mean of 0.8 ± 0.08 ($P < 0.05$, t-test). Similarly the closed eye monocular response increased from the 3dMD mean of 0.8 ± 0.08 to a 5-6dMD mean of 1.1 ± 0.09 ($P < 0.05$, t-test). This data demonstrates that the plasticity deficit in 6JOlaHsd mice is specific to the later homeostatic plasticity period and suggests that plasticity during this time seems to be entirely accounted for by this homeostatic mechanism (Figure 6.5).

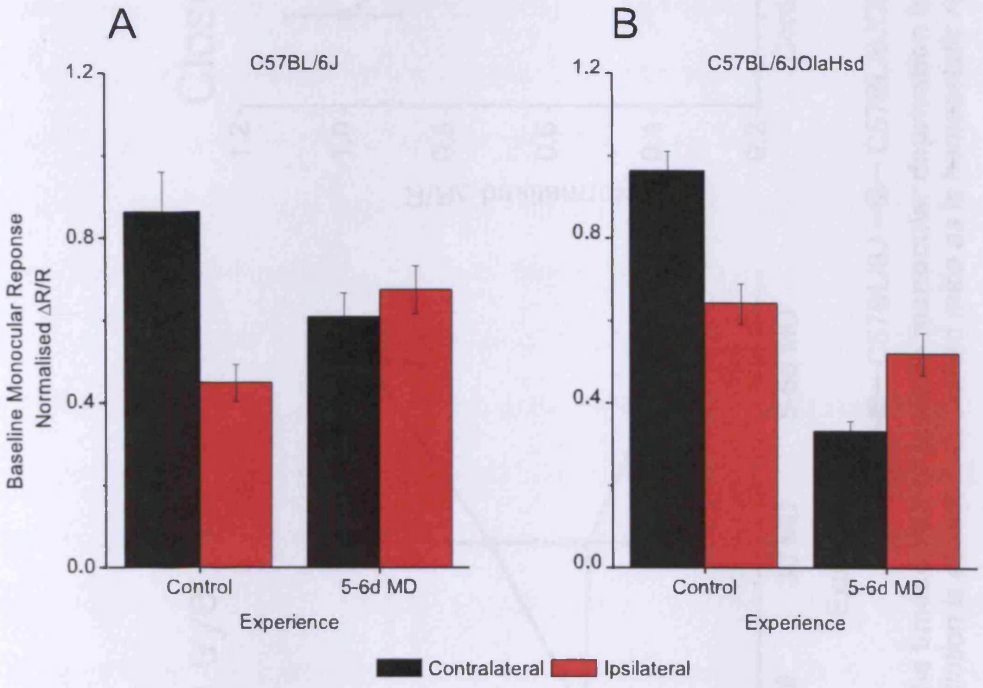

Figure 6.4 Effects of longer (5-6d) monocular experience.
A: 5-6d MD results in open eye potentiation in 6J mice. B: Open eye potentiation is absent in 6JOlaHsd mice after 5-6d MD.

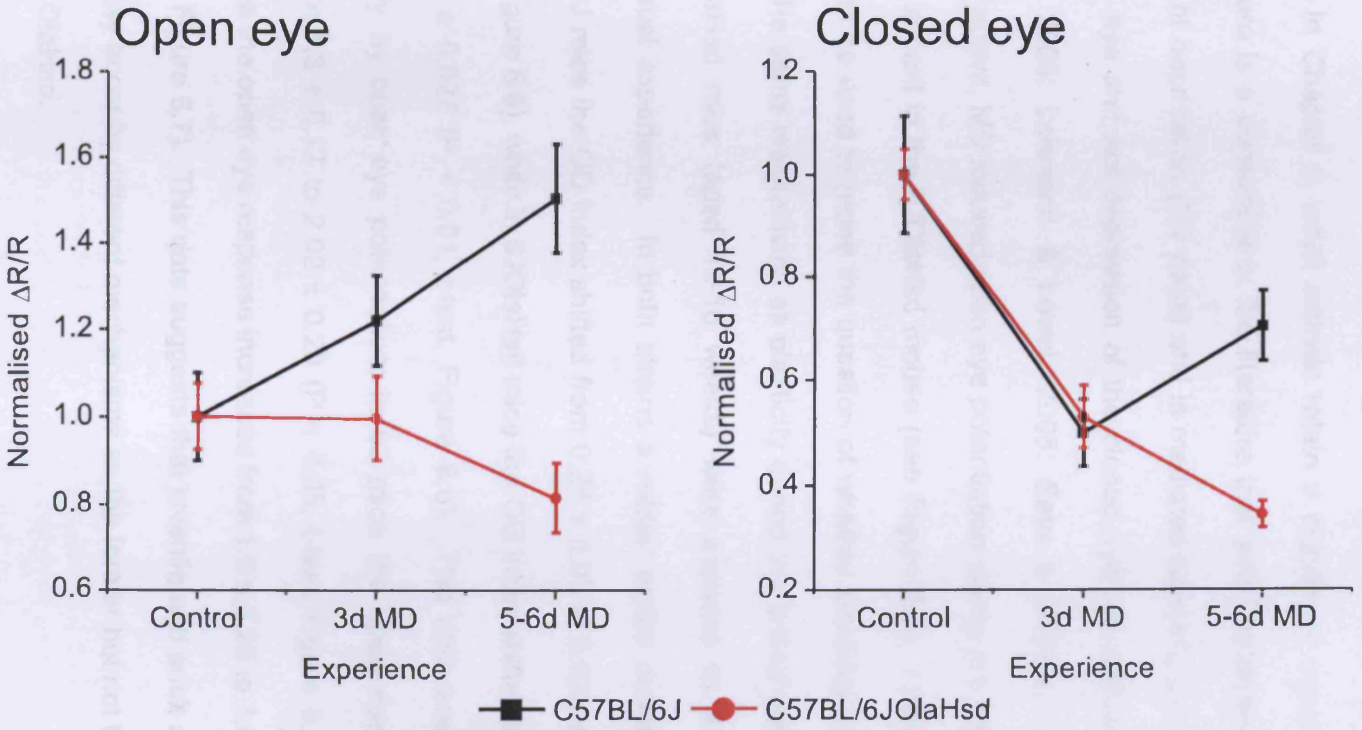

Figure 6.5 The timecourse of juvenile monocular deprivation in 6J versus 6JOlaHsd mice.
Open eye potentiation is absent in 6JOlaHsd mice as is homeostatic recovery of closed eye response.

6.3.4 Deficit in synaptic scaling leaves adult spared eye potentiation intact

As discussed in Chapter 5, adult animals retain a significant capacity for OD plasticity. There is a consensus in the literature that adult plasticity requires a longer period of deprivation (5-7 days) and is mediated primarily by potentiation of the spared eye and not depression of the closed eye (Sawtell *et al.*, 2003; Hofer *et al.*, 2006; Lehmann & Lowel, 2008; Sato & Stryker, 2008). As demonstrated above, MD induced open eye potentiation *during the critical period* is completely absent in the 6JOlaHsd mouse (see Figure 6.5), I reasoned that the strain could be used to probe the question of whether plasticity in adulthood proceeds by the same mechanisms as plasticity during the critical period. Adult 6J and 6JOlaHsd mice (aged 15-16 weeks) were exposed to 6-7 days of monocular visual experience. In both strains a robust ocular dominance shift occurred; in 6J mice the OD index shifted from 0.28 ± 0.07 to 0.023 ± 0.04 ($P < 0.01$, t-test, Figure 6.6), while in 6JOlaHsd mice the OD index shifted from 0.23 ± 0.05 to -0.05 ± 0.027 ($P < 0.01$, t-test, Figure 6.6). This shift was mediated almost entirely by open eye potentiation; in 6J mice the open eye response increased from 1.3 ± 0.17 to 2.02 ± 0.29 ($P < 0.05$, t-test, Figure 6.7) while in 6JOlaHsd mice the open eye response increased from 1.9 ± 0.26 to 3.0 ± 0.42 ($P < 0.05$, t-test, Figure 6.7). This data suggests that juvenile and adult spared eye potentiation may occur by different mechanisms as the former but not the latter is impaired in 6JOlaHsd.

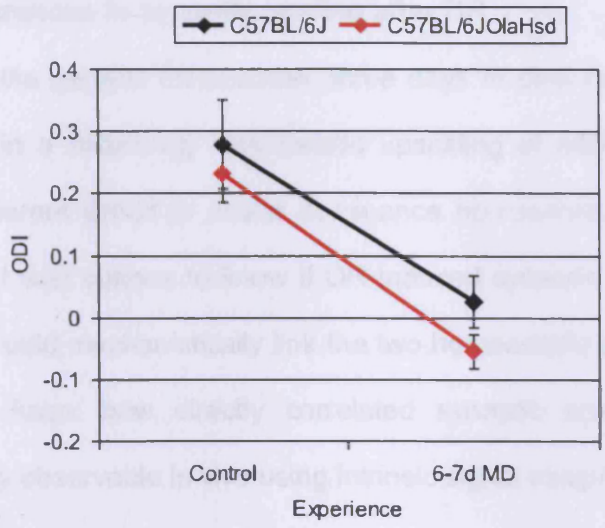

Figure 6.6 ODI shift is normal in adult C57BL/6JOlaHsd.

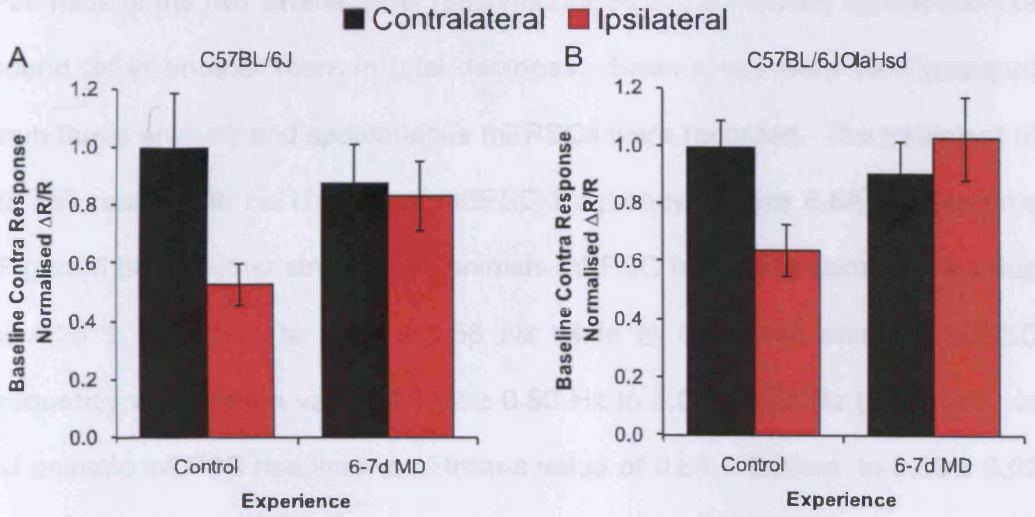

Figure 6.7 Ocular dominance plasticity is normal in adult C57BL/6JOlaHsd. As in C57BL/6J mice it is mediated primarily by open eye potentiation.

6.3.5 Strain differences in synaptic scaling after DR

As discussed in the general introduction, three days of dark rearing (3d DR) is known to result in a saturating homeostatic upscaling of mEPSPs. As I had identified an apparent deficit in ocular dominance homeostatic plasticity in the 6JOlaHsd strain I was curious to know if DR induced synaptic scaling was also impaired. This would mechanistically link the two homeostatic processes. I was also curious to know how directly correlated synaptic scaling is with the population activity observable in vivo using intrinsic signal imaging.

We first examined synaptic scaling ex vivo in 6J and 6JOlaHsd. Beginning at P26 mice of the two strains either remained for 3d in the normally lighted room or spend 3d in another room in total darkness. Brain slices were then prepared from these animals and spontaneous mEPSCs were recorded. The treatment of 3d DR resulted in no change of mEPSC frequency (Figure 6.8A) or rise time (Figure 6.8B) in either strain. In 6J animals mEPSC frequency went from a value of 4.25 ± 0.25 Hz to 4.43 ± 0.68 Hz while in 6JOlaHsd animals mEPSC frequency went from a value of 4.82 ± 0.60 Hz to 4.60 ± 0.57 Hz ($P = 0.90$). In 6J animals mEPSC rise time went from a value of 0.88 ± 0.03ms to 0.89 ± 0.02 ms while in 6JOlaHsd animals mEPSC rise time went from a value of 0.90 ± 0.02 ms to 0.87 ± 0.03 ms ($P = 0.88$).

A clear strain difference was however observed in the effect of DR on mEPSC amplitude. The 6J strain mice exhibited an upscaling of mEPSC amplitude after

3d DR relative to controls (Figure 6.9). Specifically in 6J mice the mEPSC amplitude increased by approximately 22% from 10.39 ± 0.43 pA to 12.72 ± 0.22 pA ($P < 0.01$). In contrast 6JOlaHsd animals showed no such scaling of synaptic currents; control amplitude was 9.65 ± 0.19 pA and deprived amplitude was 10.06 ± 0.71 pA ($P > 0.05$). This suggests firstly that synaptic scaling is disrupted in the C57BL/6JOlaHsd mouse strain. Secondly that there is some mechanistic overlap in the homeostatic processes engaged during MD and DR. And thirdly that in vivo intrinsic signal studies and ex vivo acute slice studies are likely to be providing a readout of the same phenomenon of homeostatic plasticity.

I next examined whether the DR induced scaling of mEPSCs observed ex vivo are correlated with scaling up of intrinsic signal magnitudes in vivo. Animals received identical conditioning to that in the ex vivo studies (either 3d in normally lighted conditions or 3dDR) after which they were prepared for intrinsic signal imaging.

In the case of 6J animals mEPSC scaling was observed ex vivo and I therefore hypothesised that if there was a simple linear relationship between mEPSC and

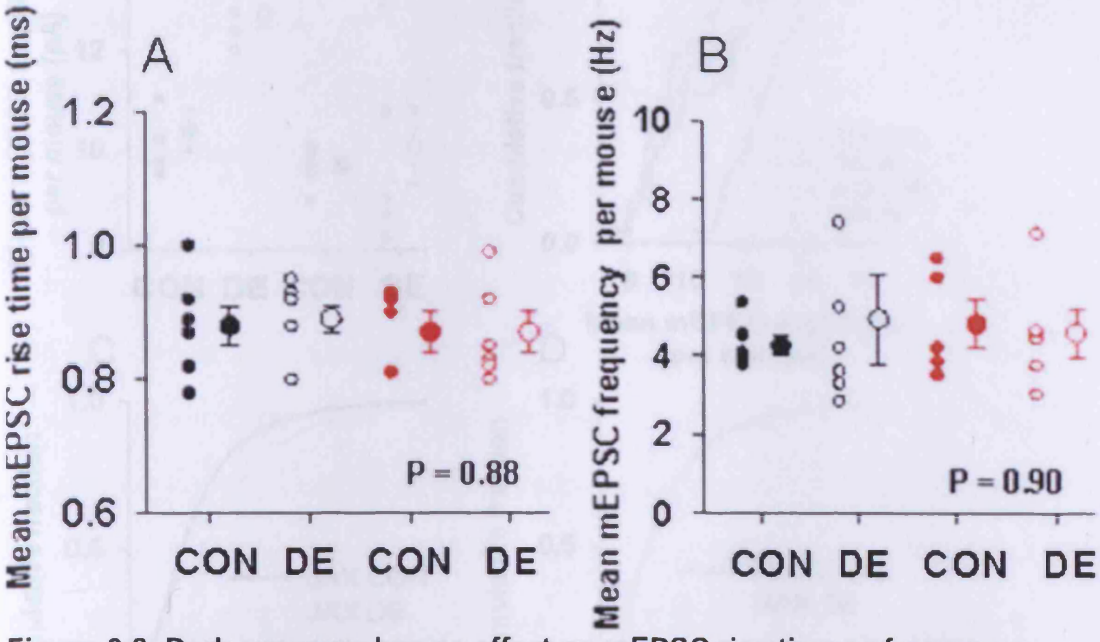

Figure 6.8 Dark exposure has no effect on mEPSC rise time or frequency.
CON are control values while DE are dark exposed.

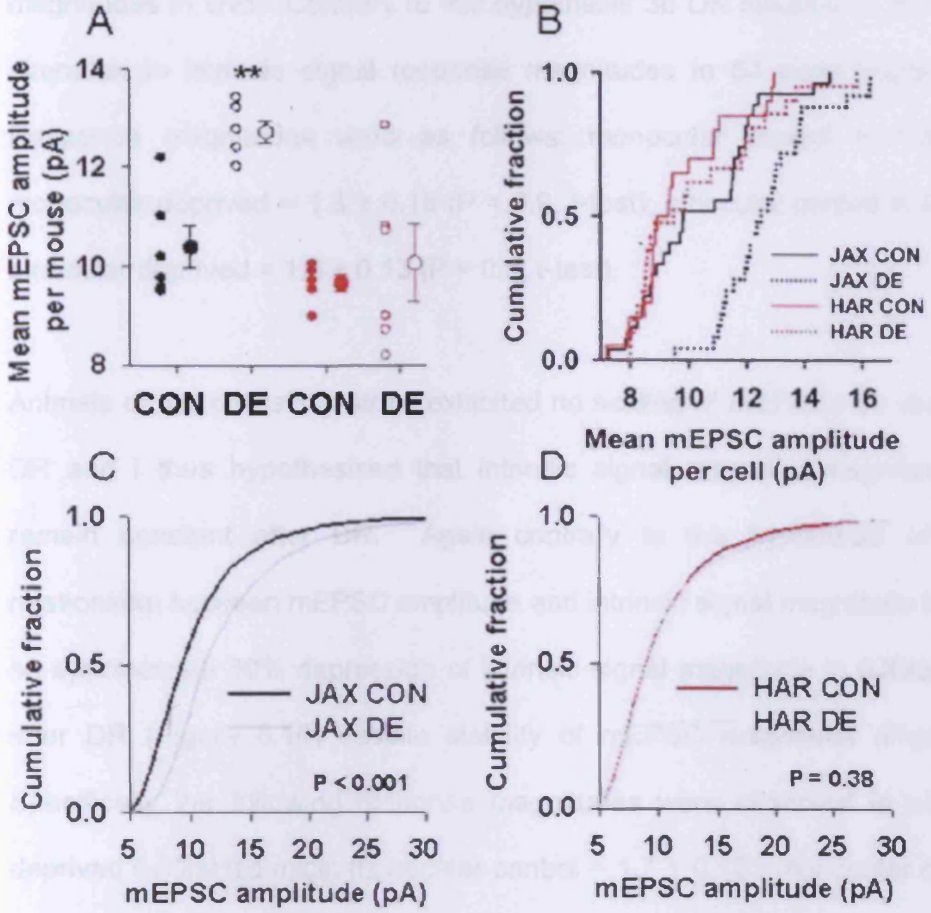

Figure 6.9 Synaptic scaling is impaired in C57BL/6JOlaHsd mice.
A: After 3d dark exposure, per mouse mean mEPSC amplitude increases in C57BL/6J mice (black) while that of C57BL/6JOlaHsd mice (red) remains the same on average. CON are control values while DE are dark exposed. B: Cumulative frequency distribution of cells recorded in each condition. C & D: Distribution of mEPSC events shifts to a greater amplitude in C57BL/6J mice after dark exposure (C), while that of C57BL/6JOlaHsd mice remains the same (D).

intrinsic signal amplitude then I might observe a scaling of intrinsic signal magnitudes in vivo. Contrary to this hypothesis 3d DR resulted in no significant alteration in intrinsic signal response magnitudes in 6J mice (Figure 6.10A). Response magnitudes were as follows: monocular control = 1.3 ± 0.11, monocular deprived = 1.3 ± 0.18 (P = 0.9, t-test); binocular control = 1.4 ± 0.11, binocular deprived = 1.6 ± 0.13 (P = 0.5, t-test).

Animals of the 6JOlaHsd strain exhibited no scaling of mEPSCs ex vivo after 3d DR and I thus hypothesised that intrinsic signal response magnitudes might remain constant after DR. Again contrary to the hypothesis of a direct relationship between mEPSC amplitude and intrinsic signal magnitude I observed an approximate 30% depression of intrinsic signal magnitude in 6JOlaHsd mice after DR (Figure 6.10) despite stability of mEPSC magnitude (Figure 6.9A). Specifically the following response magnitudes were observed in control and deprived 6JOlaHsd mice: monocular control = 1.7 ± 0.12 , monocular deprived = 1.3 ± 0.13 (P = 0.054, t-test); binocular control = 2.1 ± 0.15, binocular deprived = 1.5 ± 0.13 (P < 0.05 , t-test).

It is known from ex vivo experiments that dark exposure induced synaptic scaling is reversed entirely after one day of light exposure (Goel *et al.*, 2006) and this process might occur even more rapidly. Although animals were anaesthetised while still in the dark before being prepared for imaging and then imaged as rapidly as possible, there is still the possibility that scaling could be lost,

particularly during the intense visual simulation required during functional imaging. In order to address this question, in a subset of mice visual responses were examined on a block by block basis during the imaging session. If scaling was being reversed one might expect to see a trend of loss of scaling and decreasing visual response during the imaging session, however no such trend was visible (Figure 6.11).

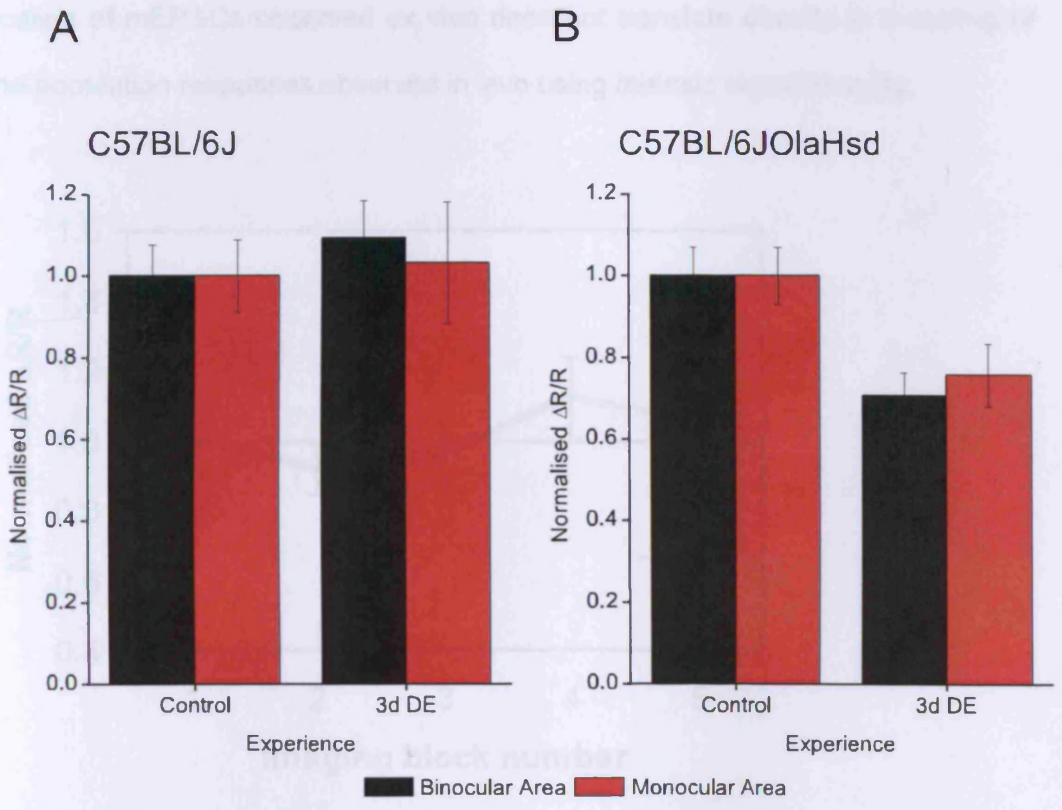

Figure 6.10 The effects of acute 3d dark exposure on visual cortical responses in juvenile 6J and 6JOlaHsd mice

The in vivo and ex vivo DR studies confirm firstly that there exists a profound difference in the manner in which the visual cortices of C57BL/6J and C57BL/6JOlaHsd mice respond to reduced visual input. C57BL/6J mice exhibit the previously reported phenomenon of DR induced synaptic scaling and perhaps through this mechanism maintain population activity at a constant level. In contrast C57BL/6JOlaHsd mice do not show DR induced synaptic scaling and perhaps as a result of this exhibit a general trend towards an atrophy of visual cortical responses during DR. A second finding of these studies is that the scaling of mEPSCs observed ex vivo does not translate directly to a scaling of the population responses observed in vivo using intrinsic signal imaging.

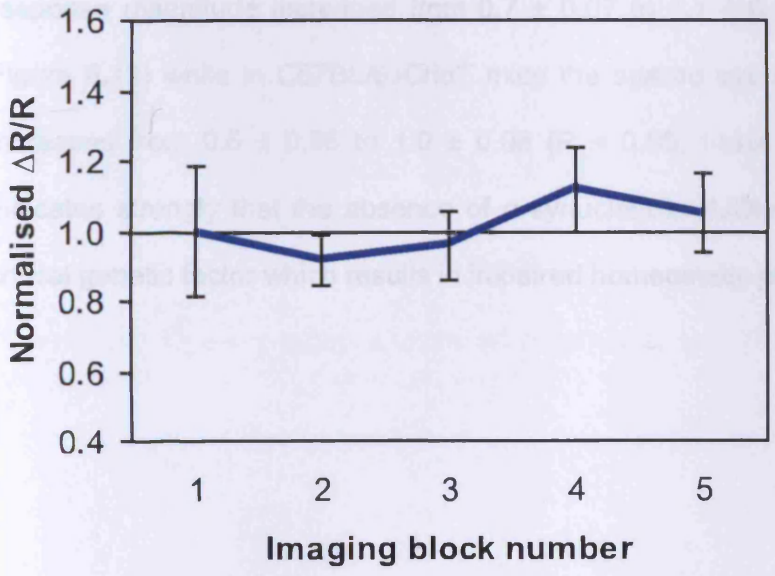

Figure 6.11 Binocular visual responses are stable during imaging session following 3d dark exposure.

6.3.6 Homeostatic plasticity is unimpaired during the critical period in non-C57BL/6JOlaHsd α -synuclein$^{-/-}$ mice

As the α-synuclein gene is known to be absent in the 6JOlaHsd mouse strain I decided to test whether homeostatic plasticity was disrupted in C57BL/6JCrl mice which had the α-synuclein gene deliberately ablated while leaving other genes that are absent in 6JOlaHsd intact (C57BL/6JCrlα$^{-/-}$ mice). α-synuclein$^{-/-}$ mice were monocularly deprived for 5d (5d MD) and then the spared eye response magnitude was compared with the spared eye response magnitude of non-deprived animals of matched genetic background by intrinsic signal imaging. C57BL/6JCrl and C57BL/6JCrlα$^{-/-}$ mice exhibited comparable degree of potentiation of the spared eye. In C57BL/6JCrl mice the spared eye mean response magnitude increased from 0.7 ± 0.07 to 1.1 ± 0.13 ($P < 0.05$, t-test, Figure 6.12) while in C57BL/6JCrlα$^{-/-}$ mice the spared eye response magnitude increased from 0.6 ± 0.06 to 1.0 ± 0.08 ($P < 0.05$, t-test, Figure 6.12). This indicates strongly that the absence of α-synuclein in 6JOlaHsd mice is not the critical genetic factor which results in impaired homeostatic plasticity.

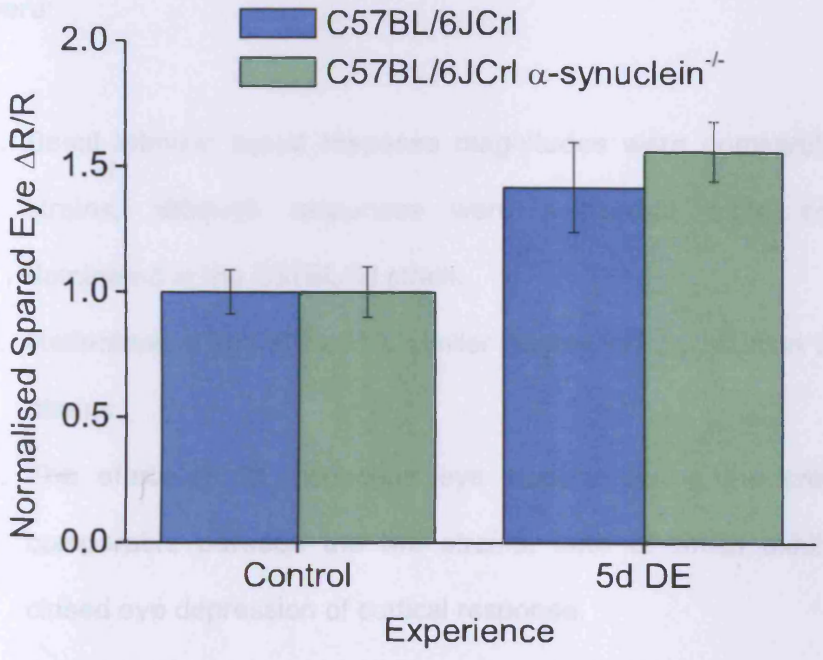

Figure 6.12 Open-eye potentiation after 5d MD is preserved in mice lacking α-synuclein.

6.4 Summary of findings

The aim of the experiments presented in this chapter was to characterise a serendipitous discovery which I made of a homeostatic plasticity deficit in a common inbred mouse strain (C57BL/6JOlaHsd, Harlan). In most experiments C57BL/6JOlaHsd mice were compared to C57BL/6J mice. The key findings were:

1. Basal intrinsic signal response magnitudes were comparable between the strains, although responses were somewhat more contralateral eye dominated in the C57BL/6J strain.
2. Retinotopic maps showed a similar degree of organisation between the two strains.
3. The effect of 3d monocular eye closure during the critical period was comparable between the two strains, both of which exhibited the typical closed eye depression of cortical response.
4. C57BL/6JOlaHsd mice exhibited a specific deficit during the critical period in the homeostatic response increase observable after 5-6d monocular eye closure in C57BL/6J mice.
5. Similarly C57BL/6JOlaHsd mice, unlike C57BL/6J mice, exhibited a failure to maintain normal cortical responses after a brief period of dark exposure during the critical period.
6. C57BL/6JOlaHsd mice exhibited a comparable deficit in homeostatic synaptic scaling of mEPSC amplitude in vitro after 3 days of critical period dark

exposure. This suggests that the homeostatic plasticity phenomena described in vivo after prolonged eye closure and in vitro after dark exposure are mechanistically linked.

7. The role in homeostatic plasticity of α–synuclein (coded by a gene known to be deleted in the C57BL/6JOlaHsd strain) was tested, and it was found to be non-essential during the critical period.

Chapter 7.General discussion

7.1 Summary of studies conducted

The aim of this study was to examine the extent to which plasticity processes that have been described in detail *in vitro* are actually utilised in the living brain. The general approach has been to take well described *in vivo* plasticity phenomena and examine whether they are disrupted by manipulations that are known to disrupt plasticity observable *in vitro*. Specifically in this thesis the consequence of the knockout of the AMPA receptor subunit GluR1 (that disrupts some forms of LTP/LTD in vitro) was studied. Additionally an inbred mouse strain (C57BL/6JOlaHsd) that exhibits previously unknown impaired homeostatic plasticity, both *in vitro* and *in vivo,* was described.

7.2 Chapter 2: Methodological considerations

Several recent studies have described experiments conducted by repeated imaging of intrinsic signals (Kaneko *et al.*, 2008a; Kaneko *et al.*, 2008b; Kaneko *et al.*, 2010). This allows a within animal longitudinal experiment to be conducted. However there is some difficulty with stabilising the imaging preparation over the course of a week. My own experience and that of others (Hofer *et al.*, 2006) is that the skull becomes progressively less transparent with repeated imaging and intrinsic signal magnitude drops as a consequence. A compromise is that the ratio of contralateral to ipsilateral eye response can be calculated allowing longitudinal imaging without ambiguities in results related to unstable signal magnitude.

Experiments in chapter 3 highlight one difficulty with drawing conclusions about retinotopic map organisation from intrinsic signal imaging data collected using the periodic imaging paradigm developed by Kalatsky & Stryker (2003), additionally see section 7.3 below. By modulating stimulus contrast, that in turn modulates intrinsic signal magnitude, I demonstrated that the degree of map scatter is strongly correlated with the magnitude of the intrinsic signal. Although Smith & Trachtenberg (2007) have shown that it is possible to observe low scatter, and apparently well organised maps despite a weak signal magnitude, it is clear that a weak signal can be a cause of intrinsic signal map scatter when combined with a degree of biological noise. A lower magnitude signal results in a map with greater scatter because the signal to noise ratio is less favourable. More stimulus presentations and more averaging of the resultant signal increases the signal to noise ratio and reduces the map scatter. The reduction in map scatter due to increasing signal averaging will plateau for a given stimulus after a certain number of presentations. The number of stimulus presentations required to reach a plateau of the map scatter value will vary as a function of the initial unaveraged signal to noise ratio. Therefore the number stimulus presentations must be tailored to the strength of signal being elicited, with lower contrast stimuli for example requiring more stimulus presentations, in order to achieve, ideally, an equal signal to noise ratio between different stimuli after averaging.

7.3 Chapter 3: Basal cortical visual responses of GluR1 knockout mouse

Several differences were found functionally under baseline conditions between GluR1$^{-/-}$ mice and their WT littermates. First, a reduction in visual cortical population response magnitude was observed in knockout mice in vivo. A similar depressed response was observed both in the superficial layers using intrinsic signal imaging and in the primary thalamorecipient layer 4 by measuring visually evoked electrical field potentials. No such recordings have previously been made in the visual cortex of GluR1$^{-/-}$ mice, however, single unit recordings made in the somatosensory cortex have reported no abnormalities in average spike rates in vivo (Wright *et al.*, 2008) in agreement with preliminary somatosensory intrinsic signal data that also reported no difference in cortical responses (see appendix figure 8.4). This suggests there may be some unexpected difference between these cortical areas in normal AMPAR subunit composition or homeostatic neuronal excitability compensation mechanisms. Some evidence has previously been reported for a difference in AMPAR subunit composition between V1 and S1 in rat cortex, however this work indicated that at 5 weeks GluR1 expression relative to GluR2 expression is greater in S1 than V1, suggesting that any deficit in synaptic strength due to GluR1 knockout would be more severe in S1 (Goel *et al.*, 2006). Another possible explanation is that there is a sampling bias in extracellular recordings towards recording neurons that are more responsive. In contrast the two approaches used in this study (VEPs and intrinsic signal imaging) are relatively unbiased in this respect and are also sensitive to subthreshold activity.

An alternative explanation could be that the reduction in visual cortical response in GluR1$^{-/-}$ mice is a deficit that is being inherited from an earlier stage of the visual pathway; i.e. either the retina or the thalamic relay cells both of which normally express GluR1. That the deficit isn't present at the L4 → L2/3 synapse is supported to some extent by the observation that the degree of basal response depression appears no greater in layer 2/3 than in layer 4. However the situation may be more complex than this canonical model of the cortex suggests as previous studies have illustrated that in the mouse visual cortex at least, plastic changes of ocular dominance in layer 4 need not be inherited by layer 2/3 and vice versa (Liu *et al.*, 2008; Yoon *et al.*, 2009). GluR1 is known to be expressed in the retina (Xue *et al.*, 2001) and this could be the locus of the basal response depression observed in GluR1$^{-/-}$ mice. This question could be addressed by making recordings from the optic nerve or performing an electroretinogram.

An apparent difference in the degree of primary visual cortex retinotopic map organisation was also observed in GluR1$^{-/-}$ relative to WT littermates. This difference was observed in retinotopic maps collected using a periodic drifting bar visual stimulus (Kalatsky & Stryker, 2003) and analysed by using the well established method of calculating average map scatter (Cang *et al.*, 2005a; Cang *et al.*, 2005b; Smith & Trachtenberg, 2007). Using this metric the degree of scatter observed in retinotopic maps of GluR1$^{-/-}$ mice was approximately twice that observed in WT littermates. One interpretation of this finding is that correct retinotopic connectivity might normally be established by something analogous to

the LTP or LTD processes that are disrupted in the cortex of GluR1$^{-/-}$ mice (Hardingham & Fox, 2006; Wright *et al.*, 2008). It is known that spontaneous retinal waves, which are mediated by cholinergic transmission, are required for normal cortical retinotopic map refinement (Cang *et al.*, 2005c) which occurs after the prototypic map is formed by a process dependent upon gradients of guidance molecules such as ephrins (Cang *et al.*, 2005b). However it remains unknown what the molecular mechanism of the former process is and the degree to which it involves synaptic or structural plasticity.

As discussed in section 7.2 there is some question of the validity of measuring retinotopic map organisation using the periodic intrinsic signal methodology of Kalatsky & Stryker (2003), specifically signal magnitude and map scatter can be confounded. In the case of GluR1$^{-/-}$ mice the intrinsic signal and VEP were both shown to be weaker than those observed in WT littermates. When the response magnitudes of GluR1$^{-/-}$ vs. WT mice are plotted on to the curve of response magnitude vs. scatter obtained by altering the stimulus contrast the difference in scatter between the genotypes is as would be expected given the difference in response magnitudes. The question of whether retinotopic maps are less organised in GluR1$^{-/-}$ mice could be further addressed by making single unit recordings and mapping receptive fields of individual neurons which would be predicted to be larger in GluR1$^{-/-}$ mice.

7.4 Chapter 4: GluR1 as a substrate of critical period experience dependent plasticity

The importance of GluR1 in critical period ocular dominance plasticity was assessed using the standard methods of intrinsic signal imaging and visual evoked potentials (Sawtell *et al.*, 2003; Cang *et al.*, 2005a). Cortical responses to visual stimulation were measured in normal mice and mice that had had either 3 or 5-6 days of monocular visual experience.

The intrinsic optical signal has previously been presumed to be dominated by activity in the superficial layers of the cortex in the mouse, similar to other species (Bonhoeffer & Grinvald, 1996). This idea was supported by preliminary experiments presented in chapter 4 in which the cortex was gradually deactivated from the surface downwards by surface application of the GABA-a agonist muscimol (Wright & Fox, 2010). Simultaneous intrinsic signal, layer 4 VEP and surface VEP recording showed that the intrinsic signal and surface VEP rapidly reduced by ~80% while over the same time period the layer 4 VEP remained stable, suggesting the intrinsic signal is superficial in origin. This meant that plasticity measurements could be made from either the superficial layers of the cortex using intrinsic signal imaging or from the primary thalamorecipient layer 4 using visual evoked potentials.

7.4.1 The effect of short monocular deprivation (3d) on layer 2/3 cortical responses to visual stimulation in GluR1$^{-/-}$ mice

After a short period of monocular experience (3d) the cortical responsiveness to the closed eye decreases upon eye reopening (Gordon & Stryker, 1996). In order to measure the loss of response to the closed eye intrinsic signal imaging was conducted in both the binocular and monocular areas of the primary visual cortex of control or deprived WT or GluR1$^{-/-}$ mice. In the binocular area both WT and GluR1 KO mice exhibited ocular dominance plasticity while in the monocular area the normal depression of closed eye response was absent.

Although the ODI (a ratio measure of the response of the two eyes) of WT and GluR1$^{-/-}$ mice shifted in an identical manner the absolute shift in the response magnitude to stimulation of the closed eye differed. This was due to the baseline differences between the two genotypes in all response magnitudes described above. This meant that the absolute reduction in closed eye response was greater in WT than GluR1$^{-/-}$ mice but the reduction relative to the genotypic baseline (approximately 30% in both genotypes) was identical. This prompts the question of whether the *absolute* intrinsic signal or the *relative-to-genotypic-baseline* intrinsic signal provides the most informative picture.

From the *absolute* intrinsic signal perspective closed eye depression is interpreted as partially impaired in GluR1$^{-/-}$ mice. This impairment may be due to a partial occlusion of plasticity in GluR1$^{-/-}$ animals in the sense that GluR1$^{-/-}$ mice may have less functional membrane inserted AMPARs and thus less capacity to

exhibit plasticity due to post translational modification or internalisation of AMPARs. This view is supported by the evidence that baseline intrinsic signal is reduced in GluR1$^{-/-}$ animals. A second interpretation is that plasticity may be impaired because a specific molecular interaction that requires GluR1 can not take place. In this scheme, if synapses were at a similar level of excitability as that observed in GluR1$^{-/-}$ mice but did hold GluR1 containing AMPARs then a similar absolute degree of synaptic depression would occur.

Alternatively from the intrinsic signal *relative-to-genotypic-baseline* perspective, baseline responses are depressed in GluR1$^{-/-}$ mice due to a reduction in AMPAR mediated current but closed eye depression plasticity is normal. In this scheme closed ye depression does not mechanistically require an interaction to occur involving GluR1.

In both schemes some plasticity occurs in the binocular cortex of mice lacking GluR1. Interestingly, in the monocular area intrinsic signal imaging showed a reduction of closed eye response after 3dMD in WT mice as previously reported (Kaneko *et al.*, 2008b), but this depression was completely absent in GluR1$^{-/-}$ mice. This suggests that the binocular cortex might have multiple forms of plasticity it can exploit, some of which are non-GluR1 dependent, while the monocular cortex only has access to GluR1 dependent plasticity. It seems unlikely that there is some intrinsic biological difference between the neighbouring neurons of binocular cortex and monocular cortex, however one

profound factor that differs between the areas is the nature of the input they receive during monocular eyelid closure.

In the case of the monocular cortex all input arrives through the eyelid of the closed eye and may be insufficient to drive spiking in cortical neurons. Indeed even when a high contrast bar stimulus is presented, lid closure in the mouse has been shown to result in approximately a 50% reduction in intrinsic signal magnitude and a dramatic loss of spatial information (Faguet *et al.*, 2009) although it is unclear to what extent this signal represents spiking versus subthreshold activity. In the home cage of laboratory mice nothing of such high contrast typically exists so the amount of spiking of monocular cortex neurons is likely to be very low. Monocular neurons may instead be receiving constant low frequency and mostly subthreshold stimulation.

In contrast in the binocular cortex, well correlated input continues to arrive to almost all neurons via ipsilateral eye driven synapses while simultaneously poorly correlated input arrives via contralateral eye driven synapses.

To draw parallels with in vitro protocols of plasticity induction, the monocular area may depress through a process analogous to low frequency stimulation induced LTD (Kirkwood *et al.*, 1993). In the binocular cortex this process of low frequency stimulation induced LTD may also be occurring but in parallel spike timing dependent depression (Markram *et al.*, 1997) is possible as binocular cortex neurons are still producing large numbers of spikes. Spike timing dependent

plasticity has been shown to depend upon retrograde cannabinoid signalling (Sjostrom *et al.*, 2003) and a number of studies have shown that disrupting endocannabinoid signalling disrupts developmental cortical sensory map plasticity including ocular dominance plasticity in layer 2/3 (Liu *et al.*, 2008; Li *et al.*, 2009).

If the binocular cortex in WT mice has two plasticity mechanisms for synaptic depression open to it but the monocular cortex only has one then a greater amount of depression might be expected to be observed in binocular versus monocular cortex after a certain period of eye closure. This was found to be the case, with a 27% depression observed in monocular cortex versus a 43% depression in binocular cortex.

Interestingly, in the mouse barrel cortex a highly penetrant phenotype of impaired experience dependent depression in response to whisker removal has been reported in GluR1$^{-/-}$ mice (Wright *et al.*, 2008). This may be because the input being received in a deprived barrel is more analogous to monocular cortex input than binocular cortex input during MD, as neurons within a barrel are highly dominated in their receptive fields by their 'principal whisker'. Another explanation is that the barrel cortex phenotype may differ from that of the visual cortex because of the different developmental time courses of the two areas (Cheetham & Fox, 2010). Indeed in the somatosensory cortex it has been shown that cannabinoid dependent plasticity is critical for barrel map developmental plasticity only during an early postnatal period (Li *et al.*, 2009). In the study

conducted by Wright et al. (2008) experiments were performed outside of this critical period. In contrast the experiments described here in the visual cortex were conducted during a period at which cannabinoid dependent plasticity is known to occur (Liu *et al.*, 2008).

In summary ocular dominance plasticity in layer 2/3 of the binocular cortex seems to be partially dependent upon interactions involving GluR1, but can also precede to a lesser degree by GluR1 independent mechanisms, one possibility being presynaptically expressed spike timing dependent plasticity. In contrast MD induced depression of layer 2/3 monocular cortex responsiveness appears to be entirely dependent upon interaction involving GluR1 as it is absent in GluR1$^{-/-}$ mice. One possible reason for the difference in the degree of dependence of the two cortical areas on GluR1 is a difference is the quality and quantity of visual drive being received by neurons in the two areas.

7.4.2 The effect of short monocular deprivation (3d) on layer 4 cortical responses to visual stimulation in GluR1$^{-/-}$ mice

After a short period of monocular experience (3d) during the critical period the cortical responsiveness to the closed eye also decreases upon eye reopening in layer 4 (Frenkel & Bear, 2004). In order to measure the loss of response to the closed eye visually evoked potentials were recorded in the binocular area of the primary visual cortex of control or deprived WT or GluR1$^{-/-}$ mice. WT mice exhibited OD plasticity as has previously been reported (Frenkel & Bear, 2004). However, in GluR1$^{-/-}$ mice the normal depression of closed eye response was

absent, indicating an important role for interactions involving GluR1 in OD plasticity in layer 4.

Interestingly, none of the residual ocular dominance plasticity observed in layer 2/3 of GluR1$^{-/-}$ mice was present in layer 4. This is consistent with previous reports that cannabinoid signalling dependent plasticity is limited to the superficial layers of the mouse visual cortex (Crozier *et al.*, 2007; Liu *et al.*, 2008) and with anatomic observations of low expression of CB1 receptors in layer 4 of the somatosensory cortex (Deshmukh *et al.*, 2007).

As discussed above and in accord with observations made using intrinsic signal imaging, the layer 4 VEP is basally depressed in GluR1$^{-/-}$ mice. This again raises the question of whether plasticity is occluded in GluR1$^{-/-}$ mice owing simply to the fact that there are less functional AMPARs available to be removed from the membrane or whether the plasticity deficit is due specifically to the lack of GluR1 containing receptors. If the former were the case this would suggest there was some lower limit to the degree of synaptic depression that could occur and that GluR1$^{-/-}$ mice are already at this limit. The data do not permit to distinguish between these two possibilities.

7.4.3 The effect of long monocular deprivation (5-6d) on layer 2/3 cortical responses to visual stimulation in GluR1$^{-/-}$ mice

After a longer period of monocular experience (5-6d), the cortical responsiveness in layer 2/3 to the open eye has been observed to be potentiated (Frenkel &

Bear, 2004). This was measured in the binocular area of the primary visual cortex of control or deprived WT or GluR1$^{-/-}$ mice. WT mice exhibited potentiation of the open eye as has previously been reported. However, in GluR1$^{-/-}$ mice the normal potentiation of open eye responses was absent. This suggests GluR1 containing AMPARs may be driven into the membrane or phosphorylated as a critical stage in the process of open eye potentiation. This is consistent with several studies that have shown increased PSD GluR1 expression in acutely dark exposed (1 week of dark exposure) rats (Goel *et al.*, 2006) and increased surface GluR1 expression after activity blockade in culture (Shepherd *et al.*, 2006).

As discussed in Chapter 6, the C57BL/6JOlaHsd (Harlan, UK) background into which the GluR1$^{-/-}$ mice were generated has a severe homeostatic plasticity deficit that results in a total lack of open eye potentiation during the critical period as well as impaired synaptic scaling. The GluR1$^{-/-}$ mice therefore had to be outbred onto a background that does possess homeostatic plasticity, namely C57BL/6J (Charles River, UK). The mice used in the GluR1$^{-/-}$ 5-6d MD experiments had been backcrossed twice and will be referred to as JaxGluR1$^{-/-}$. This was found to be sufficient to restore normal open eye potentiation in WT littermates, however the normally observed closed eye depression in WT animals was almost absent. This may be due in part to an unanticipated phenotype due to interbreeding strains. A large degree of variability in capacity for OD plasticity has previously been reported in recombinant mouse strains derived from mixed C57BL/6J and DBA/2J inbred mice (Heimel *et al.*, 2008) although not from

interbreeding the presumably more closely related C57BL/6J substrains (although see Specht & Schoepfer, 2001 and discussion of strain differences below). Curiously the closed eye depresses normally in JaxGluR1$^{-/-}$ mice suggesting that homeostatic plasticity might be enhanced rather than depression impaired in the C57BL/6J x C57BL/6JOlaHsd cross.

7.5 Chapter 5: GluR1 as a substrate of adult plasticity.

Early work on the rodent visual cortex suggested that ocular dominance plasticity could only occur during a brief postnatal critical period as had been found to be the case in many other mammals. However, other studies provided evidence that plasticity was possible in adult mice but that it requires a slightly longer period of altered visual experience in order for it to be induced. In Chapter 5 the GluR1 dependence of a number of forms of adult plasticity was investigated.

7.5.1 Adult ocular dominance plasticity does not require GluR1

The reliability of adult ocular dominance plasticity was first assessed in adult animals with a mean age of 90 days. Consistent with previous reports, it was found that a significant shift in ocular dominance occurred after 6 days of monocular eye closure. In contrast, a shorter 3d eye closure resulted in no such OD shift. This adult OD shift has previously been shown to be mediated by potentiation of the open eye response (Sawtell *et al.*, 2003; Sato & Stryker, 2008). In order to test if a substrate of this potentiation is GluR1, adult WT and GluR1$^{-/-}$ mice were imaged before and after having experienced 6d monocular

visual experience. Both genotypes exhibited an OD shift of a comparable degree towards the open eye indicating that layer 2/3 open eye adult potentiation can operate through mechanisms independent of the GluR1 subunit.

In this study absolute response strengths were not available as mice were chronically imaged, resulting in an unstable absolute response magnitude (see methodological discussion above and Hofer et al., 2006 for further details). The interpretation that GluR1$^{-/-}$ does not disrupt adult plasticity makes the assumption that the closed versus open eye plasticity underlying the OD shift in GluR1$^{-/-}$ and WT mice is the same. Additionally the conclusion that adult open eye potentiation does not require GluR1 makes a further assumption that adult open eye potentiation actually occurs in WT mice of the genetic background on which the knockout was generated (C57BL/6JOlaHsd) – this was confirmed to be the case in chapter 6. See section 7.6 below for a discussion of this issue.

7.5.2 Adult recovery of binocularity does not require GluR1

Recovery of normal contralateral dominated binocular responsiveness of the visual cortex after monocular deprivation has been described both in critical period and adult mice (Hofer *et al.*, 2006; Kaneko *et al.*, 2008a; Hofer *et al.*, 2009). In juvenile mice 5 days of monocular experience results in a depression of the closed eye and a potentiation of the open eye response. It has been demonstrated that 4 days of normal binocular experience is sufficient for these two plasticity events to be reversed and for the normal contralateral bias to be restored (Kaneko *et al.*, 2008a). This process has been found to depend upon

TrkB/BDNF signalling as pharmacological inhibition of the TrkB receptor abolishes recovery. Interestingly, blocking the TrkB receptor both blocks de-potentiation of the spared eye and de-depression of the closed eye (Kaneko *et al.*, 2008a). The rapid process of recovery following MD, at least in ferrets, has been shown to be independent of protein synthesis (Krahe *et al.*, 2005). One hypothesised mechanism by which BDNF-TrkB signalling might mediate the plasticity involved in binocular recovery in the absence of protein synthesis is through phosphorylation of the NMDAR by BDNF-activated tyrosine kinases. Phosphorylation of a tyrosine kinase substrate of the NMDAR is known to potentiate synaptic transmission at least in part by an increase in channel open probability (Blum & Konnerth, 2005). The GluR1 receptor is one substrate of calcium dependent kinases such as CaMKII which would be activated by increased NMDAR function. Also rapid reversal of deprivation induced dephosphorylation of the GluR1 PKA site, serine 845, would be another protein synthesis-independent means of reversing deprivation effects.

The role of GluR1 in recovery following MD was investigated in adult mice by inducing MD with 6 days of monocular experience, verifying that an ocular dominance shift had occurred by intrinsic signal imaging, allowing a 4 week period of binocular recovery and then reimaging. There was however no difference observed in the degree of recovery between GluR1$^{-/-}$ mice and WT littermates suggesting GluR1 is non-critical in this process.

OD plasticity seems to occur normally in adult mice who lack GluR1. Therefore one obvious issue with this study is that because GluR1 receptors did not participate during the deprivation stage, they did not undergo phosphorylation alterations, and these changes can not therefore be reversed. An implicit assumption is therefore that there is a degree of degeneracy or compensation in the process of plasticity induction that allows it to occur through a GluR1 independent means with the consequence that the reversal mechanism is absent (Edelman & Gally, 2001).

Another limitation with this study is that the recovery period is extremely long compared to that of many other studies of recovery following monocular deprivation (greater than 4 weeks recovery). The recovery period was this length because the recovery experiment was an incidental sub-experiment within the longer term imaging study which required a long recovery period. Other studies have typically used recovery periods of 3-5 days (Liao *et al.*, 2002; Kaneko *et al.*, 2008) although recovery has been reported after as short a period as a few hours (Krahe *et al.*, 2005). It is entirely possible that in parallel to the rapid recovery that is protein synthesis independent, other processes are occurring over other timescales to mediate recovery. It would therefore be interesting to investigate whether very rapid recovery following MD is impaired in GluR1$^{-/-}$ mice.

The relationship between the ODI prior to the first deprivation and that after recovery was also examined. It has previously been noted that individual mice have signature ocular dominance indexes that persist over time under normal

conditions and can be observed by repeated intrinsic signal imaging of the same mouse (Kaneko *et al.*, 2008b). The origin of the baseline ODI, and the bias towards the contralateral eye, has been suggested to be dictated by the input from the dLGN (Coleman *et al.*, 2009). Therefore one might expect the recovered ODI to be related in some way to the ODI observed at baseline. No such relationship was observed. This may be because the precise ODI is fine tuned in the cortex or because some retino-cortical plasticity takes place during MD.

7.5.3 Partially impaired ocular dominance plasticity facilitation by prior experience in GluR1$^{-/-}$ mice

As discussed above and demonstrated in other studies, a short period of monocular experience (3d) is insufficient to induce an ocular dominance shift in mice outside of the critical period (Gordon & Stryker, 1996; Sawtell *et al.*, 2003). However two studies have shown that if a mouse has prior experience of ocular dominance plasticity, either during the critical period or during adulthood then plasticity during a second short episode of monocular experience is facilitated (Hofer *et al.*, 2006, 2009). This has the effect that a significant ocular dominance shift occurs after 3 days in previously experienced adult mice. This finding was confirmed in the present study by exposing either MD-naïve or MD-experienced adult mice to 3 days of monocular experience. Consistent with previous reports mice with prior experience of ocular dominance plasticity exhibited an ocular dominance shift while naïve mice did not.

Hofer et al. (2009) propose that prior experience dependent facilitation of adult plasticity occurs as a result of conserved structural changes to dendritic arbors from the first episode of monocular experience being reused during the second episode of monocular experience. This idea is supported by longitudinal dendritic imaging studies which show that the first episode of MD results in a dramatic increase in density of persistent new spines while the second episode of MD does not. Additionally persistent spines that appear during the first episode of MD selectively increase in size during the second MD episode (Hofer *et al.*, 2009). Previous work has pointed to a permissive role of GluR1 containing AMPARs in stable spine enlargement (Kopec *et al.*, 2007). In support of this idea preliminary work in our lab has provided evidence of an increased density of immature spines in the cortex of GluR1$^{-/-}$ mice (C. Cheetham, personal communication).

While ocular dominance shifts appear to be normal after 6d monocular experience in GluR1$^{-/-}$ mice, structural changes that are the correlate of this plasticity might be less stable. I tested indirectly the importance of GluR1 in stabilising new spines using the paradigm of facilitation by prior experience (Hofer *et al.*, 2006). Under the scheme proposed by Hofer et al. (2009), spines created during the first MD must persist until the second MD if they are to facilitate plasticity. If spines are less stable in GluR1$^{-/-}$ mice then one would predict less facilitation due to prior experience. In the study presented here a 4 week recovery period elapsed between the first MD and the second, this is the period over which new spines must persist.

In support of a role of GluR1 in spine stabilisation, facilitation due to prior experience was partially impaired in GluR1$^{-/-}$ mice relative to WT littermates despite an apparently normal first ocular dominance shift. This impairment consisted of a partial but significant reduction in the adult plasticity facilitation effect of prior plasticity experience. One explanation for this result might be that GluR1 has a role in stabilising new spines. Alternatively, plasticity may be occurring in adult GluR1$^{-/-}$ mice through a degenerate mechanism which may not require dendritic remodelling, such as presynaptic modifications. Again in this case the persistent structural changes to dendritic spines that are thought to mediate facilitation due to prior experience will be absent. Longitudinal structural imaging would be required to distinguish between these accounts, the pertinent questions being Cross-modal regulation of synaptic AMPA receptors in primary sensory cortices whether normal post synaptic structural plasticity occurs in GluR1$^{-/-}$ mice and if it does whether spines are less persistent than in WT mice.

7.6 Strain differences in plastic responses to monocular deprivation and dark exposure

7.6.1 Impaired homeostatic plasticity in GluR1 WT littermates

During the investigation of ocular dominance plasticity in GluR1$^{-/-}$ mice I noticed that WT littermates of the original genetic background on which the knockout was generated (C57BL/6JOlaHsd, Harlan, UK) did not exhibit the plasticity profile

previous described by others in the literature. Specifically after 5-6d of critical period monocular experience a potentiation of the open eye response is normally observed, as well as a partial recovery of the closed eye response relative to that at 3d (Frenkel & Bear, 2004; Kaneko *et al.*, 2008b). This plasticity is typically described as a homeostatic reaction to reduced visual input to the cortex, as suggested by the otherwise paradoxical partial recovery of closed eye response. This form of homeostatic plasticity was observed to be absent in WT littermates of GluR1$^{-/-}$ mice of the C57BL/6JOlaHsd background. One reason that this finding is of importance is that although the full nomenclature of the C57BL/6JOlaHsd mouse makes it sound obscure it is in fact the default C57BL/6J mouse provided by the Harlan mouse company in many parts of Europe including the UK.

7.6.2 Impaired homeostatic plasticity is a general feature of the C57BL/6JOlaHsd inbred mouse strain

In order to confirm that this lack of homeostatic plasticity was not a result of inadvertent contamination of the genetic background of GluR1$^{-/-}$ WT littermate mice, homeostatic ocular dominance plasticity was next investigated in C57BL/6JOlaHsd (referred to from here as 6JOlaHsd) mice purchased directly from Harlan UK and compared with C57BL/6J (referred to from here as 6J) purchased from Charles River UK under licence from Jackson, USA.

The two strains exhibited almost identical plasticity after 3d monocular experience but deviated sharply after 5-6d at which point 6J mice showed robust

open eye potentiation and significant recovery of closed eye response, both of which were absent in 6JOlaHsd mice. Results from 6JOlaHsd mice were consistent with data from WT littermates of GluR1$^{-/-}$ mice.

7.6.3 No differences in basal responses of C57BL/6J vs. C57BL/6JOlaHsd

Under baseline conditions visual responses were very similar between the strains but not identical. Retinotopic map scatter was measured using period intrinsic signal imaging and no difference was found between the two strains. Similarly no significant difference was observed in intrinsic signal magnitude between the strains in response to the relatively high spatial frequency stimulus used suggesting no significant differences in visual acuity. Binocular responses were observed to be slightly less contralateral dominated in the 6JOlaHsd strain and this was as a result of a larger ipsilateral response.

7.6.4 Impairments of MD induced homeostatic plasticity and synaptic scaling are correlated

Having established that a clear and robust deficit in homeostatic plasticity exists in 6JOlaHsd mice we next sought to exploit this finding to probe whether another model system of homeostatic plasticity operates by the same impaired mechanism, namely synaptic scaling. Ex vivo recordings of mEPSCs were made in brain slices of mice of each strain after 3 days in either a normally lighted or completely dark room. This form of dark exposure is known to result in a multiplicative synaptic scaling of spontaneous mEPSCs that is thought to be a homeostatic response to reduced visual drive. Synaptic scaling was completely

absent in the 6JOlaHsd strain where as the 6J strain showed a degree of scaling comparable to previous reports in the literature. This strongly suggests that the homeostatic plasticity engaged during MD and that engaged during dark rearing induced synaptic scaling are mechanistically closely linked.

7.6.5 Synaptic scaling not directly correlated with intrinsic signal scaling

Despite many years of brief dark exposure induced synaptic scaling experiments no study to my knowledge has examined directly the consequences of this synaptic scaling on visual evoked population activity in vivo. Synaptic scaling has been described as a homeostatic mechanism that operates to adjust the excitability of excitatory neurons in order to stabilise neuronal networks (Turrigiano, 2008). In ex vivo studies it has consistently been observed that activity deprivation results in a shift in the excitatory/inhibitory balance such that excitatory neurons become more excitable (Maffei & Turrigiano, 2008). Therefore in imaging visual responses immediately following 3d dark expose relative 3d normal lighting it was expected that dark exposed responses would be greater, at least in mice with normally operating homeostatic plasticity. Intrinsic signal magnitudes were compared in the two mouse strains after 3d dark exposure, a manipulation known to saturate scaling of mEPSCs ex vivo (Goel & Lee, 2007). Unexpectedly the 6J strain, which showed ex vivo synaptic scaling after this manipulation, showed no change in intrinsic signal magnitude in response to either monocular or binocular stimulation, relative to mice that had lived under normal lighting. In contrast 6JOlaHsd mice showed a depression of intrinsic signal responses relative to normally reared mice.

This indicates firstly that there is not a direct linear relationship between mEPSC amplitude and intrinsic signal magnitude. And it secondly suggests that at the population level homeostatic plasticity is required to maintain normal cortical responsiveness during periods of reduced activity. One possible explanation for the lack of potentiation in 6J mice is that synaptic scaling is reversed so rapidly after light exposure, even in the anaesthetised mouse, that responses have returned to normal by the time imaging proceeds. It is known that 1d of light exposure is sufficient to completely reverse 2d dark exposure induced synaptic scaling (Goel *et al.*, 2006) although the minimum requirements for scaling reversal have not been determined. In a subset of data from 6J mice that had been dark exposed for 3d, an analysis was conducted to search for any indication of a gradual reduction in intrinsic signal response strength during the course of each imaging session. This showed that responses are stable during post dark rearing imaging, although loss of scaling could still have occurred during surgery when mice are light exposed. It seems unlikely that this is the case as I have observed that the scaling of intrinsic signal magnitude that occurs during ocular dominance plasticity is preserved stably for at least two hours under these anaesthetic conditions.

7.6.6 A genetic factor that permits homeostatic plasticity

The lack of homeostatic plasticity in the C57BL/6JOlaHsd is assumed to be due to some genetic difference between it and the other strain examined, C57BL/6J. It seems that the 6JOlaHsd strain is the 'odd one out' in not possessing this form

of homeostatic plasticity as I have shown that another C57BL/6J sub-strain (C57BL/6JCrl) does possess normal homeostatic plasticity. Similarly several other studies have shown homeostatic plasticity in vivo in mixed background mice (Mrsic-Flogel *et al.*, 2007) and most tellingly in rats (Desai *et al.*, 2002; Goel *et al.*, 2006). Very little work has compared plasticity in these two strains as they had previously been assumed to be genetically equivalent. One study examined spatial learning and found no difference between strains (Chen *et al.*, 2002) while another series of experiments found that fear conditioning induction was normal while extinction was absent in 6JOlaHsd (Stiedl et al., 1999; Siegmund et al., 2005).

The finding of a profound homeostatic plasticity deficit prompted the question of what is the critical genetic difference between 6JOlaHsd mice and these other strains and species. One known genetic difference between the two strains I have examined is that C57BL/6JOlaHsd mice harbour a spontaneous mutation that results in deletion of the gene Sncg (Specht & Schoepfer, 2001, 2004). This gene codes for the presynaptic protein α-synuclein and was thus a promising candidate for the plasticity disrupting genetic difference between the strains. As α-synuclein knockout mice on a non-6JOlaHsd background were available to me I assayed homeostatic plasticity in these animals in vivo. Homeostasis was induced by 5d monocular experience during the critical period however no difference was observed between mice possessing of lacking the Sncg gene. It thus seems that α-synuclein is not the critical homeostasis associated protein.

There are many other minor genetic differences between 6JOlaHsd and 6J mice, many of which are in genes of unknown function or that are not expressed in the brain. For example following the discovery of the Sncg deletion, Specht & Schoepfer (2004) went on to describe complete deletion of MMRN1 in the same strain, a gene that codes for a protein involved in haemostasis. Similarly another study has identified many loci at which various inbred mouse strains differ, which includes complete gene deletions and single nucleotide polymorphisms (Egan *et al.*, 2007). Additionally the plasticity phenotype may be due to interactions between a number of genes.

Despite the absence of this homeostatic plasticity mechanism C57BL/6JOlaHsd mice display no obvious under control conditions. Indeed C57BL/6JOlaHsd continue to be used interchangeably with other C57BL/6J strains. Interestingly a reoccurring theme in studies of plasticity in knockout mice is that brain function appears approximately normal until the system is perturbed in some way and this unmasks a deficit (Glazewski *et al.*, 2000; Hardingham *et al.*, 2008; Kaneko *et al.*, 2008b; Wright *et al.*, 2008; McCurry *et al.*, 2010). This may be due to a high degree of degeneracy which is thought to be an ubiquitous feature of biological systems, and refers to the existence of systems which operate in parallel to serve the same function by different mechanistic means (Edelman & Gally, 2001). As neuronal excitability appears to be within a normal range in C57BL/6JOlaHsd mice, presumably other homeostatic plasticity mechanisms must act in parallel and over a longer timecourse to regulate excitation levels.

7.6.7 Mechanism of adult OD plasticity differs from that of juvenile OD plasticity

Adult ocular dominance plasticity, that can be observed to have occurred after 6 days of monocular experience, is known to be mediated exclusively by open eye potentiation (Sawtell *et al.*, 2003; Hofer *et al.*, 2006; Sato & Stryker, 2008). As part of the series of adult plasticity experiments discussed in chapter 5, WT mice of the C57BL/6JOlaHsd background were subjected to 6 days monocular experience which robustly induced an ocular dominance shift. As these were longitudinal intrinsic signal imaging experiments absolute response magnitudes are unreliable (the skull becomes progressively less transparent, a problem also noted by Hofer et al., 2006) thus only a ratio measure of contralateral to ipsilateral response was available. In chapter 6 these experiments were repeated with acute imaging and the 6J and 6JOlaHsd were found to have identical open eye potentiation. This suggests that juvenile and adult open eye potentiation occurs by different mechanisms.

Interestingly an early study by Kirkwood et al. (1997) showed that this might be the case by providing evidence of a striking age dependent increase in the importance of αCaMKII in visual cortex LTP induction by theta burst stimulation. At the time of the Kirkwood et al. study ocular dominance plasticity was believed to be confined to a postnatal critical period and studies investigating the importance of CaMKII and CaMKII autophosphorylation in OD plasticity starting during this critical period yielded mixed results (Gordon *et al.*, 1996; Taha *et al.*, 2002; Taha & Stryker, 2005). In contrast in the mouse somatosensory cortex,

vibrissae removal induced plasticity was found to be severely impaired in either mice that were lacking CaMKII all together or lacking autophosphorylating CaMKII (Glazewski *et al.*, 1996; Glazewski *et al.*, 2000). It will be interesting to test the dependence of adult OD plasticity in C57BL/6JOlaHsd mice that lack αCaMKII or possess αCaMKII with impaired autophosphorylation. A preliminary experiment has suggested that mice possessing αCaMKII with impaired autophosphorylation do show impaired adult plasticity (see appendix figure 8.4).

7.7 Future directions

Unsurprisingly there appear to be multiple semi-discrete mechanisms of synaptic plasticity operating in parallel during the process of activity dependent cortical sensory circuit development and refinement. Additionally the cortical areas responsible for different sensory modalities appear to develop on different timescales (Fox, 1992; Gordon & Stryker, 1996; Cheetham & Fox, 2010). Therefore in order to assess the importance of a sensory cortical plasticity mechanism one must compare cortical areas at matched developmental stages (Cheetham & Fox, 2010).

In in vitro slice electrophysiology synaptic plasticity experiments the stimulus for plasticity induction is central to experiment design and predominantly determines the properties of plasticity induced. This is similarly the case in in vivo experiments, but less control is typically possible of the plasticity inducing stimulus. When comparing plasticity between sensory areas and attempting to make generalisations it is also therefore of importance to consider what the most analogous in vitro model of the stimulus inducing the plasticity might be.

In order to further complete the picture of the role of GluR1 in visual cortical and somatosensory plasticity a number of knowledge gaps must be filled. Firstly in the somatosensory cortex the GluR1 dependence of plasticity must be assessed at earlier time points during which cannabinoid signalling dependent presynaptic

mechanisms are still active (Li *et al.*, 2009). If the somatosensory cortex and visual cortex develop by essentially the same plasticity mechanisms then at this time one might expect to see residual somatosensory depression plasticity in GluR1$^{-/-}$ mice after a period of single vibrissae experience. Additionally at this early somatosensory developmental time point something analogous to the monocular cortex MD condition could be explored, perhaps by total whisker deprivation. In this case somatosensory cortex may receive something analogous to a low frequency stimulus and produce few spikes, that might induce a GluR1 dependent, LFS-LTD like form of plasticity. Indeed it is known that in barrel cortex plasticity effects in deprived barrels are more significant if surround whiskers are preserved suggesting that competition and postsynaptic spikes are critical for some aspects of plasticity (Glazewski *et al.*, 1998; Wallace *et al.*, 2001).

In adulthood the studies presented here suggest that ocular dominance plasticity is not a GluR1 dependent process. Adult plasticity also appears to be unimpaired in C57BL/6JOlaHsd mice which lack homeostatic plasticity suggesting that adult open eye potentiation operates by a distinct mechanism from juvenile open eye potentiation. Early studies in the visual cortex in vitro suggested that an age dependent increase occurs in the dependence of visual cortex LTP on CaMKII (Kirkwood *et al.*, 1997). The inconsistencies in the literature regarding the importance of CaMKII and CaMKII autophosphorylation suggests that this may be the case (Gordon *et al.*, 1996; Taha *et al.*, 2002b; Taha & Stryker, 2005). It will be interesting to further test if this increased dependence

of LTP on CaMKII as animals age is accompanied by an increased dependence on the same protein of the process of open eye potentiation (see appendix figure 8.4).

Retinotopic maps measured in mice lacking GluR1 were found to be less well organised than their WT littermates. Further work is required to determine whether this is in fact the case the case or whether it is an artefact of the measurement technique used. This question can be addressed by measuring retinotopic maps in a more rigorous way by applying the principles discussed in the methodological discussion above. Additionally single unit recordings could be made to map receptive field sizes.

Recovery from MD was found to be normal in GluR1$^{-/-}$ mice after a recovery period of 4 weeks. It would be informative to undertake a dedicated study of the minimum time required to recover from MD and to determine if short term protein synthesis independent recovery (Krahe *et al.*, 2005) is impaired in GluR1$^{-/-}$ mice, which could not recover by reversing dephosphorylation of this receptor subunit. More generally it will be important to determine the degree to which the recovery following MD described in the mouse consists of recovery of visual acuity. Previous studies have used relatively low spatial frequency stimuli to probe recovery of cortical responses (Hofer *et al.*, 2006; Kaneko *et al.*, 2008a) and there is evidence that visual responses at higher spatial frequencies do not recover (Prusky & Douglas, 2003).

Preliminary ex vivo dendritic imaging studies from our group have suggested elevated spine density and a greater proportion of immature spines in sensory cortex of mice lacking GluR1. Additionally several studies have concluded that GluR1 is permissive for spine enlargement and stabilisation (Kopec et al., 2006). In agreement with this conclusion the data presented here suggests that facilitation of adult plasticity by prior experience (a process that is hypothesised to depend upon reuse of spines that developed during the episode of prior experience (Hofer et al., 2009)) is disrupted in GluR1-/- mice. Further work is required to associate GluR1 more directly with the process of new spine stabilisation, ideally longitudinal imaging of spine turnover in GluR1-/- mice. Additionally it would be interesting to know whether spine turnover increases in GluR1$^{-/-}$ mice during the an initial naïve episode of MD or whether adult plasticity is occurring in these mice through presynaptic mechanisms.

8.1 Appendix figures

Figure 8.1 Schematic of somatosensory cortex imaging.

Figure 8.2 Functional maps of somatosensory cortex obtained by intrinsic signal imaging with periodic whicker stimulation.

Chapter 8. Appendix

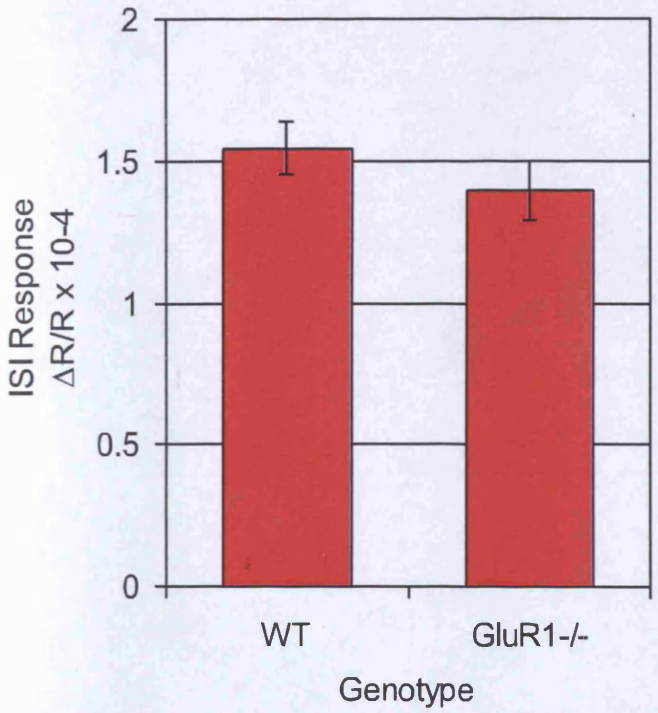

Figure 8.3 Somatosensory cortex intrinsic signal responses to whisker inflections. No significant difference between WT and GluR1$^{-/-}$ mice was observed.

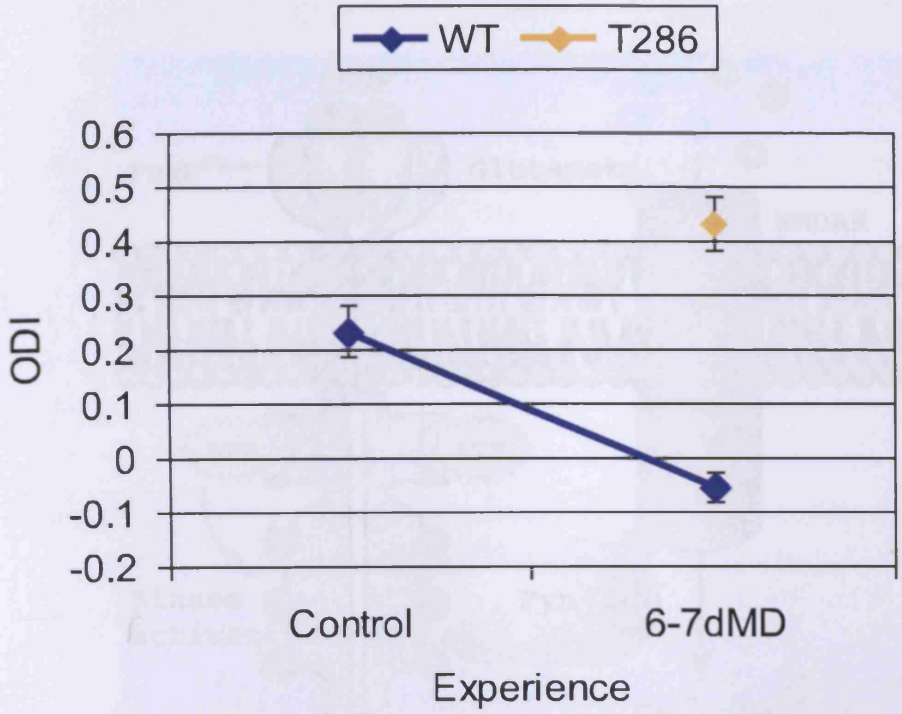

Figure 8.4 Preliminary data suggests adult ocular dominance plasticity is absent in mice lacking autophosphorylating CaMKII (T286 mice). Note T286 group n = 2.

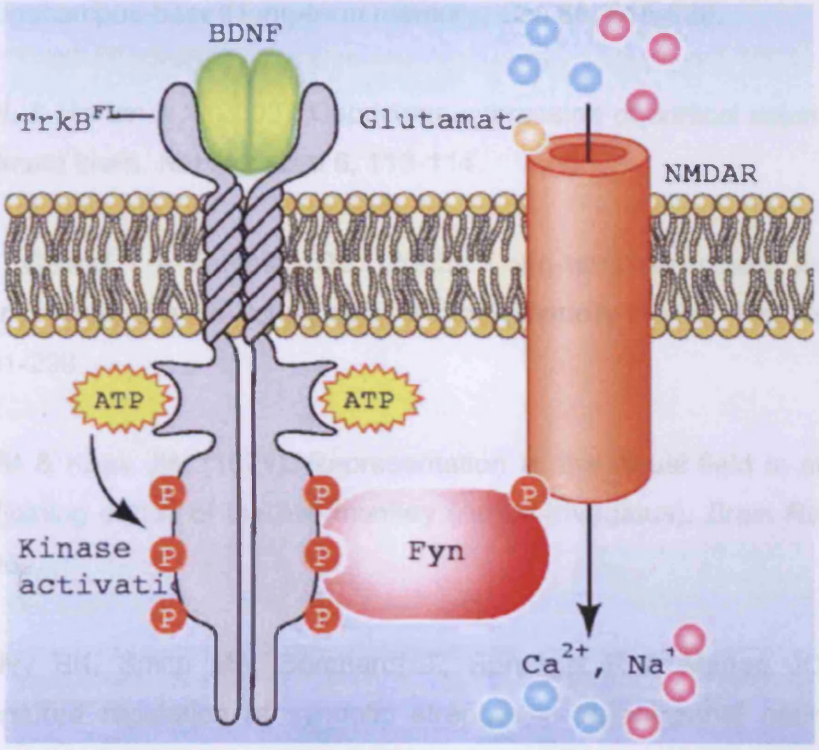

Figure 8.5 The interaction between BDNF/TrkB and the NMDA receptor is mediated by the thyrosine kinase Fyn (adapted from Blum & Konnerth, 2005).

References

Abel T, Nguyen PV, Barad M, Deuel TA, Kandel ER & Bourtchouladze R. (1997). Genetic demonstration of a role for PKA in the late phase of LTP and in hippocampus-based long-term memory. *Cell* **88,** 615-626.

Adams DL & Horton JC. (2003). Capricious expression of cortical columns in the primate brain. *Nat Neurosci* **6,** 113-114.

Allen CB, Celikel T & Feldman DE. (2003). Long-term depression induced by sensory deprivation during cortical map plasticity in vivo. *Nat Neurosci* **6,** 291-299.

Allman JM & Kaas JH. (1971). Representation of the visual field in striate and adjoining cortex of the owl monkey (Aotus trivirgatus). *Brain Res* **35,** 89-106.

Andrasfalvy BK, Smith MA, Borchardt T, Sprengel R & Magee JC. (2003). Impaired regulation of synaptic strength in hippocampal neurons from GluR1-deficient mice. *J Physiol* **552,** 35-45.

Aroniadou VA & Teyler TJ. (1991). The role of NMDA receptors in long-term potentiation (LTP) and depression (LTD) in rat visual cortex. *Brain Res* **562,** 136-143.

Artola A & Singer W. (1987). Long-term potentiation and NMDA receptors in rat visual cortex. *Nature* **330,** 649-652.

Artola A & Singer W. (1990). The Involvement of N-Methyl-D-Aspartate Receptors in Induction and Maintenance of Long-Term Potentiation in Rat Visual Cortex. *Eur J Neurosci* **2,** 254-269.

Banke TG, Bowie D, Lee H, Huganir RL, Schousboe A & Traynelis SF. (2000). Control of GluR1 AMPA receptor function by cAMP-dependent protein kinase. *J Neurosci* **20,** 89-102.

Bannerman DM, Chapman PF, Kelly PA, Butcher SP & Morris RG. (1994). Inhibition of nitric oxide synthase does not prevent the induction of long-term potentiation in vivo. *J Neurosci* **14,** 7415-7425.

Barria A, Derkach V & Soderling T. (1997). Identification of the Ca2+/calmodulin-dependent protein kinase II regulatory phosphorylation site in the alpha-amino-3-hydroxyl-5-methyl-4-isoxazole-propionate-type glutamate receptor. *J Biol Chem* **272,** 32727-32730.

Bear MF, Cooper LN & Ebner FF. (1987). A physiological basis for a theory of synapse modification. *Science* **237,** 42-48.

Bear MF, Kleinschmidt A, Gu Q & Singer W. (1990a). Disruption of Experience-Dependent Synaptic Modifications in Striate Cortex by Infusion of an Nmda Receptor Antagonist. *Journal of Neuroscience* **10,** 909-925.

Bear MF, Kleinschmidt A, Gu QA & Singer W. (1990b). Disruption of experience-dependent synaptic modifications in striate cortex by infusion of an NMDA receptor antagonist. *J Neurosci* **10,** 909-925.

Beattie EC, Stellwagen D, Morishita W, Bresnahan JC, Ha BK, Von Zastrow M, Beattie MS & Malenka RC. (2002). Control of synaptic strength by glial TNFalpha. *Science* **295,** 2282-2285.

Beaver CJ, Ji Q, Fischer QS & Daw NW. (2001). Cyclic AMP-dependent protein kinase mediates ocular dominance shifts in cat visual cortex. *Nat Neurosci* **4,** 159-163.

Beique JC, Na Y, Kuhl D, Worley PF & Huganir RL. (2010). Arc-dependent synapse-specific homeostatic plasticity. *Proc Natl Acad Sci U S A* **108,** 816-821.

Bekkers JM & Stevens CF. (1990). Presynaptic mechanism for long-term potentiation in the hippocampus. *Nature* **346,** 724-729.

Berardi N, Pizzorusso T, Ratto GM & Maffei L. (2003). Molecular basis of plasticity in the visual cortex. *Trends Neurosci* **26,** 369-378.

Beretta F, Sala C, Saglietti L, Hirling H, Sheng M & Passafaro M. (2005). NSF interaction is important for direct insertion of GluR2 at synaptic sites. *Mol Cell Neurosci* **28,** 650-660.

Bienenstock EL, Cooper LN & Munro PW. (1982). Theory for the development of neuron selectivity: orientation specificity and binocular interaction in visual cortex. *J Neurosci* **2,** 32-48.

Bliss TV & Collingridge GL. (1993). A synaptic model of memory: long-term potentiation in the hippocampus. *Nature* **361,** 31-39.

Bliss TV & Gardner-Medwin AR. (1973). Long-lasting potentiation of synaptic transmission in the dentate area of the unanaestetized rabbit following stimulation of the perforant path.[see comment]. *Journal of Physiology* **232,** 357-374.

Bliss TV & Lomo T. (1973). Long-lasting potentiation of synaptic transmission in the dentate area of the anaesthetized rabbit following stimulation of the perforant path.[see comment]. *Journal of Physiology* **232,** 331-356.

Blum R & Konnerth A. (2005). Neurotrophin-mediated rapid signaling in the central nervous system: mechanisms and functions. *Physiology (Bethesda)* **20,** 70-78.

Bonhoeffer T & Grinvald A. (1996). *Optical Imaging Based on Intrisic Signals. The Methodology.* Academic Press, London.

Brandon EP, Idzerda RL & McKnight GS. (1997). PKA isoforms, neural pathways, and behaviour: making the connection. *Curr Opin Neurobiol* **7,** 397-403.

Brandon EP, Zhuo M, Huang YY, Qi M, Gerhold KA, Burton KA, Kandel ER, McKnight GS & Idzerda RL. (1995). Hippocampal long-term depression and depotentiation are defective in mice carrying a targeted disruption of the gene encoding the RI beta subunit of cAMP-dependent protein kinase. *Proc Natl Acad Sci U S A* **92,** 8851-8855.

Bredt DS & Snyder SH. (1989). Nitric oxide mediates glutamate-linked enhancement of cGMP levels in the cerebellum. *Proc Natl Acad Sci U S A* **86,** 9030-9033.

Buzsaki G, Kaila K & Raichle M. (2007). Inhibition and brain work. *Neuron* **56,** 771-783.

Cang J, Kalatsky VA, Lowel S & Stryker MP. (2005a). Optical imaging of the intrinsic signal as a measure of cortical plasticity in the mouse. *Vis Neurosci* **22,** 685-691.

Cang J, Kaneko M, Yamada J, Woods G, Stryker MP & Feldheim DA. (2005b). Ephrin-as guide the formation of functional maps in the visual cortex. *Neuron* **48,** 577-589.

Cang J, Niell CM, Liu X, Pfeiffenberger C, Feldheim DA & Stryker MP. (2008). Selective disruption of one Cartesian axis of cortical maps and receptive fields by deficiency in ephrin-As and structured activity. *Neuron* **57,** 511-523.

Cang J, Renteria RC, Kaneko M, Liu X, Copenhagen DR & Stryker MP. (2005c). Development of precise maps in visual cortex requires patterned spontaneous activity in the retina. *Neuron* **48,** 797-809.

Chalupa LM & Williams RW. (2008). *Eye, retina, and visual system of the mouse*. MIT, Cambridge, Mass. ; London.

Cheetham CE & Fox K. (2010). Presynaptic development at L4 to l2/3 excitatory synapses follows different time courses in visual and somatosensory cortex. *J Neurosci* **30,** 12566-12571.

Cheetham CE, Hammond MS, Edwards CE & Finnerty GT. (2007). Sensory experience alters cortical connectivity and synaptic function site specifically. *J Neurosci* **27,** 3456-3465.

Chen PE, Specht CG, Morris RG & Schoepfer R. (2002). Spatial learning is unimpaired in mice containing a deletion of the alpha-synuclein locus. *Eur J Neurosci* **16,** 154-158.

Chen W, Prithviraj R, Mahnke AH, McGloin KE, Tan JW, Gooch AK & Inglis FM. (2009). AMPA glutamate receptor subunits 1 and 2 regulate dendrite

complexity and spine motility in neurons of the developing neocortex. *Neuroscience* **159,** 172-182.

Chetkovich DM, Gray R, Johnston D & Sweatt JD. (1991). N-methyl-D-aspartate receptor activation increases cAMP levels and voltage-gated Ca2+ channel activity in area CA1 of hippocampus. *Proc Natl Acad Sci U S A* **88,** 6467-6471.

Chung HJ, Xia J, Scannevin RH, Zhang X & Huganir RL. (2000). Phosphorylation of the AMPA receptor subunit GluR2 differentially regulates its interaction with PDZ domain-containing proteins. *J Neurosci* **20,** 7258-7267.

Cingolani LA, Thalhammer A, Yu LM, Catalano M, Ramos T, Colicos MA & Goda Y. (2008). Activity-dependent regulation of synaptic AMPA receptor composition and abundance by beta3 integrins. *Neuron* **58,** 749-762.

Coleman JE, Law K & Bear MF. (2009). Anatomical origins of ocular dominance in mouse primary visual cortex. *Neuroscience*.

Collingridge GL, Kehl SJ & McLennan H. (1983). Excitatory amino acids in synaptic transmission in the Schaffer collateral-commissural pathway of the rat hippocampus. *J Physiol* **334,** 33-46.

Contestabile A. (2000). Roles of NMDA receptor activity and nitric oxide production in brain development. *Brain Research Reviews* **32,** 476-509.

Contractor A & Heinemann SF. (2002). Glutamate receptor trafficking in synaptic plasticity. *Science's Stke [Electronic Resource]: Signal Transduction Knowledge Environment* **2002,** RE14.

Cooke SF & Bear MF. (2010). Visual experience induces long-term potentiation in the primary visual cortex. *J Neurosci* **30,** 16304-16313.

Crair MC, Gillespie DC & Stryker MP. (1998). The role of visual experience in the development of columns in cat visual cortex. *Science* **279,** 566-570.

Crair MC & Malenka RC. (1995). A critical period for long-term potentiation at thalamocortical synapses. *Nature* **375,** 325-328.

Cramer KS, Angelucci A, Hahm JO, Bogdanov MB & Sur M. (1996). A role for nitric oxide in the development of the ferret retinogeniculate projection. *J Neurosci* **16,** 7995-8004.

Cramer KS, Leamey CA & Sur M. (1998). Nitric oxide as a signaling molecule in visual system development. *Prog Brain Res* **118,** 101-114.

Cramer KS, Moore CI & Sur M. (1995). Transient expression of NADPH-diaphorase in the lateral geniculate nucleus of the ferret during early postnatal development. *J Comp Neurol* **353,** 306-316.

Cramer KS & Sur M. (1999). The neuronal form of nitric oxide synthase is required for pattern formation by retinal afferents in the ferret lateral geniculate nucleus. *Brain Res Dev Brain Res* **116,** 79-86.

Crowley JC & Katz LC. (2000). Early development of ocular dominance columns. *Science* **290,** 1321-1324.

Crozier RA, Wang Y, Liu CH & Bear MF. (2007). Deprivation-induced synaptic depression by distinct mechanisms in different layers of mouse visual cortex. *Proc Natl Acad Sci U S A* **104,** 1383-1388.

Daw NW, Gordon B, Fox KD, Flavin HJ, Kirsch JD, Beaver CJ, Ji Q, Reid SN & Czepita D. (1999). Injection of MK-801 affects ocular dominance shifts more than visual activity. *J Neurophysiol* **81,** 204-215.

Dawson TM & Snyder SH. (1994). Gases as biological messengers: nitric oxide and carbon monoxide in the brain. *J Neurosci* **14,** 5147-5159.

Derkach VA, Oh MC, Guire ES & Soderling TR. (2007). Regulatory mechanisms of AMPA receptors in synaptic plasticity. *Nat Rev Neurosci* **8,** 101-113.

Desai NS, Cudmore RH, Nelson SB & Turrigiano GG. (2002). Critical periods for experience-dependent synaptic scaling in visual cortex. *Nat Neurosci* **5,** 783-789.

Desai NS, Rutherford LC & Turrigiano GG. (1999). Plasticity in the intrinsic excitability of cortical pyramidal neurons. *Nat Neurosci* **2,** 515-520.

Deshmukh S, Onozuka K, Bender KJ, Bender VA, Lutz B, Mackie K & Feldman DE. (2007). Postnatal development of cannabinoid receptor type 1 expression in rodent somatosensory cortex. *Neuroscience* **145,** 279-287.

Dews PB & Wiesel TN. (1970). Consequences of monocular deprivation on visual behaviour in kittens. *J Physiol* **206,** 437-455.

Di Cristo G, Chattopadhyaya B, Kuhlman SJ, Fu Y, Belanger MC, Wu CZ, Rutishauser U, Maffei L & Huang ZJ. (2007). Activity-dependent PSA expression regulates inhibitory maturation and onset of critical period plasticity. *Nat Neurosci* **10,** 1569-1577.

Dingledine R. (1983). N-methyl aspartate activates voltage-dependent calcium conductance in rat hippocampal pyramidal cells. *J Physiol* **343,** 385-405.

Dingledine R, Borges K, Bowie D & Traynelis SF. (1999). The glutamate receptor ion channels. *Pharmacol Rev* **51,** 7-61.

Dong H, Wang Q, Valkova K, Gonchar Y & Burkhalter A. (2004). Experience-dependent development of feedforward and feedback circuits between lower and higher areas of mouse visual cortex. *Vision Res* **44,** 3389-3400.

Drager UC. (1975). Receptive fields of single cells and topography in mouse visual cortex. *J Comp Neurol* **160,** 269-290.

Drager UC & Olsen JF. (1980). Origins of crossed and uncrossed retinal projections in pigmented and albino mice. *J Comp Neurol* **191,** 383-412.

Drager UC & Olsen JF. (1981). Ganglion cell distribution in the retina of the mouse. *Invest Ophthalmol Vis Sci* **20,** 285-293.

Dudek SM & Bear MF. (1992). Homosynaptic long-term depression in area CA1 of hippocampus and effects of N-methyl-D-aspartate receptor blockade. *Proc Natl Acad Sci U S A* **89,** 4363-4367.

Dugas JP, Garbow JR, Kobayashi DK & Conradi MS. (2004). Hyperpolarized (3)He MRI of mouse lung. *Magn Reson Med* **52,** 1310-1317.

Edelman GM & Gally JA. (1992). Nitric oxide: linking space and time in the brain. *Proc Natl Acad Sci U S A* **89,** 11651-11652.

Edelman GM & Gally JA. (2001). Degeneracy and complexity in biological systems. *Proc Natl Acad Sci U S A* **98,** 13763-13768.

Egan CM, Sridhar S, Wigler M & Hall IM. (2007). Recurrent DNA copy number variation in the laboratory mouse. *Nat Genet* **39,** 1384-1389.

Eliasson MJ, Blackshaw S, Schell MJ & Snyder SH. (1997). Neuronal nitric oxide synthase alternatively spliced forms: prominent functional localizations in the brain. *Proc Natl Acad Sci U S A* **94,** 3396-3401.

Esteban JA, Shi SH, Wilson C, Nuriya M, Huganir RL & Malinow R. (2003). PKA phosphorylation of AMPA receptor subunits controls synaptic trafficking underlying plasticity. *Nat Neurosci* **6,** 136-143.

Faber DJ, Mik EG, Aalders MC & van Leeuwen TG. (2003). Light absorption of (oxy-)hemoglobin assessed by spectroscopic optical coherence tomography. *Opt Lett* **28,** 1436-1438.

Fagiolini M, Fritschy JM, Low K, Mohler H, Rudolph U & Hensch TK. (2004). Specific GABAA circuits for visual cortical plasticity. *Science* **303,** 1681-1683.

Faguet J, Maranhao B, Smith SL & Trachtenberg JT. (2009). Ipsilateral eye cortical maps are uniquely sensitive to binocular plasticity. *J Neurophysiol* **101,** 855-861.

Farley BJ, Yu H, Jin DZ & Sur M. (2007). Alteration of visual input results in a coordinated reorganization of multiple visual cortex maps. *J Neurosci* **27,** 10299-10310.

Feldman DE. (2000). Inhibition and plasticity. *Nat Neurosci* **3,** 303-304.

Feldman DE. (2002). Synapses, scaling and homeostasis in vivo. *Nat Neurosci* **5,** 712-714.

Fischer M, Kaech S, Wagner U, Brinkhaus H & Matus A. (2000). Glutamate receptors regulate actin-based plasticity in dendritic spines. *Nat Neurosci* **3,** 887-894.

Fitzpatrick D, Lund JS, Schmechel DE & Towles AC. (1987). Distribution of GABAergic neurons and axon terminals in the macaque striate cortex. *J Comp Neurol* **264,** 73-91.

Fox K, Daw N, Sato H & Czepita D. (1992). The effect of visual experience on development of NMDA receptor synaptic transmission in kitten visual cortex. *J Neurosci* **12,** 2672-2684.

Fox K & Daw NW. (1993). Do NMDA receptors have a critical function in visual cortical plasticity? *Trends Neurosci* **16,** 116-122.

Franklin KBJ & Paxinos G. (2008). *The mouse brain in stereotaxic coordinates*. Elsevier Academic Press, Amsterdam ; London.

Frenkel MY & Bear MF. (2004a). How Monocular Deprivation Shifts Ocular Dominance in Visual Cortex of Young Mice. *Neuron* **44,** 917-923.

Frenkel MY & Bear MF. (2004b). How monocular deprivation shifts ocular dominance in visual cortex of young mice. *Neuron* **44,** 917-923.

Frenkel MY, Sawtell NB, Diogo AC, Yoon B, Neve RL & Bear MF. (2006). Instructive effect of visual experience in mouse visual cortex. *Neuron* **51,** 339-349.

Froemke RC & Dan Y. (2002). Spike-timing-dependent synaptic modification induced by natural spike trains. *Nature* **416,** 433-438.

Frostig RD, Lieke EE, Ts'o DY & Grinvald A. (1990). Cortical functional architecture and local coupling between neuronal activity and the microcirculation revealed by in vivo high-resolution optical imaging of intrinsic signals. *Proc Natl Acad Sci U S A* **87,** 6082-6086.

Gainey MA, Hurvitz-Wolff JR, Lambo ME & Turrigiano GG. (2009). Synaptic scaling requires the GluR2 subunit of the AMPA receptor. *J Neurosci* **29,** 6479-6489.

Gandhi SP, Yanagawa Y & Stryker MP. (2008). Delayed plasticity of inhibitory neurons in developing visual cortex. *Proc Natl Acad Sci U S A* **105,** 16797-16802.

Garthwaite J & Boulton CL. (1995). Nitric-Oxide Signaling in the Central-Nervous-System. *Annual Review of Physiology* **57,** 683-706.

Garthwaite J, Charles SL & Chess-Williams R. (1988). Endothelium-derived relaxing factor release on activation of NMDA receptors suggests role as intercellular messenger in the brain. *Nature* **336,** 385-388.

Garthwaite J & Garthwaite G. (1987). Cellular origins of cyclic GMP responses to excitatory amino acid receptor agonists in rat cerebellum in vitro. *J Neurochem* **48,** 29-39.

Ge S, Yang CH, Hsu KS, Ming GL & Song H. (2007). A critical period for enhanced synaptic plasticity in newly generated neurons of the adult brain. *Neuron* **54,** 559-566.

Glazewski S, Chen CM, Silva A & Fox K. (1996). Requirement for alpha-CaMKII in experience-dependent plasticity of the barrel cortex. *Science* **272,** 421-423.

Glazewski S, Giese KP, Silva A & Fox K. (2000). The role of alpha-CaMKII autophosphorylation in neocortical experience-dependent plasticity. *Nature Neuroscience* **3,** 911-918.

Glazewski S, McKenna M, Jacquin M & Fox K. (1998). Experience-dependent depression of vibrissae responses in adolescent rat barrel cortex. *Eur J Neurosci* **10,** 2107-2116.

Godecke I & Bonhoeffer T. (1996). Development of identical orientation maps for two eyes without common visual experience. *Nature* **379,** 251-254.

Goel A, Jiang B, Xu LW, Song L, Kirkwood A & Lee HK. (2006). Cross-modal regulation of synaptic AMPA receptors in primary sensory cortices by visual experience. *Nat Neurosci* **9,** 1001-1003.

Goel A & Lee HK. (2007). Persistence of experience-induced homeostatic synaptic plasticity through adulthood in superficial layers of mouse visual cortex. *J Neurosci* **27,** 6692-6700.

Goldreich D, Peterson BE & Merzenich MM. (1998). Optical imaging and electrophysiology of rat barrel cortex. II. Responses to paired-vibrissa deflections. *Cerebral Cortex* **8,** 184-192.

Goodman CS & Shatz CJ. (1993). Developmental mechanisms that generate precise patterns of neuronal connectivity. *Cell* **72 Suppl,** 77-98.

Gordon JA. (1997). Cellular mechanisms of visual cortical plasticity: a game of cat and mouse. *Learn Mem* **4,** 245-261.

Gordon JA, Cioffi D, Silva AJ & Stryker MP. (1996). Deficient plasticity in the primary visual cortex of alpha-calcium/calmodulin-dependent protein kinase II mutant mice. *Neuron* **17,** 491-499.

Gordon JA & Stryker MP. (1996). Experience-dependent plasticity of binocular responses in the primary visual cortex of the mouse. *J Neurosci* **16,** 3274-3286.

Greenberg JH, Sohn NW & Hand PJ. (1999). Nitric oxide and the cerebral-blood-flow response to somatosensory activation following deafferentation. *Exp Brain Res* **129,** 541-550.

Grinvald A, Lieke E, Frostig RD, Gilbert CD & Wiesel TN. (1986). Functional architecture of cortex revealed by optical imaging of intrinsic signals. *Nature* **324,** 361-364.

Groth RD & Tsien RW. (2008). A role for retinoic acid in homeostatic plasticity. *Neuron* **60,** 192-194.

Grubb MS & Thompson ID. (2003). Quantitative characterization of visual response properties in the mouse dorsal lateral geniculate nucleus. *J Neurophysiol* **90,** 3594-3607.

Gu X & Han S. (2007). Attention and reality constraints on the neural processes of empathy for pain. *Neuroimage* **36,** 256-267.

Guido W. (2008). Refinement of the retinogeniculate pathway. *J Physiol* **586,** 4357-4362.

Guire ES, Lickey ME & Gordon B. (1999). Critical period for the monocular deprivation effect in rats: assessment with sweep visually evoked potentials. *J Neurophysiol* **81,** 121-128.

Haas K, Li J & Cline HT. (2006). AMPA receptors regulate experience-dependent dendritic arbor growth in vivo. *Proc Natl Acad Sci U S A* **103,** 12127-12131.

Hahm JO, Langdon RB & Sur M. (1991). Disruption of retinogeniculate afferent segregation by antagonists to NMDA receptors. *Nature* **351,** 568-570.

Hamassaki-Britto DE, Hermans-Borgmeyer I, Heinemann S & Hughes TE. (1993). Expression of glutamate receptor genes in the mammalian retina: the localization of GluR1 through GluR7 mRNAs. *J Neurosci* **13,** 1888-1898.

Hardingham N & Fox K. (2006). The role of nitric oxide and GluR1 in presynaptic and postsynaptic components of neocortical potentiation. *J Neurosci* **26,** 7395-7404.

Hardingham N, Glazewski S, Pakhotin P, Mizuno K, Chapman PF, Giese KP & Fox K. (2003). Neocortical long-term potentiation and experience-dependent synaptic plasticity require alpha-calcium/calmodulin-dependent protein kinase II autophosphorylation. *J Neurosci* **23,** 4428-4436.

Hardingham N, Wright N, Dachtler J & Fox K. (2008). Sensory deprivation unmasks a PKA-dependent synaptic plasticity mechanism that operates in parallel with CaMKII. *Neuron* **60,** 861-874.

Hasenstaub AR & Callaway EM. (2010). Paint it black (or red, or green): optical and genetic tools illuminate inhibitory contributions to cortical circuit function. *Neuron* **67,** 681-684.

Hayashi Y, Shi SH, Esteban JA, Piccini A, Poncer JC & Malinow R. (2000). Driving AMPA receptors into synapses by LTP and CaMKII: requirement for GluR1 and PDZ domain interaction. *Science* **287,** 2262-2267.

He HY, Hodos W & Quinlan EM. (2006). Visual deprivation reactivates rapid ocular dominance plasticity in adult visual cortex. *Journal of Neuroscience* **26,** 2951-2955.

Hebb DO. (1949). *The Organisation of Behaviour.* Wiley, New York.

Heimel JA, Hartman RJ, Hermans JM & Levelt CN. (2007). Screening mouse vision with intrinsic signal optical imaging. *Eur J Neurosci* **25,** 795-804.

Heimel JA, Hermans JM, Sommeijer JP & Levelt CN. (2008). Genetic control of experience-dependent plasticity in the visual cortex. *Genes Brain Behav* **7,** 915-923.

Hensch TK. (2004). Critical period regulation. *Annual Review of Neuroscience* **27,** 549-579.

Hensch TK, Fagiolini M, Mataga N, Stryker MP, Baekkeskov S & Kash SF. (1998a). Local GABA circuit control of experience-dependent plasticity in developing visual cortex. *Science* **282,** 1504-1508.

Hensch TK, Gordon JA, Brandon EP, McKnight GS, Idzerda RL & Stryker MP. (1998b). Comparison of plasticity in vivo and in vitro in the developing

visual cortex of normal and protein kinase A RIbeta-deficient mice. *J Neurosci* **18,** 2108-2117.

Heynen AJ & Bear MF. (2001). Long-term potentiation of thalamocortical transmission in the adult visual cortex in vivo. *J Neurosci* **21,** 9801-9813.

Heynen AJ, Yoon BJ, Liu CH, Chung HJ, Huganir RL & Bear MF. (2003). Molecular mechanism for loss of visual cortical responsiveness following brief monocular deprivation. *Nat Neurosci* **6,** 854-862.

Higley MJ & Strittmatter SM. Neuroscience. Lynx for braking plasticity. *Science* **330,** 1189-1190.

Hill DK & Keynes RD. (1949). Opacity changes in stimulated nerve. *J Physiol* **108,** 278-281.

Hofer SB, Mrsic-Flogel TD, Bonhoeffer T & Hubener M. (2006). Prior experience enhances plasticity in adult visual cortex. *Nat Neurosci* **9,** 127-132.

Hofer SB, Mrsic-Flogel TD, Bonhoeffer T & Hubener M. (2009). Experience leaves a lasting structural trace in cortical circuits. *Nature* **457,** 313-317.

Hoffman DA, Sprengel R & Sakmann B. (2002). Molecular dissection of hippocampal theta-burst pairing potentiation. *Proc Natl Acad Sci U S A* **99,** 7740-7745.

Holtmaat AJ, Trachtenberg JT, Wilbrecht L, Shepherd GM, Zhang X, Knott GW & Svoboda K. (2005). Transient and persistent dendritic spines in the neocortex in vivo. *Neuron* **45,** 279-291.

Hopper RA & Garthwaite J. (2006). Tonic and phasic nitric oxide signals in hippocampal long-term potentiation. *J Neurosci* **26,** 11513-11521.

Hou Q, Zhang D, Jarzylo L, Huganir RL & Man HY. (2008). Homeostatic regulation of AMPA receptor expression at single hippocampal synapses. *Proc Natl Acad Sci U S A* **105,** 775-780.

Houweling AR & Brecht M. (2008). Behavioural report of single neuron stimulation in somatosensory cortex. *Nature* **451,** 65-68.

Howard MA, Elias GM, Elias LA, Swat W & Nicoll RA. (2010). The role of SAP97 in synaptic glutamate receptor dynamics. *Proc Natl Acad Sci U S A* **107,** 3805-3810.

Huang W, Plyka I, Li H, Eisenstein EM, Volkow ND & Springer CS, Jr. (1996). Magnetic resonance imaging (MRI) detection of the murine brain response to light: temporal differentiation and negative functional MRI changes. *Proc Natl Acad Sci U S A* **93,** 6037-6042.

Huang ZJ & Di Cristo G. (2008). Time to change: retina sends a messenger to promote plasticity in visual cortex. *Neuron* **59,** 355-358.

Hubel DH & Wiesel TN. (1959). Receptive fields of single neurones in the cat's striate cortex. *J Physiol* **148,** 574-591.

Hubel DH & Wiesel TN. (1962). Receptive fields, binocular interaction and functional architecture in the cat's visual cortex. *J Physiol* **160,** 106-154.

Hubel DH & Wiesel TN. (1963a). Receptive Fields of Cells in Striate Cortex of Very Young, Visually Inexperienced Kittens. *J Neurophysiol* **26,** 994-1002.

Hubel DH & Wiesel TN. (1963b). Shape and arrangement of columns in cat's striate cortex. *J Physiol* **165,** 559-568.

Hubel DH & Wiesel TN. (1965). Binocular interaction in striate cortex of kittens reared with artificial squint. *J Neurophysiol* **28,** 1041-1059.

Hubel DH & Wiesel TN. (1970). The period of susceptibility to the physiological effects of unilateral eye closure in kittens. *J Physiol* **206,** 419-436.

Hubel DH & Wiesel TN. (1998). Early exploration of the visual cortex. *Neuron* **20,** 401-412.

Hubener M. (2003). Mouse visual cortex. *Curr Opin Neurobiol* **13,** 413-420.

Huber D, Petreanu L, Ghitani N, Ranade S, Hromadka T, Mainen Z & Svoboda K. (2008). Sparse optical microstimulation in barrel cortex drives learned behaviour in freely moving mice. *Nature* **451,** 61-64.

Imura T, Kanatani S, Fukuda S, Miyamoto Y & Hisatsune T. (2005). Layer-specific production of nitric oxide during cortical circuit formation in postnatal mouse brain. *Cereb Cortex* **15,** 332-340.

Isaac JT, Crair MC, Nicoll RA & Malenka RC. (1997). Silent synapses during development of thalamocortical inputs. *Neuron* **18,** 269-280.

Isaac JT, Nicoll RA & Malenka RC. (1995). Evidence for silent synapses: implications for the expression of LTP. *Neuron* **15,** 427-434.

Iwai Y, Atapour N, Renger J, Roder J, Seeburg P & Hensch TK. (2006). Sequential role of AMPA receptor subunits in ocular dominance plasticity. In *Society for Neuroscience*. Atlanta.

Iwai Y, Fagiolini M, Obata K & Hensch TK. (2003). Rapid critical period induction by tonic inhibition in visual cortex. *J Neurosci* **23,** 6695-6702.

Jensen V, Kaiser KM, Borchardt T, Adelmann G, Rozov A, Burnashev N, Brix C, Frotscher M, Andersen P, Hvalby O, Sakmann B, Seeburg PH & Sprengel R. (2003). A juvenile form of postsynaptic hippocampal long-term potentiation in mice deficient for the AMPA receptor subunit GluR-A. *J Physiol* **553,** 843-856.

Jiang B, Trevino M & Kirkwood A. (2007). Sequential development of long-term potentiation and depression in different layers of the mouse visual cortex. *J Neurosci* **27,** 9648-9652.

Kalatsky VA, Polley DB, Merzenich MM, Schreiner CE & Stryker MP. (2005). Fine functional organization of auditory cortex revealed by Fourier optical imaging. *Proceedings of the National Academy of Sciences of the United States of America* **102,** 13325-13330.

Kalatsky VA & Stryker MP. (2003). New paradigm for optical imaging: temporally encoded maps of intrinsic signal. *Neuron* **38,** 529-545.

Kaneko M, Cheetham CE, Lee YS, Silva AJ, Stryker MP & Fox K. (2010). Constitutively active H-ras accelerates multiple forms of plasticity in developing visual cortex. *Proc Natl Acad Sci U S A* **107,** 19026-19031.

Kaneko M, Hanover JL, England PM & Stryker MP. (2008a). TrkB kinase is required for recovery, but not loss, of cortical responses following monocular deprivation. *Nat Neurosci* **11,** 497-504.

Kaneko M, Stellwagen D, Malenka RC & Stryker MP. (2008b). Tumor necrosis factor-alpha mediates one component of competitive, experience-dependent plasticity in developing visual cortex. *Neuron* **58,** 673-680.

Karmarkar UR & Dan Y. (2006). Experience-dependent plasticity in adult visual cortex. *Neuron* **52,** 577-585.

Katz LC & Shatz CJ. (1996). Synaptic activity and the construction of cortical circuits. *Science* **274,** 1133-1138.

Keck T, Mrsic-Flogel TD, Vaz Afonso M, Eysel UT, Bonhoeffer T & Hubener M. (2008). Massive restructuring of neuronal circuits during functional reorganization of adult visual cortex. *Nat Neurosci* **11,** 1162-1167.

Kerlin AM, Andermann ML, Berezovskii VK & Reid RC. (2010). Broadly tuned response properties of diverse inhibitory neuron subtypes in mouse visual cortex. *Neuron* **67,** 858-871.

Kielland A, Bochorishvili G, Corson J, Zhang L, Rosin DL, Heggelund P & Zhu JJ. (2009). Activity patterns govern synapse-specific AMPA receptor trafficking between deliverable and synaptic pools. *Neuron* **62,** 84-101.

Kilman V, van Rossum MC & Turrigiano GG. (2002). Activity deprivation reduces miniature IPSC amplitude by decreasing the number of postsynaptic GABA(A) receptors clustered at neocortical synapses. *J Neurosci* **22,** 1328-1337.

Kim CH, Takamiya K, Petralia RS, Sattler R, Yu S, Zhou W, Kalb R, Wenthold R & Huganir R. (2005). Persistent hippocampal CA1 LTP in mice lacking the C-terminal PDZ ligand of GluR1. *Nat Neurosci* **8,** 985-987.

Kirkwood A & Bear MF. (1994). Homosynaptic long-term depression in the visual cortex. *J Neurosci* **14,** 3404-3412.

Kirkwood A, Dudek SM, Gold JT, Aizenman CD & Bear MF. (1993). Common forms of synaptic plasticity in the hippocampus and neocortex in vitro. *Science* **260,** 1518-1521.

Kirkwood A, Lee HK & Bear MF. (1995). Co-regulation of long-term potentiation and experience-dependent synaptic plasticity in visual cortex by age and experience. *Nature* **375,** 328-331.

Kirkwood A, Rioult MC & Bear MF. (1996). Experience-dependent modification of synaptic plasticity in visual cortex. *Nature* **381,** 526-528.

Kirkwood A, Silva A & Bear MF. (1997). Age-dependent decrease of synaptic plasticity in the neocortex of alphaCaMKII mutant mice. *Proc Natl Acad Sci U S A* **94,** 3380-3383.

Knott GW, Holtmaat A, Wilbrecht L, Welker E & Svoboda K. (2006). Spine growth precedes synapse formation in the adult neocortex in vivo. *Nat Neurosci* **9,** 1117-1124.

Kopec CD, Li B, Wei W, Boehm J & Malinow R. (2006). Glutamate receptor exocytosis and spine enlargement during chemically induced long-term potentiation. *J Neurosci* **26,** 2000-2009.

Kopec CD, Real E, Kessels HW & Malinow R. (2007). GluR1 links structural and functional plasticity at excitatory synapses. *J Neurosci* **27,** 13706-13718.

Krahe TE, Medina AE, de Bittencourt-Navarrete RE, Colello RJ & Ramoa AS. (2005). Protein synthesis-independent plasticity mediates rapid and precise recovery of deprived eye responses. *Neuron* **48,** 329-343.

Lambo ME & Turrigiano GG. (2010). Delayed synaptic scaling in binocular visual cortex during monocular deprivation In *Society For Neuroscience Meeting*. San Diego.

Lamprecht R & LeDoux J. (2004). Structural plasticity and memory. *Nat Rev Neurosci* **5,** 45-54.

Lee HK, Barbarosie M, Kameyama K, Bear MF & Huganir RL. (2000). Regulation of distinct AMPA receptor phosphorylation sites during bidirectional synaptic plasticity. *Nature* **405,** 955-959.

Lee HK, Kameyama K, Huganir RL & Bear MF. (1998). NMDA induces long-term synaptic depression and dephosphorylation of the GluR1 subunit of AMPA receptors in hippocampus. *Neuron* **21,** 1151-1162.

Lee HK, Takamiya K, Han JS, Man H, Kim CH, Rumbaugh G, Yu S, Ding L, He C, Petralia RS, Wenthold RJ, Gallagher M & Huganir RL. (2003). Phosphorylation of the AMPA receptor GluR1 subunit is required for synaptic plasticity and retention of spatial memory. *Cell* **112,** 631-643.

Lee HK, Takamiya K, Kameyama K, He K, Yu S, Rossetti L, Wilen D & Huganir RL. (2007). Identification and characterization of a novel phosphorylation site on the GluR1 subunit of AMPA receptors. *Mol Cell Neurosci* **36,** 86-94.

Lehmann K & Lowel S. (2008). Age-dependent ocular dominance plasticity in adult mice. *PLoS One* **3,** e3120.

Lettvin JY. (1968). What the frog's eye tells the frogs brain.

LeVay S, Wiesel TN & Hubel DH. (1980). The development of ocular dominance columns in normal and visually deprived monkeys. *J Comp Neurol* **191,** 1-51.

Levenson JM & Sweatt JD. (2005). Epigenetic mechanisms in memory formation. *Nature Reviews Neuroscience* **6,** 108-118.

Li L, Bender KJ, Drew PJ, Jadhav SP, Sylwestrak E & Feldman DE. (2009). Endocannabinoid signaling is required for development and critical period plasticity of the whisker map in somatosensory cortex. *Neuron* **64,** 537-549.

Liao D, Hessler NA & Malinow R. (1995). Activation of postsynaptically silent synapses during pairing-induced LTP in CA1 region of hippocampal slice. *Nature* **375,** 400-404.

Liao DS, Mower AF, Neve RL, Sato-Bigbee C & Ramoa AS. (2002). Different mechanisms for loss and recovery of binocularity in the visual cortex. *J Neurosci* **22,** 9015-9023.

Lisman J & Raghavachari S. (2006). A unified model of the presynaptic and postsynaptic changes during LTP at CA1 synapses. *Sci STKE* **2006,** re11.

Liu BH, Li P, Sun YJ, Li YT, Zhang LI & Tao HW. (2010). Intervening inhibition underlies simple-cell receptive field structure in visual cortex. *Nat Neurosci* **13,** 89-96.

Liu CH, Heynen AJ, Shuler MG & Bear MF. (2008). Cannabinoid receptor blockade reveals parallel plasticity mechanisms in different layers of mouse visual cortex. *Neuron* **58,** 340-345.

Lomo T. (2003). The discovery of long-term potentiation. *Philosophical Transactions of the Royal Society of London Series B-Biological Sciences* **358,** 617-620.

Lu W, Man H, Ju W, Trimble WS, MacDonald JF & Wang YT. (2001). Activation of synaptic NMDA receptors induces membrane insertion of new AMPA receptors and LTP in cultured hippocampal neurons. *Neuron* **29,** 243-254.

Lu W, Shi Y, Jackson AC, Bjorgan K, During MJ, Sprengel R, Seeburg PH & Nicoll RA. (2009). Subunit composition of synaptic AMPA receptors revealed by a single-cell genetic approach. *Neuron* **62,** 254-268.

Ludwig CJ, Ranson A & Gilchrist ID. (2008). Oculomotor capture by transient events: a comparison of abrupt onsets, offsets, motion, and flicker. *J Vis* **8,** 11 11-16.

Luo L, Callaway EM & Svoboda K. (2008). Genetic dissection of neural circuits. *Neuron* **57,** 634-660.

Luscher C, Xia H, Beattie EC, Carroll RC, von Zastrow M, Malenka RC & Nicoll RA. (1999). Role of AMPA receptor cycling in synaptic transmission and plasticity. *Neuron* **24,** 649-658.

Mack V, Burnashev N, Kaiser KM, Rozov A, Jensen V, Hvalby O, Seeburg PH, Sakmann B & Sprengel R. (2001). Conditional restoration of hippocampal synaptic potentiation in Glur-A-deficient mice. *Science* **292,** 2501-2504.

Maffei A, Lambo ME & Turrigiano GG. (2010). Critical period for inhibitory plasticity in rodent binocular V1. *J Neurosci* **30,** 3304-3309.

Maffei A, Nelson SB & Turrigiano GG. (2004). Selective reconfiguration of layer 4 visual cortical circuitry by visual deprivation. *Nat Neurosci* **7,** 1353-1359.

Maffei A & Turrigiano GG. (2008). Multiple modes of network homeostasis in visual cortical layer 2/3. *J Neurosci* **28,** 4377-4384.

Malenka RC, Kauer JA, Zucker RS & Nicoll RA. (1988). Postsynaptic calcium is sufficient for potentiation of hippocampal synaptic transmission. *Science* **242,** 81-84.

Malenka RC & Nicoll RA. (1999). Long-term potentiation--a decade of progress? *Science* **285,** 1870-1874.

Malinow R, Madison DV & Tsien RW. (1988). Persistent protein kinase activity underlying long-term potentiation. *Nature* **335,** 820-824.

Mangini NJ & Pearlman AL. (1980). Laminar distribution of receptive field properties in the primary visual cortex of the mouse. *J Comp Neurol* **193,** 203-222.

Martin LJ, Blackstone CD, Levey AI, Huganir RL & Price DL. (1993). AMPA glutamate receptor subunits are differentially distributed in rat brain. *Neuroscience* **53,** 327-358.

Masino SA. (2003). Quantitative comparison between functional imaging and single-unit spiking in rat somatosensory cortex. *Journal of Neurophysiology* **89,** 1702-1712.

Matsuo N, Reijmers L & Mayford M. (2008). Spine-type-specific recruitment of newly synthesized AMPA receptors with learning. *Science* **319,** 1104-1107.

McCormack SG, Stornetta RL & Zhu JJ. (2006). Synaptic AMPA receptor exchange maintains bidirectional plasticity. *Neuron* **50,** 75-88.

McCurry CL, Shepherd JD, Tropea D, Wang KH, Bear MF & Sur M. (2010). Loss of Arc renders the visual cortex impervious to the effects of sensory experience or deprivation. *Nat Neurosci* **13,** 450-457.

Meliza CD & Dan Y. (2006). Receptive-field modification in rat visual cortex induced by paired visual stimulation and single-cell spiking. *Neuron* **49,** 183-189.

Metin C, Godement P & Imbert M. (1988). The primary visual cortex in the mouse: receptive field properties and functional organization. *Exp Brain Res* **69,** 594-612.

Mize RR, Wu HH, Cork RJ & Scheiner CA. (1998). The role of nitric oxide in development of the patch-cluster system and retinocollicular pathways in the rodent superior colliculus. *Prog Brain Res* **118,** 133-152.

Mizuno H, Hirano T & Tagawa Y. (2007). Evidence for activity-dependent cortical wiring: formation of interhemispheric connections in neonatal mouse visual cortex requires projection neuron activity. *J Neurosci* **27,** 6760-6770.

Molnar E, Baude A, Richmond SA, Patel PB, Somogyi P & McIlhinney RA. (1993). Biochemical and immunocytochemical characterization of antipeptide antibodies to a cloned GluR1 glutamate receptor subunit:

cellular and subcellular distribution in the rat forebrain. *Neuroscience* **53,** 307-326.

Mooser F, Bosking WH & Fitzpatrick D. (2004). A morphological basis for orientation tuning in primary visual cortex. *Nat Neurosci* **7,** 872-879.

Morishita H, Miwa JM, Heintz N & Hensch TK. (2010). Lynx1, a cholinergic brake, limits plasticity in adult visual cortex. *Science* **330,** 1238-1240.

Mrsic-Flogel T, Hubener M & Bonhoeffer T. (2003). Brain mapping: new wave optical imaging. *Curr Biol* **13,** R778-780.

Mrsic-Flogel TD, Hofer SB, Creutzfeldt C, Cloez-Tayarani I, Changeux JP, Bonhoeffer T & Hubener M. (2005). Altered map of visual space in the superior colliculus of mice lacking early retinal waves. *J Neurosci* **25,** 6921-6928.

Mrsic-Flogel TD, Hofer SB, Ohki K, Reid RC, Bonhoeffer T & Hubener M. (2007). Homeostatic regulation of eye-specific responses in visual cortex during ocular dominance plasticity. *Neuron* **54,** 961-972.

Nauhaus I, Benucci A, Carandini M & Ringach DL. (2008). Neuronal selectivity and local map structure in visual cortex. *Neuron* **57,** 673-679.

Nelken I, Bizley JK, Nodal FR, Ahmed B, Schnupp JW & King AJ. (2004). Large-scale organization of ferret auditory cortex revealed using continuous acquisition of intrinsic optical signals. *Journal of Neurophysiology* **92,** 2574-2588.

Niell CM & Stryker MP. (2008). Highly selective receptive fields in mouse visual cortex. *J Neurosci* **28,** 7520-7536.

Nikonenko I, Boda B, Steen S, Knott G, Welker E & Muller D. (2008). PSD-95 promotes synaptogenesis and multiinnervated spine formation through nitric oxide signaling. *J Cell Biol* **183,** 1115-1127.

Northoff G, Walter M, Schulte RF, Beck J, Dydak U, Henning A, Boeker H, Grimm S & Boesiger P. (2007). GABA concentrations in the human anterior cingulate cortex predict negative BOLD responses in fMRI. *Nat Neurosci* **10,** 1515-1517.

Nowak L, Bregestovski P, Ascher P, Herbet A & Prochiantz A. (1984). Magnesium gates glutamate-activated channels in mouse central neurones. *Nature* **307,** 462-465.

O'Dell TJ, Hawkins RD, Kandel ER & Arancio O. (1991). Tests of the roles of two diffusible substances in long-term potentiation: evidence for nitric oxide as a possible early retrograde messenger. *Proc Natl Acad Sci U S A* **88,** 11285-11289.

O'Dell TJ, Huang PL, Dawson TM, Dinerman JL, Snyder SH, Kandel ER & Fishman MC. (1994). Endothelial NOS and the blockade of LTP by NOS inhibitors in mice lacking neuronal NOS. *Science* **265,** 542-546.

Ohki K, Chung S, Ch'ng YH, Kara P & Reid RC. (2005). Functional imaging with cellular resolution reveals precise micro-architecture in visual cortex. *Nature* **433,** 597-603.

Osten P, Khatri L, Perez JL, Kohr G, Giese G, Daly C, Schulz TW, Wensky A, Lee LM & Ziff EB. (2000). Mutagenesis reveals a role for ABP/GRIP binding to GluR2 in synaptic surface accumulation of the AMPA receptor. *Neuron* **27,** 313-325.

Park M, Penick EC, Edwards JG, Kauer JA & Ehlers MD. (2004). Recycling endosomes supply AMPA receptors for LTP. *Science* **305,** 1972-1975.

Perez JL, Khatri L, Chang C, Srivastava S, Osten P & Ziff EB. (2001). PICK1 targets activated protein kinase Calpha to AMPA receptor clusters in spines of hippocampal neurons and reduces surface levels of the AMPA-type glutamate receptor subunit 2. *J Neurosci* **21,** 5417-5428.

Peterson BE, Goldreich D & Merzenich M. (1998). Optical imaging and electrophysiology of rat barrel cortex. I. Responses to small single-vibrissa deflections. *Cerebral Cortex* **8,** 173-183.

Pham TA, Graham SJ, Suzuki S, Barco A, Kandel ER, Gordon B & Lickey ME. (2004). A semi-persistent adult ocular dominance plasticity in visual cortex is stabilized by activated CREB. *Learn Mem* **11,** 738-747.

Phillips KG, Hardingham NR & Fox K. (2008). Postsynaptic action potentials are required for nitric-oxide-dependent long-term potentiation in CA1 neurons of adult GluR1 knock-out and wild-type mice. *J Neurosci* **28,** 14031-14041.

Pinker S. (1994). *The Language Instinct*. Harper Collins., New York

Plant K, Pelkey KA, Bortolotto ZA, Morita D, Terashima A, McBain CJ, Collingridge GL & Isaac JT. (2006). Transient incorporation of native GluR2-lacking AMPA receptors during hippocampal long-term potentiation. *Nat Neurosci* **9,** 602-604.

Plath N, Ohana O, Dammermann B, Errington ML, Schmitz D, Gross C, Mao X, Engelsberg A, Mahlke C, Welzl H, Kobalz U, Stawrakakis A, Fernandez E, Waltereit R, Bick-Sander A, Therstappen E, Cooke SF, Blanquet V, Wurst

W, Salmen B, Bosl MR, Lipp HP, Grant SG, Bliss TV, Wolfer DP & Kuhl D. (2006). Arc/Arg3.1 is essential for the consolidation of synaptic plasticity and memories. *Neuron* **52,** 437-444.

Porciatti V, Pizzorusso T & Maffei L. (1999). The visual physiology of the wild type mouse determined with pattern VEPs. *Vision Res* **39,** 3071-3081.

Prusky GT & Douglas RM. (2003). Developmental plasticity of mouse visual acuity. *Eur J Neurosci* **17,** 167-173.

Putignano E, Lonetti G, Cancedda L, Ratto G, Costa M, Maffei L & Pizzorusso T. (2007). Developmental Downregulation of histone posttranslational modifications regulates visual cortical plasticity. *Neuron* **53,** 747-759.

Rajagopalan UM & Tanifuji M. (2007). Functional optical coherence tomography reveals localized layer-specific activations in cat primary visual cortex in vivo. *Opt Lett* **32,** 2614-2616.

Reid SN, Daw NW, Gregory DS & Flavin H. (1996a). cAMP levels increased by activation of metabotropic glutamate receptors correlate with visual plasticity. *J Neurosci* **16,** 7619-7626.

Reid SNM, Daw NW, Czepita D, Flavin HJ & Sessa WC. (1996b). Inhibition of nitric oxide synthase does not alter ocular dominance shifts in kitten visual cortex. *Journal of Physiology-London* **494,** 511-517.

Restani L, Cerri C, Pietrasanta M, Gianfranceschi L, Maffei L & Caleo M. (2009). Functional masking of deprived eye responses by callosal input during ocular dominance plasticity. *Neuron* **64,** 707-718.

Ridder W, 3rd, Nusinowitz S & Heckenlively JR. (2002). Causes of cataract development in anesthetized mice. *Exp Eye Res* **75,** 365-370.

Roberson ED & Sweatt JD. (1996). Transient activation of cyclic AMP-dependent protein kinase during hippocampal long-term potentiation. *J Biol Chem* **271,** 30436-30441.

Roberts EB, Meredith MA & Ramoa AS. (1998). Suppression of NMDA receptor function using antisense DNA block ocular dominance plasticity while preserving visual responses. *J Neurophysiol* **80,** 1021-1032.

Roche KW, O'Brien RJ, Mammen AL, Bernhardt J & Huganir RL. (1996). Characterization of multiple phosphorylation sites on the AMPA receptor GluR1 subunit. *Neuron* **16,** 1179-1188.

Rumpel S, Hatt H & Gottmann K. (1998). Silent synapses in the developing rat visual cortex: evidence for postsynaptic expression of synaptic plasticity. *J Neurosci* **18,** 8863-8874.

Runyan CA, Schummers J, Van Wart A, Kuhlman SJ, Wilson NR, Huang ZJ & Sur M. (2010). Response features of parvalbumin-expressing interneurons suggest precise roles for subtypes of inhibition in visual cortex. *Neuron* **67,** 847-857.

Ruthazer ES, Gillespie DC, Dawson TM, Snyder SH & Stryker MP. (1996). Inhibition of nitric oxide synthase does not prevent ocular dominance plasticity in kitten visual cortex. *Journal of Physiology* **494,** 519-527.

Sato M & Stryker MP. (2008). Distinctive features of adult ocular dominance plasticity. *J Neurosci* **28,** 10278-10286.

Sawtell NB, Frenkel MY, Philpot BD, Nakazawa K, Tonegawa S & Bear MF. (2003). NMDA receptor-dependent ocular dominance plasticity in adult visual cortex. *Neuron* **38,** 977-985.

Schmitt WB, Sprengel R, Mack V, Draft RW, Seeburg PH, Deacon RM, Rawlins JN & Bannerman DM. (2005). Restoration of spatial working memory by genetic rescue of GluR-A-deficient mice. *Nat Neurosci* **8,** 270-272.

Schuett S, Bonhoeffer T & Hubener M. (2002). Mapping retinotopic structure in mouse visual cortex with optical imaging. *J Neurosci* **22,** 6549-6559.

Schuman EM & Madison DV. (1991). A requirement for the intercellular messenger nitric oxide in long-term potentiation. *Science* **254,** 1503-1506.

Schuman EM & Madison DV. (1994). Nitric oxide and synaptic function. *Annu Rev Neurosci* **17,** 153-183.

Sengpiel F, Godecke I, Stawinski P, Hubener M, Lowel S & Bonhoeffer T. (1998). Intrinsic and environmental factors in the development of functional maps in cat visual cortex. *Neuropharmacology* **37,** 607-621.

Serulle Y, Zhang S, Ninan I, Puzzo D, McCarthy M, Khatri L, Arancio O & Ziff EB. (2007). A GluR1-cGKII interaction regulates AMPA receptor trafficking. *Neuron* **56,** 670-688.

Shepherd JD & Bear MF. (2011). New views of Arc, a master regulator of synaptic plasticity. *Nat Neurosci* **14,** 279-284.

Shepherd JD & Huganir RL. (2007). The cell biology of synaptic plasticity: AMPA receptor trafficking. *Annu Rev Cell Dev Biol* **23,** 613-643.

Shepherd JD, Rumbaugh G, Wu J, Chowdhury S, Plath N, Kuhl D, Huganir RL & Worley PF. (2006). Arc/Arg3.1 mediates homeostatic synaptic scaling of AMPA receptors. *Neuron* **52,** 475-484.

Sherman SM, Guillery RW, Kaas JH & Sanderson KJ. (1974). Behavioral, electrophysiological and morphological studies of binocular competition in the development of the geniculo-cortical pathways of cats. *J Comp Neurol* **158,** 1-18.

Shi S, Hayashi Y, Esteban JA & Malinow R. (2001). Subunit-specific rules governing AMPA receptor trafficking to synapses in hippocampal pyramidal neurons. *Cell* **105,** 331-343.

Shi SH, Hayashi Y, Petralia RS, Zaman SH, Wenthold RJ, Svoboda K & Malinow R. (1999). Rapid spine delivery and redistribution of AMPA receptors after synaptic NMDA receptor activation. *Science* **284,** 1811-1816.

Siegmund A, Langnaese K & Wotjak CT. (2005). Differences in extinction of conditioned fear in C57BL/6 substrains are unrelated to expression of alpha-synuclein. *Behav Brain Res* **157,** 291-298.

Silva AJ, Paylor R, Wehner JM & Tonegawa S. (1992a). Impaired Spatial-Learning in Alpha-Calcium-Calmodulin Kinase-Ii Mutant Mice. *Science* **257,** 206-211.

Silva AJ, Stevens CF, Tonegawa S & Wang YY. (1992b). Deficient Hippocampal Long-Term Potentiation in Alpha-Calcium-Calmodulin Kinase-Ii Mutant Mice. *Science* **257,** 201-206.

Singer W. (1995). Development and plasticity of cortical processing architectures. *Science* **270,** 758-764.

Sjostrom PJ, Turrigiano GG & Nelson SB. (2003). Neocortical LTD via coincident activation of presynaptic NMDA and cannabinoid receptors. *Neuron* **39,** 641-654.

Smith GB, Heynen AJ & Bear MF. (2009). Bidirectional synaptic mechanisms of ocular dominance plasticity in visual cortex. *Philos Trans R Soc Lond B Biol Sci* **364,** 357-367.

Smith MA, Ellis-Davies GC & Magee JC. (2003). Mechanism of the distance-dependent scaling of Schaffer collateral synapses in rat CA1 pyramidal neurons. *J Physiol* **548,** 245-258.

Smith SL & Hausser M. (2010). Parallel processing of visual space by neighboring neurons in mouse visual cortex. *Nat Neurosci* **13,** 1144-1149.

Smith SL & Trachtenberg JT. (2007). Experience-dependent binocular competition in the visual cortex begins at eye opening. *Nat Neurosci* **10,** 370-375.

Smith SL & Trachtenberg JT. (2010). The Refinement of Ipsilateral Eye Retinotopic Maps Is Increased by Removing the Dominant Contralateral Eye in Adult Mice. *Plos One* **5,** -.

Sohya K, Kameyama K, Yanagawa Y, Obata K & Tsumoto T. (2007). GABAergic neurons are less selective to stimulus orientation than excitatory neurons in layer II/III of visual cortex, as revealed by in vivo functional Ca2+ imaging in transgenic mice. *J Neurosci* **27,** 2145-2149.

Son H, Hawkins RD, Martin K, Kiebler M, Huang PL, Fishman MC & Kandel ER. (1996). Long-term potentiation is reduced in mice that are doubly mutant in endothelial and neuronal nitric oxide synthase. *Cell* **87,** 1015-1023.

Song I & Huganir RL. (2002). Regulation of AMPA receptors during synaptic plasticity. *Trends Neurosci* **25,** 578-588.

Specht CG & Schoepfer R. (2001). Deletion of the alpha-synuclein locus in a subpopulation of C57BL/6J inbred mice. *BMC Neurosci* **2,** 11.

Specht CG & Schoepfer R. (2004). Deletion of multimerin-1 in alpha-synuclein-deficient mice. *Genomics* **83,** 1176-1178.

Stefanovic B, Schwindt W, Hoehn M & Silva AC. (2007). Functional uncoupling of hemodynamic from neuronal response by inhibition of neuronal nitric oxide synthase. *Journal of Cerebral Blood Flow and Metabolism* **27,** 741-754.

Steinert JR, Kopp-Scheinpflug C, Baker C, Challiss RA, Mistry R, Haustein MD, Griffin SJ, Tong H, Graham BP & Forsythe ID. (2008). Nitric oxide is a volume transmitter regulating postsynaptic excitability at a glutamatergic synapse. *Neuron* **60,** 642-656.

Steinmetz CC & Turrigiano GG. (2010). Tumor necrosis factor-alpha signaling maintains the ability of cortical synapses to express synaptic scaling. *J Neurosci* **30,** 14685-14690.

Stellwagen D & Malenka RC. (2006). Synaptic scaling mediated by glial TNF-alpha. *Nature* **440,** 1054-1059.

Stiedl O, Radulovic J, Lohmann R, Birkenfeld K, Palve M, Kammermeier J, Sananbenesi F & Spiess J. (1999). Strain and substrain differences in

context- and tone-dependent fear conditioning of inbred mice. *Behav Brain Res* **104,** 1-12.

Sugiyama S, Di Nardo AA, Aizawa S, Matsuo I, Volovitch M, Prochiantz A & Hensch TK. (2008). Experience-dependent transfer of Otx2 homeoprotein into the visual cortex activates postnatal plasticity. *Cell* **134,** 508-520.

Taha S, Hanover JL, Silva AJ & Stryker MP. (2002a). Autophosphorylation of alpha CaMKII is required for ocular dominance plasticity. *Neuron* **36,** 483-491.

Taha S, Hanover JL, Silva AJ & Stryker MP. (2002b). Autophosphorylation of alphaCaMKII is required for ocular dominance plasticity. *Neuron* **36,** 483-491.

Taha SA & Stryker MP. (2005a). Molecular substrates of plasticity in the developing visual cortex. *Development, Dynamics and Pathology of Neuronal Networks: From Molecules to Functional Circuits* **147,** 103-114.

Taha SA & Stryker MP. (2005b). Ocular dominance plasticity is stably maintained in the absence of alpha calcium calmodulin kinase II (alphaCaMKII) autophosphorylation. *Proc Natl Acad Sci U S A* **102,** 16438-16442.

Takahashi T, Svoboda K & Malinow R. (2003). Experience strengthening transmission by driving AMPA receptors into synapses. *Science* **299,** 1585-1588.

Tohmi M, Kitaura H, Komagata S, Kudoh M & Shibuki K. (2006). Enduring critical period plasticity visualized by transcranial flavoprotein imaging in mouse primary visual cortex. *J Neurosci* **26,** 11775-11785.

Trachtenberg JT, Trepel C & Stryker MP. (2000). Rapid extragranular plasticity in the absence of thalamocortical plasticity in the developing primary visual cortex. *Science* **287,** 2029-2032.

Turrigiano GG. (2008). The self-tuning neuron: synaptic scaling of excitatory synapses. *Cell* **135,** 422-435.

Turrigiano GG, Leslie KR, Desai NS, Rutherford LC & Nelson SB. (1998). Activity-dependent scaling of quantal amplitude in neocortical neurons. *Nature* **391,** 892-896.

Turrigiano GG & Nelson SB. (2004). Homeostatic plasticity in the developing nervous system. *Nat Rev Neurosci* **5,** 97-107.

Van Hooser SD. (2007). Similarity and diversity in visual cortex: is there a unifying theory of cortical computation? *Neuroscientist* **13,** 639-656.

Vyazovskiy VV, Cirelli C, Pfister-Genskow M, Faraguna U & Tononi G. (2008). Molecular and electrophysiological evidence for net synaptic potentiation in wake and depression in sleep. *Nat Neurosci* **11,** 200-208.

Wallace H, Glazewski S, Liming K & Fox K. (2001). The role of cortical activity in experience-dependent potentiation and depression of sensory responses in rat barrel cortex. *J Neurosci* **21,** 3881-3894.

Wallace W & Bear MF. (2004). A morphological correlate of synaptic scaling in visual cortex. *J Neurosci* **24,** 6928-6938.

Wang BS, Sarnaik R & Cang J. Critical period plasticity matches binocular orientation preference in the visual cortex. *Neuron* **65,** 246-256.

Wang Q & Burkhalter A. (2007). Area map of mouse visual cortex. *J Comp Neurol* **502,** 339-357.

Wang Q, Gao E & Burkhalter A. (2007). In vivo transcranial imaging of connections in mouse visual cortex. *J Neurosci Methods* **159,** 268-276.

Waung MW, Pfeiffer BE, Nosyreva ED, Ronesi JA & Huber KM. (2008). Rapid translation of Arc/Arg3.1 selectively mediates mGluR-dependent LTD through persistent increases in AMPAR endocytosis rate. *Neuron* **59,** 84-97.

Weisskopf MG, Castillo PE, Zalutsky RA & Nicoll RA. (1994). Mediation of hippocampal mossy fiber long-term potentiation by cyclic AMP. *Science* **265,** 1878-1882.

Wiesel TN & Hubel DH. (1963a). Effects of Visual Deprivation on Morphology and Physiology of Cells in the Cats Lateral Geniculate Body. *J Neurophysiol* **26,** 978-993.

Wiesel TN & Hubel DH. (1963b). Single-Cell Responses in Striate Cortex of Kittens Deprived of Vision in One Eye. *Journal of Neurophysiology* **26,** 1003-1017.

Wiesel TN & Hubel DH. (1965). Comparison of the effects of unilateral and bilateral eye closure on cortical unit responses in kittens. *J Neurophysiol* **28,** 1029-1040.

Wilson RI, Godecke A, Brown RE, Schrader J & Haas HL. (1999). Mice deficient in endothelial nitric oxide synthase exhibit a selective deficit in hippocampal long-term potentiation. *Neuroscience* **90,** 1157-1165.

Wong ST, Athos J, Figueroa XA, Pineda VV, Schaefer ML, Chavkin CC, Muglia LJ & Storm DR. (1999). Calcium-stimulated adenylyl cyclase activity is critical for hippocampus-dependent long-term memory and late phase LTP. *Neuron* **23,** 787-798.

Woolsey TA & Van der Loos H. (1970). The structural organization of layer IV in the somatosensory region (SI) of mouse cerebral cortex. The description of a cortical field composed of discrete cytoarchitectonic units. *Brain Research* **17,** 205-242.

Wright N & Fox K. (2010). Origins of cortical layer V surround receptive fields in the rat barrel cortex. *J Neurophysiol* **103,** 709-724.

Wright N, Glazewski G, Hardingham N, Phillips P & Fox K. (In press). Laminar analysis of the role played by GluR1 in experience-dependent plasticity and synaptic depression responses in barrel cortex.

Wright N, Glazewski S, Hardingham N, Phillips K, Pervolaraki E & Fox K. (2008). Laminar analysis of the role of GluR1 in experience-dependent and synaptic depression in barrel cortex. *Nat Neurosci* **11,** 1140-1142.

Wu HH, Cork RJ, Huang PL, Shuman DL & Mize RR. (2000). Refinement of the ipsilateral retinocollicular projection is disrupted in double endothelial and neuronal nitric oxide synthase gene knockout mice. *Brain Research Developmental Brain Research* **120,** 105-111.

Wu K, Len GW, McAuliffe G, Ma C, Tai JP, Xu F & Black IB. (2004). Brain-derived neurotrophic factor acutely enhances tyrosine phosphorylation of the AMPA receptor subunit GluR1 via NMDA receptor-dependent mechanisms. *Brain Res Mol Brain Res* **130,** 178-186.

Xia Y, Carroll RC & Nawy S. (2006). State-dependent AMPA receptor trafficking in the mammalian retina. *J Neurosci* **26,** 5028-5036.

Xue J, Li G, Laabich A & Cooper NG. (2001). Visual-mediated regulation of retinal CaMKII and its GluR1 substrate is age-dependent. *Brain Res Mol Brain Res* **93,** 95-104.

Yang YP, Fischer QS, Zhang Y, Baumgartel K, Mansuy IM & Daw NW. (2005). Reversible blockade of experience-dependent plasticity by calcineurin in mouse visual cortex. *Nature Neuroscience* **8,** 791-796.

Yao H & Dan Y. (2001). Stimulus timing-dependent plasticity in cortical processing of orientation. *Neuron* **32,** 315-323.

Yazaki-Sugiyama Y, Kang S, Cateau H, Fukai T & Hensch TK. (2009). Bidirectional plasticity in fast-spiking GABA circuits by visual experience. *Nature* **462,** 218-221.

Yoon BJ, Smith GB, Heynen AJ, Neve RL & Bear MF. (2009). Essential role for a long-term depression mechanism in ocular dominance plasticity. *Proc Natl Acad Sci U S A.*

Yoshimura Y, Shinkawa T, Taoka M, Kobayashi K, Isobe T & Yamauchi T. (2002). Identification of protein substrates of Ca2+/calmodulin-dependent protein kinase II in the postsynaptic density by protein sequencing and mass spectrometry. *Biochemical and Biophysical Research Communications* **290,** 948-954.

Zamanillo D, Sprengel R, Hvalby O, Jensen V, Burnashev N, Rozov A, Kaiser KM, Koster HJ, Borchardt T, Worley P, Lubke J, Frotscher M, Kelly PH, Sommer B, Andersen P, Seeburg PH & Sakmann B. (1999). Importance of

AMPA receptors for hippocampal synaptic plasticity but not for spatial learning. *Science* **284,** 1805-1811.

Zepeda A, Arias C & Sengpiel F. (2004). Optical imaging of intrinsic signals: recent developments in the methodology and its applications. *J Neurosci Methods* **136,** 1-21.

Zhang F, Lofgren S & Soderberg PG. (2007). Interaction of anaesthetic drugs and UV-B irradiation in the anterior segment of the rat eye. *Acta Ophthalmol Scand* **85,** 745-752.

Zhang Y, Zhang J & Zhao B. (2004). Nitric oxide synthase inhibition prevents neuronal death in the developing visual cortex. *Eur J Neurosci* **20,** 2251-2259.

Zhou W, Zhang L, Guoxiang X, Mojsilovic-Petrovic J, Takamaya K, Sattler R, Huganir R & Kalb R. (2008). GluR1 controls dendrite growth through its binding partner, SAP97. *J Neurosci* **28,** 10220-10233.

Zhu JJ. (2009). Activity level-dependent synapse-specific AMPA receptor trafficking regulates transmission kinetics. *J Neurosci* **29,** 6320-6335.

CARDIFF UNIVERSITY
PRIFYSGOL CAERDYDD